POLITECNICO DI TORINO

Faculty of Engineering
Mechatronic Engineering

Masters Degree Thesis

Impact of Suspension Bushing's Rigidity in a Real Car's Dynamic Response

Tutor:
prof. Giovanni Maizza
ing. Umid Jamolov

Author:
Iván Sacristán Rueda

Torino, March 2020

ACKNOWLEDGEMENTS

In the first place, I would like to thank my tutor Giovanni Maizza, and Umid Jamolov for all his work and dedication in the project, without who I could not have finished this work. Thank you for giving me the opportunity to learn about a topic that really appealed to me and for teaching me so much about it.

I also want to thank my friends through the last two years, who have made me feel at hove every day ever since I arrived at Turin. Specially Maria, Paco and Patricia, who have accompanied me through these two years of mechatronic engineering and have been a source of laugh, help, love and support through all of it.

Last but not least, I have to thank my family, my parents and my brother, who gave me the opportunity to study abroad and have supported and cheered for me all this time even in the distance.

Abstract

In this thesis, an analysis of the influence of the cylindrical rubber bushings in the suspension of an Opel Astra Caravan 1999 on the dynamic response of the chassis of the vehicle under certain driving situations is developed. The objective of this analysis is to propose design recommendations for future cylindrical rubber bushings that provide a better comfort to the passengers while guaranteeing a better ride quality and handling to the vehicle.

Bushings are composed of two outer rigid surfaces joint by an elastomer material. Their main use is to absorb the vibrations of small amplitude in the elastomer, preventing them from being transferred from one rigid surface to the other, isolating, in through this method, the cabin of the vehicle from road imperfections and other vibrations, improving the comfort of the passengers.

However, recent studies have shown that suspension's rubber bushings' rigidity does not only affect vibration's absorption, but it also shows a direct and not neglectable effect in the dynamic response of the full vehicle to certain riding maneuvers.

This discovery opens a new field of improvement for vehicle suspensions as it should be possible, by designing bushings with specific properties, to improve the performance of the car while enhancing the passengers' comfort. To attain these objectives, the work was divided in four main sectors, which will now be discussed.

Firstly, the obtention of the data of the studied vehicle. Most of this data was obtained through research or in situ measurements. However, specific tests were carried out to obtain the detail characteristic curves of the dampers, springs, and specially, the bushings of the car, which are the object of study. These tests comprised vibrational tests for the dampers, tractional tests and FEM analyses for the springs, and compression and torsional tests for the bushings.

Secondly, the development and the implementation of two multibody models in ADAMS/Car. These two models are: a realistic and detailed model od the Opel Astra, with all the information, data, and parameters obtained; and a simplified model, for a better comprehension of the phenomena and for the validation of the models.

After validating the model, it was subjected to a series of analyses that included the vehicle riding over a series of bumps, that triggers a vertical and roll response of the vehicle; and a single lane change, inducing a certain lateral acceleration. The output of interest in these analyses were: the vertical displacement and de vertical and roll acceleration for the bumped road analysis; and the lateral displacement and acceleration for the lane change maneuver.

Lastly, the data was recollected from these tests at different speeds and with different bushing's rigidities configurations and was later postprocessed. Sensitivity analyses through finite differentiation were performed in order to analyze the impact that each of the rigidities of each of the cylindrical bushings had in every output of interest. After analyzing the results

obtained, it was concluded that, in order to improve the dynamic response of vehicle without damaging passenger's comfort, the following considerations should be taken:

- The radial rigidity in the horizontal direction of the front bushing of the front suspension has the greatest influence on the lateral response. Therefore, it should be increased as much as possible in order to provide a better lateral stability.

- The radial rigidity in the vertical direction of the front bushings has a negative impact on the vertical response. This effect could be mitigated reducing these rigidities or increasing the damping coefficient in this direction.

- Torsional and radial rigidity in the vertical direction in rear bushings impact every output. Therefore, a variation in any direction would prejudice some output. The best course of action would be to increase the damping coefficient of this bushings.

- A small decrease on the axial and radial rigidity in the horizontal direction of the rear bushing of the front suspension would slightly improve the lateral response while reducing the acceleration peaks experienced in the cabin of the car.

- Softer front bushings in the torsional degree of freedom would also slightly improve the satisfaction of the passengers in the body of the car.

Index

Figure index

Table index

Abbreviations

❖ Fx, Fy, Fz	Forces in x, y and z directions respectively
❖ a	Acceleration
❖ m	Mass
❖ l	Wheelbase
❖ wt	Wheel track
❖ CoG	Center of Gravity
❖ X_{CG}, Y_{CG}, Z_{CG}	Vehicle CoG coordinates
❖ $T_{U,}$ T_R	Tire unloaded and loaded radius respectively
❖ Ixx, Iyy, Izz	Vehicle roll, pitch, and yaw moments of inertia
❖ DoF	Degree of Freedom
❖ FEM	Finite Elements Model

1. Introduction

1.1. Purpose of the work

The suspension of a car is the set of components that connect the wheels to the chassis, permitting a relative motion between them. As explained by Barton D.C in [1]: "*Ride quality and handling are two of the most important issues related to vehicle refinement*". These two issues are strictly related to the suspension of the vehicles.

Due to this importance of the suspension in the ride and handling of the vehicle, there are a lot of studies on suspension configurations and key components in the suspension such as springs and dampers.

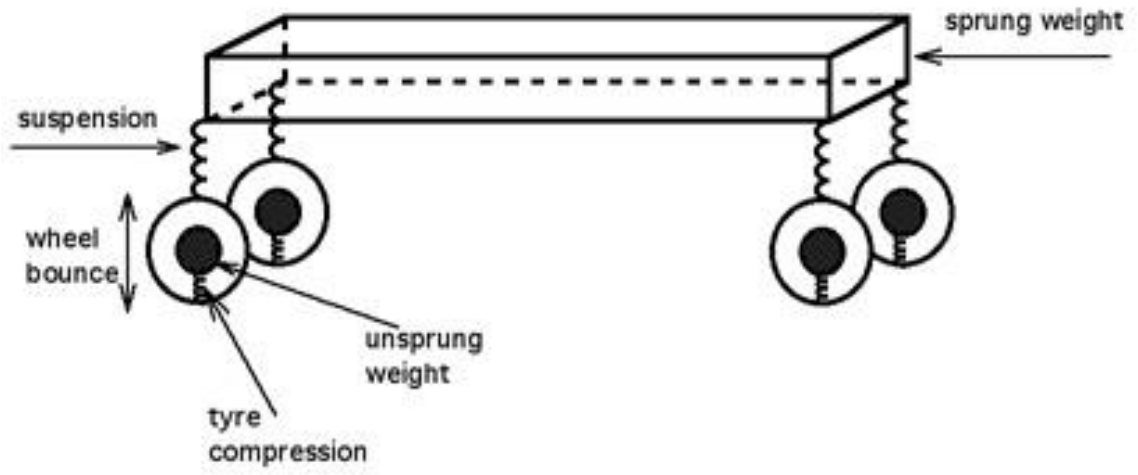

Figure 1: Sprung and unsprung masses scheme
Image by: David R. Ingham – Wikipedia

The joint of the suspension to the chassis is done through a special type of bushings called silentblocks. These silentblocks are composed of two outer rigid surfaces joint by an elastomer material. The purpose of this type of bushing is to absorb the vibrations of small amplitude in the elastomer, preventing them from being transferred from one rigid surface to the other. Since these vibrations are absorbed by the silentblocks, they do not arrive at the cabin of the car, improving in this way the comfort of the passengers.

These components were not studied in detail in the past. However, they have gained more importance in the recent times. The studies performed by Ambrósio, J., & Verissimo, P. in [6] show that they do not only serve to absorb vibrations due to road imperfections, but they also have a direct and not neglectable effect in the dynamic response of the full vehicle to certain riding maneuvers.

This discovery opens a new field of improvement for vehicle suspensions as it should be possible, by designing bushings with specific properties, to improve the performance of the car while enhancing the passengers' comfort.

It is in this field of study that this work takes place. Specifically, cylindrical rubber bushings will be analyzed in detail throughout this thesis in order to propose different improvements.

Figure 2: Cylindrical rubber bushing
Image from [11]

Since there are many different suspension configurations, the study will be performed for a common user car configuration: front Macpherson strut and a rear twist beam arrangement.

For this purpose, multibody analyses done by means of several engineering tools such as ADAMS/Car [19]; analysis methodologies like sensitivity calculations and finite differentiation; and engineering criteria application will be necessary, as it will be explain throughout this document.

1.2. State of art

Even if the study of the bushings has not had such a relevance, there have been some studies performed in the field. The works that have served as base and motivation for this works will now be explained:

- As it was stated in the introduction, there are many works on the design and development of suspension systems, analyzing and proposing different components and configurations. The *Automotive Chassis Engineering* publication by Barton D.C. and Fieldhouse J.D. [1] and *The automotive chassis*, publication by Reimpell, J., Stoll, H. and Betxler, J. [7] have been the two are the two main sources of information for general vehicle data. Another source was [10], the work by Herranz, E.E.

- The work that was taken as a reference to validate this thesis are the articles published by Ambrósio, J. and Verissimo, P.: *Improved bushing models for general multibody systems and vehicle dynamics* [6] and *Sensitivity of a vehicle ride to the suspension bushing characteristics* [2], where they study the effect of bushing rigidities in vehicle ride.

- Caputo, A., Spina, M. and Guglielmino, E., in their study *Sensitivity of Suspension System Performance to Bushing Stiffness Variation – An Evaluation Methodology* [3], propose a methodology to "*evaluate the influence of the bushings stiffness on the suspension elastokinematic performance"* In this work, they propose a methodology to analyze the impact of the bushings sensitivity in certain suspension parameters such as camber and toe angles. Blundell, M. V.'s work: *The influence of rubber bush compliance on vehicle suspension movement* [5], also analyses the impact of bushings' compliance on variation of certain suspensions' geometric parameters in order to improve computer simulations.

- The article *Experimental Study and Numerical Modeling of the Dynamic Behavior of Tyre/Suspension While Running Over an Obstacle* [4] presents the work by Gobbi, M., Giorgetta, F., Guarneri, P., Rocca, G., and Mastinu, G. in which they present different tools to perform Noise-Vibration-Harshness analyses such as experimental approaches and Recurrent-Neural-Networks-based models.

- The works by Haftka, R. T., and Adelman, H. M.: *Recent developments in structural sensitivity analysis* [8] and De Pauw, D. J., & Vanrolleghem, P. A.: *Practical aspects of sensitivity analysis for dynamic models* [9] present different methodologies to implement sensitivity analyses, an essential tool for this work. Their finite differences approach has been of priceless utility to reach the final conclusions.

Some researchers have investigated different contributions of these bushings to different parameters of the vehicle. Some of these studies are now shown:

- Lee, H. S., Shin, J. K., Msolli, S. and Kim, H. S. in their study *Prediction of the dynamic equivalent stiffness for a rubber bushing using the finite element method and empirical modeling* [11] analyze the characteristics of rubber bushings by means of a self-developed method

mixing finite elements and empirical modeling. Another study in this field was made by Dzierżek, S. in his work: *Experiment-based modeling of cylindrical rubber bushings for the simulation of wheel suspension dynamic behavior* [12] where he develops a modelling methodology based on experiments for rubber bushings.

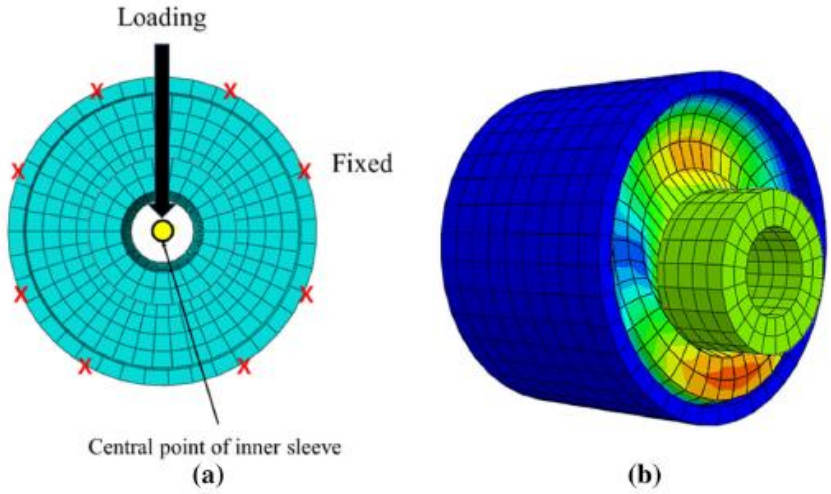

Figure 3: Cylindrical rubber bushing FEM (a) and radially deformed shape (b) Image from [11]

- Kang, B. J., Kim, N. W., Kim, J. H., Lee, Y. H., and Sin, H. C. in their work *Improving the durability of automobile suspension systems by optimizing the elastomeric bushing compliance* [14] propose a solution for the wear of suspensions by analyzing and modifying the rubber bushings of the suspensions. In the same line, Hope, S. W., Conrado, G. N. P. V., de Paula Pinto, A., Quaglia, J. L. C., Cadiot, D., and Pintos, C. in *Lower control arm rear bushing development an integrated approach* [13] explain the methodology they employed for the design of the bushings for the lower control arm of a McPherson front suspension in order to meet durability requirements. The final work considered in the field of the improvement of durability specifications is the paper by Rahman, M. M., Kadirgama, K., Noor, M. M., Rejab, M. R. M., and Kesulai, S. A.: *Fatigue life prediction of lower suspension arm using strain-life approach* where they study the life cycles to breakage independently of the bushings.

- An interesting study is the one developed by E.Y. Kuo, D. Li and W. Loh under the title: *The Efffects of Bushings Degradation on Vehicle High Mileage NVH Performance.* In this study they explain the importance of the bushings in NVH performance, since they absorb vibrations from the road before they get to the cabin. Due to this effect of the bushings, under severe mileage, the bushings degrade. The work is an analysis of this degradation

- Finally, Piquet, B., Maas, C. A., and Capou, F., in the paper: *Next Generation of Suspension Bushings: Review of Current Technologies and Expansion Upon New 3 rd Generation Product Data* [18] introduces us to a new industry set in the development of innovative solutions for bushings in order to attain quantitative benefits in passenger comfort.

Some of these innovations include solutions for variable bushing rigidities by technologies such as hydro-bushings or switchable bushings. The following figure shows some of these solutions:

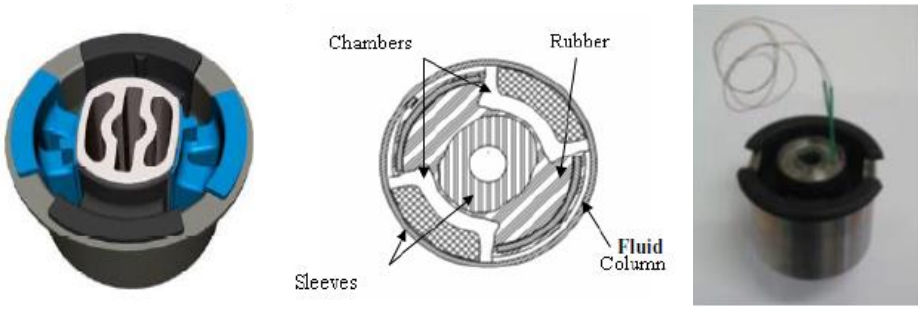

Figure 4: Dual-compound bush(a) hydro-elastic bush(b) and switchable bush(c) Images from [18]

1.3. Objectives

The objective posed for this thesis is the analysis of the influence of the cylindrical rubber bushings in the suspension of an Opel Astra Caravan 1999 on the dynamic response of the chassis of the vehicle under certain driving situations in order to proposed design recommendations for improved bushings.

For this objective a detailed multibody model of the Opel Astra is needed. In order to obtain the necessary parameters for the model, the springs and dampers of the car need to be tested, as well as the silentblocks object of study. For the development of the model ADAMS/Car software [19] has been used.

Another simplified model was developed in order to better understand the influence of the bushings and to validate the model with the results from similar analyses.

1.4. Thesis planning

As explained in the previous chapter the objective of the thesis is the analysis of the impact of rubber bushings on the dynamic response of a vehicle for the improvement of this components.

Therefore, the thesis will start with the explanation of the necessary theory to understand the work.

After setting the basis, the development of two models is explained: the realistic Opel Astra model, and the simplified model. To do this, all the performed tests and calculations will be shown and explained.

Once the models have been built, the work will proceed to validate the model by obtaining diverse results with the simplified model, evaluating and comparing them with other contrasted works.

Additionally, when the model has been contrasted, a wide variety of analyses were performed by means of ADAMS/Car. Thereafter, all the data was gathered, organized and postprocessed to make it understandable and evaluable.

With the results in hand, conclusions on the best lines to follow in order to develop cylindrical rubber bushings for an improved dynamic response of the vehicle are presented.

2. Theoretical background

The study of the effect of bushings require an adequate knowledge of the vehicle and mainly, of the suspension systems and their interaction with the sprung mass. In this chapter, the main topics in order to understand the next steps of the work will be covered.

2.1. Vehicle suspension systems

The suspension system is one of the main components of any vehicle, having a significant and active impact on the automobile's dynamic response.

Its main role has to do with the ability to hold the weight of the vehicle while providing a damping effect on the relative movement between the sprung and the unsprung masses.

We understand as sprung or suspended mass, the fraction of the vehicle's total mass due to the components hold by the suspension system (chassis, seats, engine, etc.), as well as part of the mass of those components attached both to the suspension and to any fully suspended component: the engine driveshaft as an example.

The unsprung or non-suspended mass is, therefore, all the mass that is entirely resting on the road. In this category are comprised: wheels, brakes, twist beams, etc. Figure 1 further explains these two concepts.

The joint between the suspended and non-suspended masses is done by means of components that are stiff enough to hold the desired weight while delivering a desired damping. These components conform the suspension of the vehicle.

As explained by D.C.Barton & J.D.Fieldhouse in [1], the main functions of a suspension system are the following:

- To improve ride and handling performance.
- To guarantee steering control stability during a maneuver.
- To withstand squat, dive and roll of the chassis.
- To isolate the chassis from road imperfections.
- To provide enough stiffness to hold the load imposed by the sprung mass.

All these requirements are utterly difficult to meet simultaneously, what derives in the necessity to reach a compromise that does not fully solve all of these roles perfectly. Therefore, there is not one unique and universal better suspension configuration.

2.2. Suspension system geometry

2.2.1. Suspension configurations

Conventionally, suspension systems have been grouped in three main families, depending on the grade to which the two wheels of the same axis are connected to each other: dependent, semi-dependent, and independent suspensions.

2.2.1.1. Dependent suspensions

This is the most ancient suspension configuration. It is composed of a rigid axis joining both wheels (Figure 5). With this configuration, vertical displacement of a wheel directly affects the other wheel.

Its main advantages are the simplicity, durability, and the absence of camber variation due to chassis roll. However, they tend to be heavy, and the acting forces on one wheel directly affect the other, increasing the instability of the car.

Examples of dependent configurations are the Hotchkiss suspension, employing leaf springs, widely used for trucks; and the four link arrangements, as depicted in Figure 5.

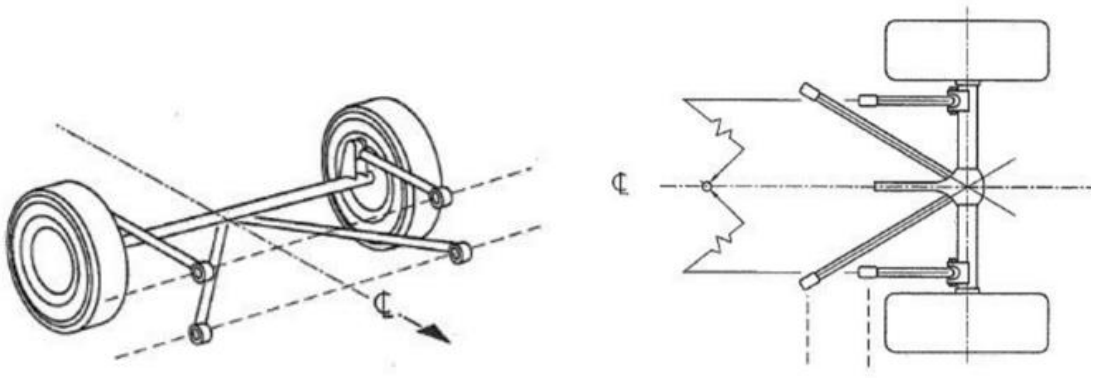

Figure 5: Four-Link Dependent suspension scheme
Image by: Elias Efler – Trabajo de Fin de Grado

2.2.1.2. Semi-dependent suspensions

These suspensions are similar in configuration to dependent suspensions. However, instead of employing rigid unions, they use links that allow certain deformations, transferring only part of the reaction on one wheel over to the other.

Figure 6: Twist Beam Semi Dependent suspension
Image from: www.invetr.com

They provide better comfort and occupy less space. Some examples are the twist beam suspension (Figure 6) or the De-Dion suspension.

2.2.1.3. Independent suspensions

In independent suspensions, both wheels are isolated, so that an action on one wheel has no effect on the other whatsoever. They offer the best vibration absorption capacity. They are the most widely used due to the design versatility they offer, and the ease to fit them into very limited space. The wheels are connected to the chassis though elements designated as arms. The number, shape, and dimension of this arms define the trajectory of the wheel from contracted to extended suspension. Some of the most widely used are McPherson strut, double wishbone multilink, or trailing arm configurations.

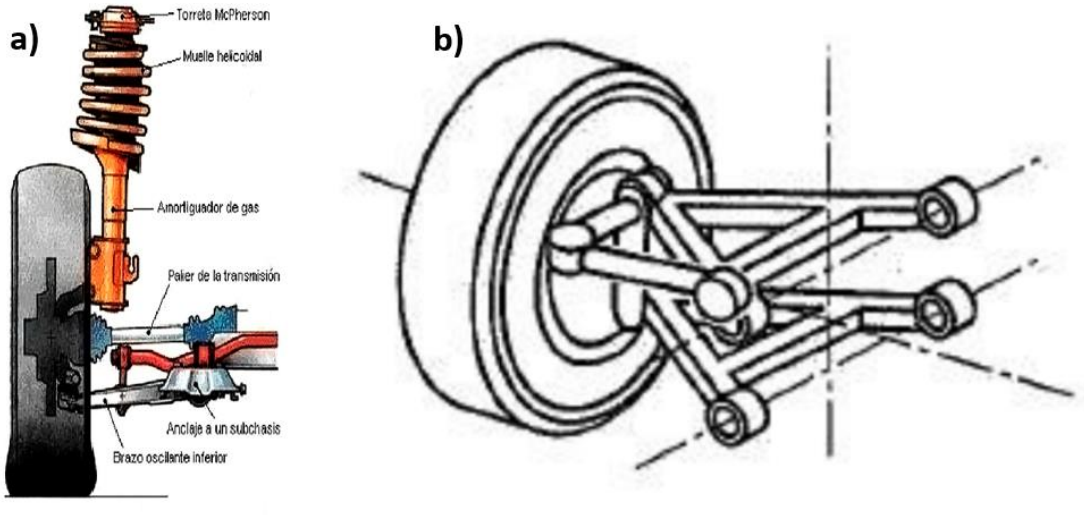

Figure 7: McPherson (a) and Double Wishbone (b) suspensions
Image by: a)www.todoautos.com b)Elias Efler – Trabajo de Fin de Grado

2.2.2. Suspension design parameters

In this chapter, the most important parameters in order to define a suspension system are described.

2.2.2.1. Wheelbase

The wheelbase is defined as the distance between the center of front and rear axis. This parameter has a big impact on the longitudinal load transfer, as expressed in the following expression, being l the wheelbase.

$$\Delta F_z = \frac{a \cdot Z_{CG} \cdot m}{l} \qquad \text{(Equation 1)}$$

2.2.2.2. Wheel track

The wheel track is the distance between the two wheels on the same axis. The front value for the wheel track could differ from the rear axis' value. In line with the wheelbase, the wheel track directly impacts the lateral load transfer, as represented in Equation 2. This implies a big influence on the turning behavior of the vehicle.

$$\Delta F_z = \frac{a \cdot Z_{CG} \cdot m}{wt} \qquad \text{(Equation 2)}$$

Figure 8 represents these two parameters:

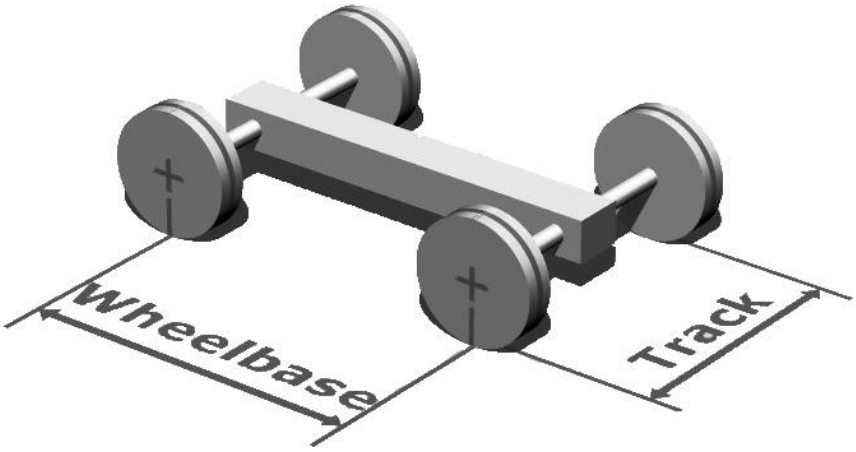

Figure 8: Wheelbase and Wheel track
Image by: Truthdowser – Wikipedia

2.2.2.3. Camber angle

The camber angle is the angle between the tire's middle axis and the vehicle's z axis seen from the front of the vehicle. This angle is considered with a negative value when the top of the wheel leans towards the body of the vehicle. This can be seen in Figure 9. The camber angle generates a lateral force on the axis with the direction of the inclination of the wheel.

A positive camber angle (around 0.1º) improves tire wear, while a negative camber angle enhances the behavior of the vehicle in bends. However, the camber angle cannot be too big, since after a certain value of the angle, the linear behavior limit is exceeded, and the effect of the camber angle is lost, phenomena known as roll-off.

It must also be noted that, in independent suspensions, since the wheels rotate to some extent, the camber angle can vary slightly when the wheel travels up.

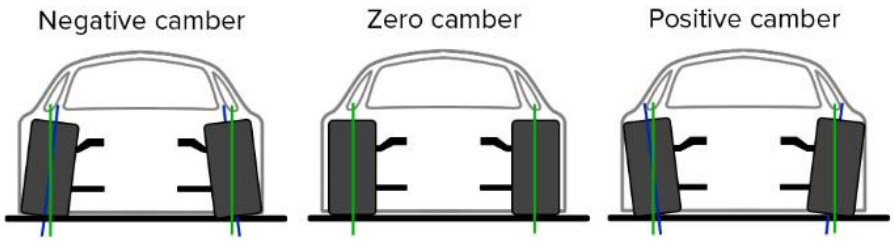

Figure 9: Camber angle
Image from: www.liberaldictionary.com

2.2.2.1. Kingpin inclination and scrub radius

The kingpin axis or steering axis is the axis about which the wheel turns at steering. Kingpin inclination is the angle between this axis and the vertical axis seen from the front. It directly affects the self-aligning torque and also impacts the tire wear. A side effect is the variation of the camber angle with steering.

The scrub radius is, as can be seen in Figure 10, the distance, seen from the front, from the intersection point of the kingpin axis and the ground to the center of the tire contact patch.

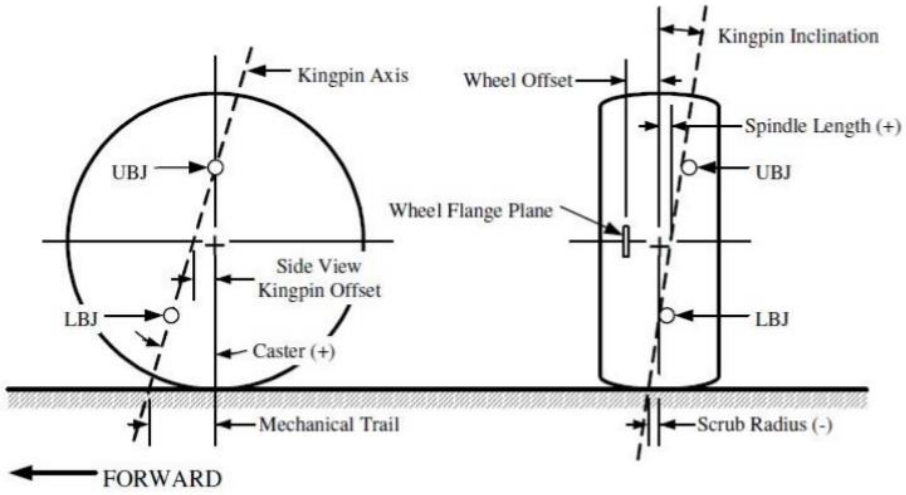

Figure 10: Kingpin angle and scrub radius
Image by: Elias Efler – Trabajo de Fin de Grado

2.2.2.2. Castor angle, castor offset and castor trail

Castor angle is a variable that only impacts the steering wheels. It is defined as the angle between the kingpin axis and the wheel's z axis, seen from the side of the vehicle. It is considered positive when the axis leans rearwards (Figure 11).

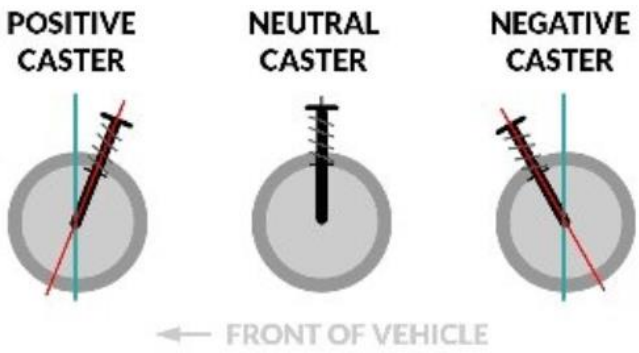

Figure 11: Castor angle sign criteria
Image by: Nitesh, Yv – 2019

Castor trail is the distance between the kingpin axis intersection point with the ground and the center of the tire. The castor offset is, on the other hand, the distance from the kingpin axis to the center of the wheel seen from the side, as shown in Figure 12.

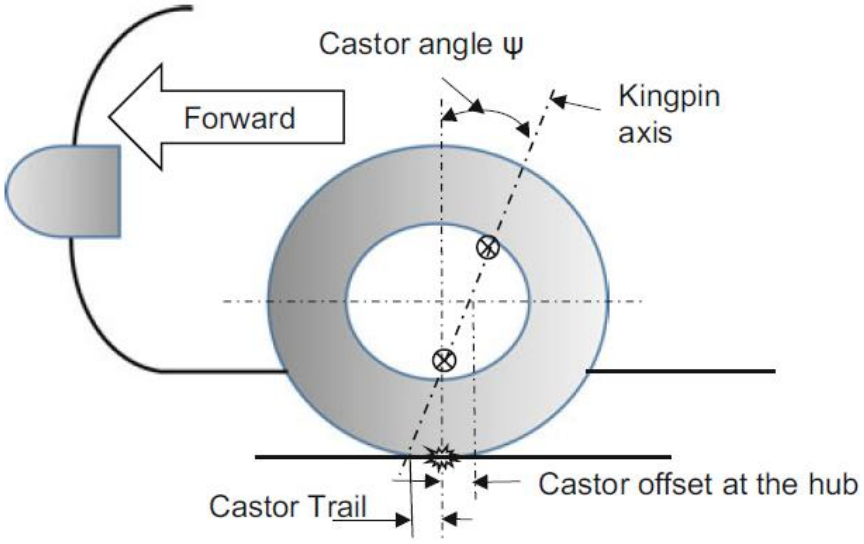

Figure 12: Castor angle sign criteria
Image by: D. C. Barton and J. D. Fieldhouse, Automotive Chassis Engineering

Castor angle and castor trail create a self-aligning torque in non-driven wheels. It impacts the torque needed for the steering of the vehicle. It also modifies the camber angle during the turning. Finally, it elevates the wheels when they are being steered, producing a rolling effect and a load transfer.

2.2.2.3. Toe in/out angle

Toe angle is the angle between the vehicle X axis of the vehicle and the middle plane of the wheel. It is positive when the middle planes of both wheels intersect towards the front of the vehicle, and negative otherwise.

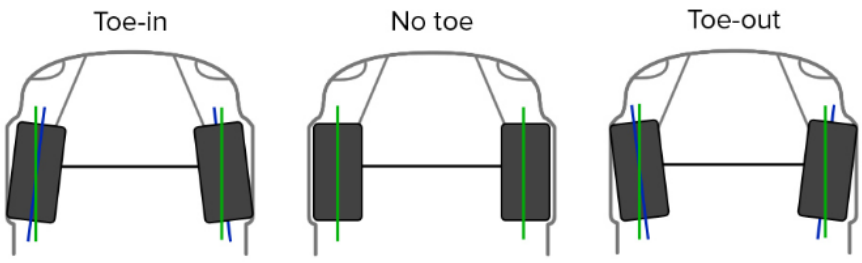

Figure 13: Toe in/out
Image from: www.liberaldictionary.com

2.3. Mechanical joints

The objective of this thesis is to analyze the impact of bushings rigidity on the overall vehicle dynamic response and passenger comfort. Therefore, understanding the different types of bushings and their impact on the vehicle's suspension is fundamental.

Bushings are components that serve the main purpose of undertaking the mechanical stresses due to relative displacements between components in different types of mechanical joints. It is, therefore, compulsory to understand the diverse mechanical joints in order to understand the bushings.

Mechanical joints are classified in base on the degrees of freedom they allow between the connected components. Since a lot of combination are possible, only the most significant will be explained. There are two main groups of

- Revolute joints: they permit only one degree of freedom: a relative rotation between the two components.

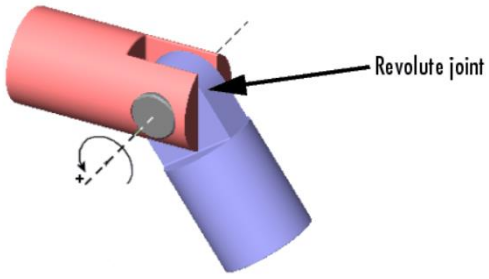

Figure 14: Revolute joint
Image from: es.mathworks.com

- Prismatic joint: one degree of freedom, a displacement along the joint axis, no rotation.

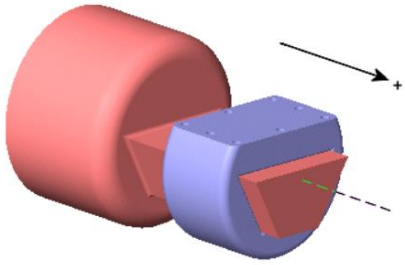

Figure 15: Prismatic joint
Image from: es.mathworks.com

- Spherical joint: this joint allows rotation around the 3 cartesian axis, granting access to any possible orientation between the parts.

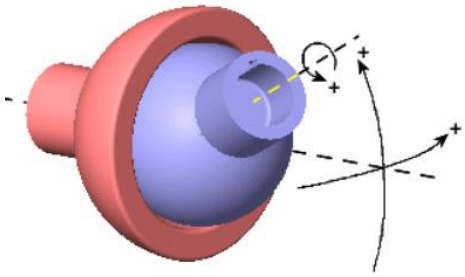

Figure 16: Spherical joint
Image from: es.mathworks.com

- Cylindrical joint: 2 degrees of freedom, a rotation and a translation, both along the same axis.

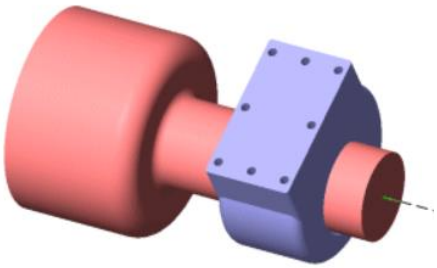

Figure 17: Cylindrical joint
Image from: es.mathworks.com

- Universal joint: also known as U joint or Cardan joint. It is formed by two revolute joint, allowing the two parts to obtain any relative angle but not allowing a rotation along the joint axis. It has therefore, 2 degrees of freedom, 2 rotations around perpendicular axis.

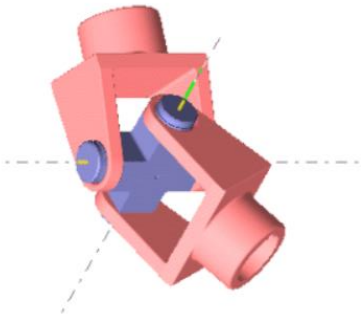

Figure 18: Universal joint
Image from: es.mathworks.com

2.4. Bushings

Bushings are components located in the interfaces of these joints. Their shapes and materials depend on the joint where they will work, and their purpose. The bushings analyzed in this thesis are a type of bushing called silentblock.

Silentblocks are composed of two outer rigid surfaces joint by an elastomer material. The purpose of this type of bushing is to absorb the vibrations of small amplitude in the elastomer, preventing them from being transferred from one rigid surface to the other.

The joints analyzed in this work are rotational. The silentblocks are, therefore, cylindrical rubber-based bushings, as in Figure 2.

It is important to understand the different deformation modes present in these components. For this purpose, Figure 19 shows the reference frame used, from this moment onwards, in the study of this components.

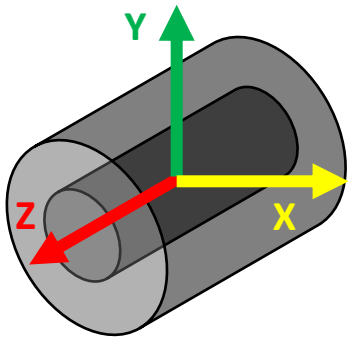

Figure 19: Cylindrical rubber bushing reference axis

From the characteristic of being cylindrical, the deformation in X and Y axis are equivalent and there are, consequently, four deformation modes.

On the one hand, the two translational deformation modes are: radial, in X and Y directions; and axial, in Z direction. On the other hand, the two rotational modes are the torsional deformation, around the Z axis, and the conical deformation, around X or Y axis, or a combination of both. This deformation modes are shown in Figure 20.

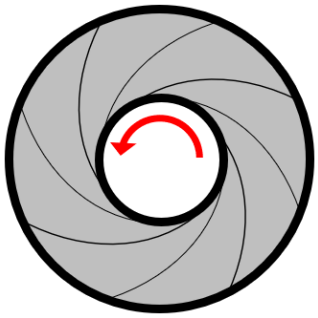

a) Torsional deformation

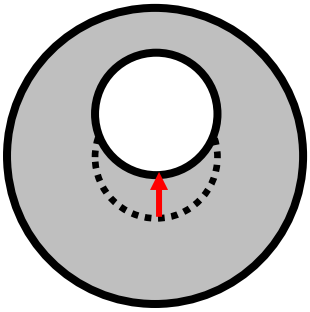

b) Radial deformation

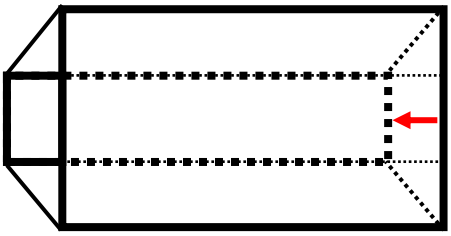

c) Axial deformation

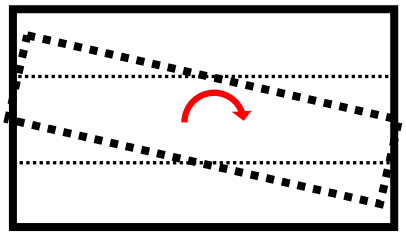

d) Conical deformation

Figure 20: Cylindrical rubber bushing deformation modes

3. Multibody model

For the analysis of the impact of the bushing's rigidity on the vehicle dynamic response, a multibody model of a vehicle was developed. In this case, the chosen model was an Opel ASTRA Caravan of the year 1999, as shown in Figure 21.

Figure 21: Modeled Car

In the following chapters, the different parameters obtained, either from tests, blueprints, measurements or calculations needed for the model will be presented.

In order to elaborate the model of the Opel Astra, MSC ADAMS/Car software was utilized. This software works through entities named subsystems, which are later assembled to produce the full car model. For a full vehicle multibody analysis, the following subsystems are requested:

- Front suspension
- Rear suspension
- Front wheels
- Rear wheels
- Body
- Engine
- Brake system
- Steering system

While these subsystems must be present for the correct behavior of the model, the software allows the implementation of other subsystems to increase the level of detail, such as anti-roll bars, transmission components or seat suspensions.

To build each of these subsystems, the process starts by employing one of the available templates given by the software, whose parameters, both geometric and dynamic, can be later modified to match those of the desired vehicle.

The geometries of the templates are based on the so-called hard-points. These points are located in all the main intersections of all de templates and allow to define the general shape through links between them.

3.1. General geometric parameters

The first step to develop the geometric model of the vehicle is to obtain the global geometric parameters of the car. These parameters were all obtained by in situ measurements on the analyzed vehicle.

Parameters	Units	Value	Obtention
Wheelbase	mm	2611	Measured
Front wheel track	mm	1464	Measured
Rear wheel track	mm	1452	Measured

Table 1: Opel Astra General Geometric Parameters

3.2. Front suspension

The front suspension of the Opel Astra Caravan 1999 is an independent suspension, allowing free displacements of one wheel with respect of the other. Specifically, the front suspension is a MacPherson strut, shown in Figure 7 a).

In this configuration, the upright of each wheel is connected to the chassis through 3 links. Firstly, the lower part of the upright is connected to an arm, which permits an oscillation with respect of the chassis. Secondly, the top of the upright is connected through the MacPherson strut, composed by an articulated spring and damper. Finally, the steering rod connects to a side in order to allow the turning of the wheel.

To develop the subsystem of the front suspension, ADAMS/Car provides us with a base template to work with. This template is shown in the following image:

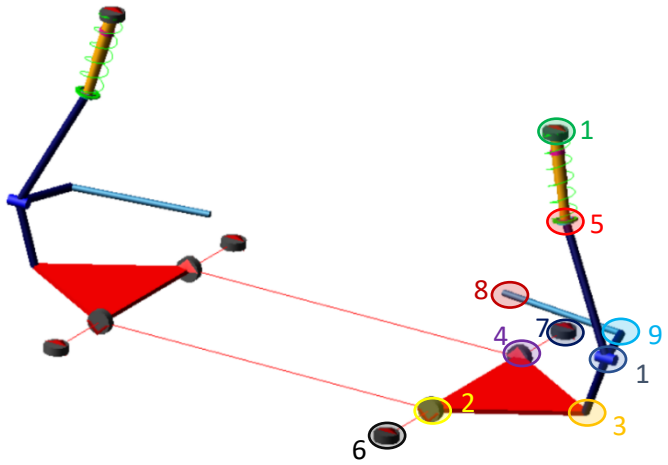

Figure 22: MacPherson suspension template

As it was previously explained, the geometry of the templates is modified by changing the position of the hard-points. This points in this template were colored in Figure 22. Right and left sides are symmetrical. In Table 2, these hard-points are defined.

	Left side		Right side	
Figure 12 Nº	**Hard Point code**	**Meaning**	**Hard Point code**	**Meaning**
1	hpl_wheel_center	left wheel center	hpr_wheel_center	right wheel center
2	hpl_lca_front	lower left control arm front point	hpr_lca_front	lower right control arm front point
3	hpl_lca_outer	lower left control arm outer point	hpr_lca_outer	lower right control arm outer point
4	hpl_lca_rear	lower left control arm rear point	hpr_lca_rear	lower right control arm rear point
5	hpl_spring_lwr_seat	left spring lower seat	hpr_spring_lwr_seat	right spring lower seat
5	hpl_strut_lwr_mount	left damper lower point	hpr_strut_lwr_mount	right damper lower point
6	hpl_subframe_front	left front subframe point	hpr_subframe_front	right front subframe point
7	hpl_subframe_rear	left rear subframe point	hpr_subframe_rear	right rear subframe point
8	hpl_tierod_inner	leftside inner tierod point	hpr_tierod_inner	rightside inner tierod point
9	hpl_tierod_outer	leftside outer tierod point	hpr_tierod_outer	rightside outer tierod point
10	hpl_top_mount	top left damper point	hpr_top_mount	top right damper point

Table 2: MacPherson suspension hard-points definition

The coordinate frame used by ADAMS/Car for the global assembly, is represented in Figure 21. To obtain the coordinates of each of the hard points, several data was analyzed.

- The default x coordinate (longitudinal) of the front wheels center was kept as a reference point from which to obtain the rest of the coordinates; and the vehicle was centered at y coordinate equal to 0.
- The general parameters shown in Table 1 were considered.

- From CAD models, it was seen that the lower control arm was set horizontally. Additionally, detailed blueprints of the lower control arm were obtained, allowing the obtention of measurement of different points.

- From [21], detailed information on the wheels of the analyzed Opel Astra was obtained. For this purpose, the needed data was the tire unloaded radius:

$$T_U = 305.7\ mm$$

  And a loaded radius of:

$$T_R = 300\ mm$$

- Suspension parameters that were obtained by in situ measurements, shown in Table 3.

Parameters	Units	Value
Camber angle	º	-1.5
Castor angle	º	6
Castor trail	mm	20
Toe angle	º	0
Kingpin inclination angle	º	10
Kingpin offset	mm	10
Spring frontal angle	º	7
Spring length	mm	247.5

Table 3: Front suspension parameters

Now, the process to stablish the geometry of the front suspension is going to be described.

To recreate the geometry and guarantee that the vehicle was tangent to the surface of the road at the beginning of the tests, the first step was to position the wheel center at a height of 300mm (wheel loaded radius), and at a y coordinate that provided the desired front track to the vehicle.

The next step was to set the location of points 3 and 5 in Table 2, as these points are the mountings of the upright and set the direction of the kingpin axis, having a direct impact in the castor and kingpin parameters. From these parameters, the location of those two points could be obtained. The main geometrical relations considered can be seen in Figure 23.

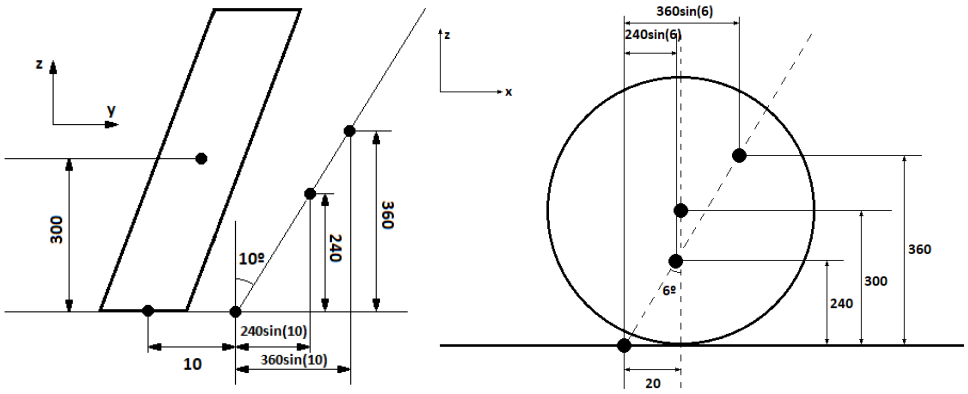

Figure 23: Castor and kingpin calculations

From this point, blueprints of the lower arm were used to set the location of points 2, 4, 6 and 7 (Table 2). Finally, hardpoint 10 location was obtained with the spring's loaded length and the orientation angle, both measured on the vehicle. The final subsystem for the front suspension is shown in Figure 24.

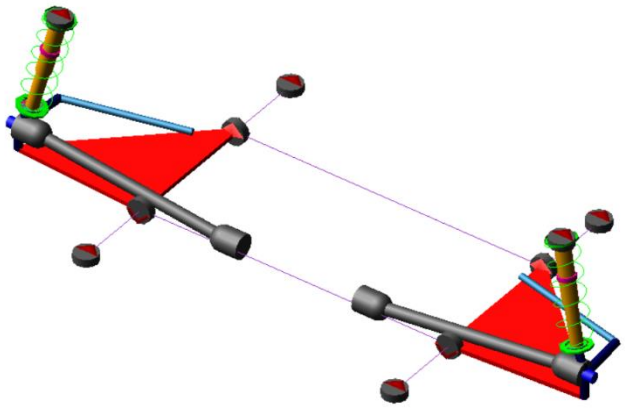

Figure 24: Opel Astra front suspension subsystem

3.3. Rear suspension

The rear suspension of the Opel Astra Caravan 1999 is a twist beam (Figure 6). This is a semi-dependent suspension. Both wheels are attached to the body of the vehicle through a trailing edge and the damper and spring. However, both trailing edges are joint by a twist beam in a way that the vertical displacement of one of the wheels directly affects the other.

As in the front suspension, ADAMS/Car provides a template to develop this type of suspension. However, this case is more complex than the previous one. For this suspension template, both trailing edge and the twist beam are modeled as a unique whole, behaving as a flexible part. Due to this characteristic, the exact shape of the rear suspension could not be

achieved. This problem was mitigated by adapting the properties of the dampers and springs so that they developed the same reactions as in the real configuration.

The full flexible body was positioned so that the height of the center of the wheels was the same as in the front axis, and so that the wheelbase of the model was the same as in the Opel Astra.

As with the front suspension, some parameters were taken into consideration for the development of this subsystem:

- The reference frame is the same as previously used.
- The general parameters shown in Table 1 were considered.
- The wheels in the rear axis are the same as in the front and, therefore, the same data from [21] was used. Unloaded radius:

$$T_U = 305.7\ mm$$

  And a loaded radius of:

$$T_R = 300\ mm$$

- Suspension parameters that were obtained by in situ measurements, shown in Table 4.

Parameters	Units	Value
Camber angle	º	-1.0
Toe angle	º	0

Table 4: Rear suspension parameters

With this information, the subsystem for the rear twist beam suspension was developed:

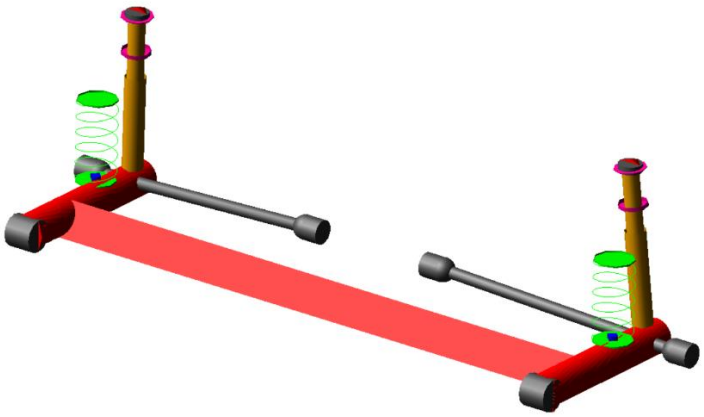

Figure 25: Opel Astra rear suspension subsystem

3.4. Other subsystems

In this chapter, other simpler subsystems for the multibody model will be described.

3.4.1. Wheels

For this model, there are two tire subsystems, one for the front tires, and one for the rear. However, all four of the wheels of the Opel Astra are equal and, therefore, have the same properties and dimensions. For this reason, these two subsystems will be described together.

The tires mounted on the Opel Astra studied were the 205/50R16. These are radial tires with a width of 205mm, an aspect ratio of 50, and mounted on a 16in (406.4mm) wheel.

The main parameters are shown in Table 5. These values are obtained from [21].

Parameter	Units	Value
Width	mm	205
Aspect Ratio	-	50
Tire type	-	Radial
Rim Diameter	mm	406.4
Tire height	mm	103
Tire diameter	mm	611.4
Unloaded radius	mm	305.7
Loaded radius	mm	300

Table 5: Wheel dimensional parameters

Other important parameters for the model were, of course, the dynamic parameters of the tires. These values were obtained from the real vehicle and are presented in the following table.

Parameter	Units	Value
Vertical stiffness	N/mm	199.4
Vertical damping	N·s/mm	0.000078
Lateral stiffness	N/mm	150
Rolling resistance	-	0.01

Table 6: Wheel dynamic parameters

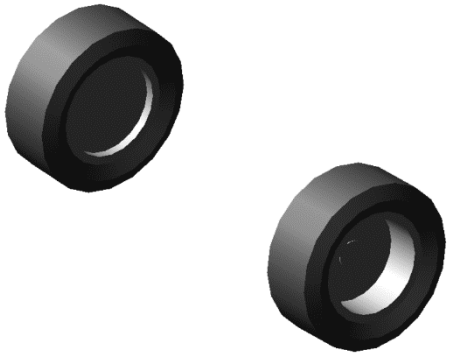

Figure 26: Opel Astra tires subsystem

3.4.2. Chassis

The chassis subsystem is in charge of joining all the other subsystems together. Therefore, it automatically adapts its main hard points to the ones present in other subsystems when included in the assembly.

3.4.3. Powertrain

The powertrain subsystem is normally only composed of the engine. However, due to the subsystem configuration employed in this model, it was not possible to use this simplistic approach. It was, the, necessary to use an intermediate subsystem to join the front suspension (driven axis) to the front mounted engine. This intermediate subsystem was modeled as a transmission shaft that only served as a transition from the engine to the front wheels.

These two subsystems are needed to provide the motional input to the assembly. They were set to 0 mass and, therefore, their geometrical location had no effect in the later tests. It was, therefore, positioned in a coherent location.

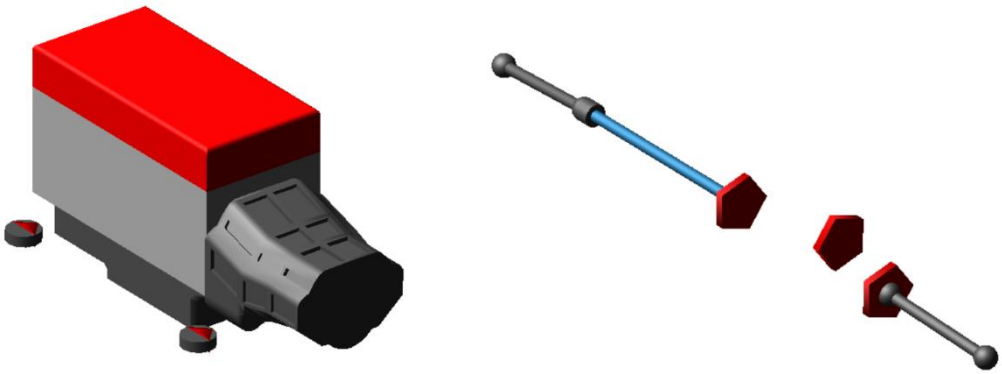

Figure 27: Opel Astra powertrain subsystem

3.4.4. Braking system

Similarly to what happened with the powertrain subsystem, the brakes are necessary in the assembly to allow the vehicle to reduce the speed, but has no specific geometrical specifications. A default braking system was, thus, employed.

3.5. Dynamic parameters

Once all of the geometrical aspects of the model were included, it is time to input other dynamic parameters that are important to the behavior of the car, including the distribution of the masses, the rigidities and damping coefficients of the suspensions and, of course, the properties of the silentblocks, object of study for this work.

3.5.1. Weight distribution

The first step was to distribute the weight among the different components. Since measuring the weight of each single component and inputting it into ADAMS was an impossibly arduous, and unnecessarily long task, a simplified approach was made.

From the full vehicle, the total weight, as well as the unsuspended masses for the right wheels was obtained. Additionally, other parameters such as the location of the center of masses and the inertia values in different directions were also measured. The following table shown all the relevant values:

Parameter	Units	Value
X coordinate of center of gravity, X_{CG}	mm	1066.00
Y coordinate of center of gravity, Y_{CG}	mm	0.00
Z coordinate of center of gravity, Z_{CG}	mm	560.00
Roll moment of inertia, Ixx	kg·m2	470.40
Pitch moment of inertia, Iyy	kg·m2	2045.80
Yaw moment of inertia, Izz	kg·m2	2234.30
Total vehicle mass	kg	1200.00
Front right unspring mass	kg	41.46
Rear right unsprung mass	kg	38.00

Table 7: Full vehicle weights and inertia values

ADAMS/Car offers an automatic approximator of vehicle masses. To optimize the calculations of the software, the following previous considerations and approximations were made:

- The priority of the software had to be the CoG positioning.
- The second priority was the obtention of the inertia values.
- The least importance was given to the total mass and sprung/unsprung ratio.
- Initially, the totality of the unsprung masses from Table 7 was placed in each of the wheels. The rest of the total mass was placed solely on the chassis.

After the internal iterations of the software, a different mass was assigned to each component. The full detail of these masses can be seen in Annex A. The global masses obtained through this process are now shown compared to the real expected values.

Mass	Real [kg]	Obtained [kg]	Error [%]
Total	1200.000	1191.420	0.71
Total Sprung	1041.080	1033.046	0.77
Total Unsprung	158.920	158.375	0.34
Front Unsprung	82.920	82.313	0.73
Rear Unsprung	76.000	76.062	0.08
Total Front	710.012	704.936	0.71
Total Rear	489.988	486.485	0.71

Table 8: Final model masses and errors

As can be seen in Table 8, the final errors are really small and, therefore, the results were considered valid. It must be noted that the errors in the total, total front, and total rear masses are the exact same. This means that the CoG location was successfully achieved, and the error from the total mass is equally distributed to the front and rear axis.

3.5.2. Spring characteristics

The characteristics of the springs of the Opel Astra were obtained by both testing and FEM analysis. The obtained curves can be seen in the following figure:

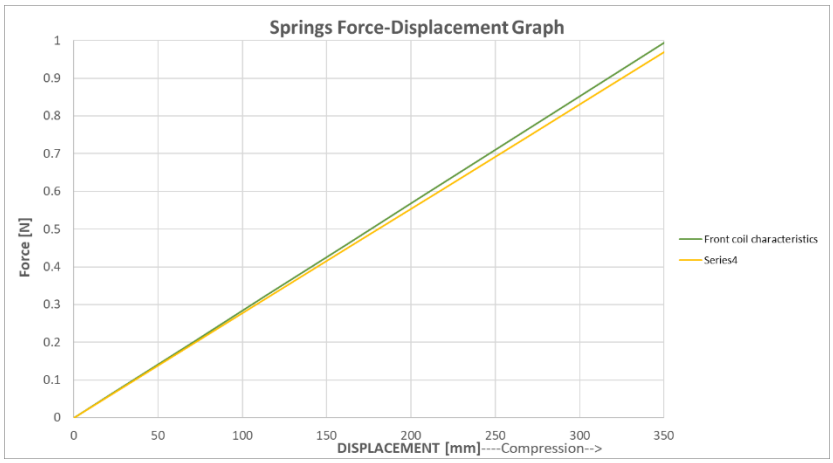

Figure 28: Opel Astra spring characteristic

3.5.3. Damper characteristics

The damper of the Opel Astra Caravan 1999 was tested in a vibrational machine named step lab. In order to mount the damper on it, a special tooling had to be developed. Once mounted, the damper went through two types of tests:

- Sets of different strokes at fixed frequencies.
- Sets of different frequencies at fixed strokes.

In order to obtain the curve of the damper, some tests were carried out and later analyzed and postprocessed with the software testcenter, which also allows the handling of the machine. Figure 29 shows the set-up for the damper tests.

Figure 29: Damper test set-up

The maximum stroke of the damper was 152mm. From The tests shown in the following table were performed:

Fixed frequency		Fixed stroke	
Frequency [Hz]	Variable stroke [mm]	Stroke [mm]	Variable frequencies [Hz]
1	130, 110, 100, 70, 40, 10	140	0.5, 1, 2, 3, 4, 5
3	130, 110, 100, 70, 40, 10	70	1.5, 3, 4, 5, 6, 7, 8
7	130, 110, 100, 70, 40, 10	55	1.5, 3, 4.5, 6, 7.5, 9
10	30, 25, 20, 15, 10, 5	40	4, 6, 9, 11, 13, 15
15	20, 16, 12, 8, 6, 4	25	5, 8, 11, 14, 17, 20
20	15, 12, 9, 6, 4, 2	10	5, 9, 13, 16, 20, 25

Table 9: Damper tests frequencies and strokes

It must be noted that for frequencies above 10Hz, the maximum stroke delivered by the machine was limited and, therefore, the strokes had to be modified for different frequencies. With these analyses, different speed configurations were analyzed. Together with a quasi-static test to study the internal and gas resistances in the cylinder, it was possible to obtain the real curve of the damper. For each test, 5 cycles were performed in order to neglect the first and las cycles due to inertial singularities, and still have 3 other cycles to obtain a more realistic approximation.

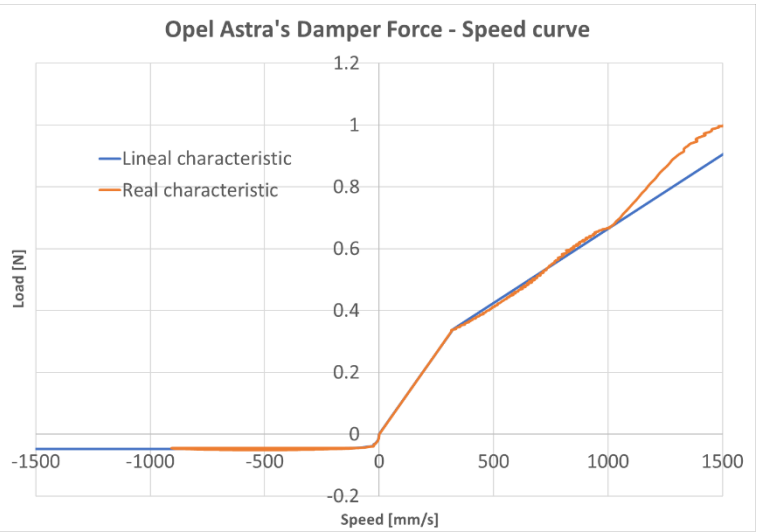

Figure 30: Opel Astra damper characteristic

Figure 30 shows the final curves obtained for the damper. The line in orange is the result obtained from the postprocessing. It can be seen clearly that it doesn't work at negative speeds (compression), where the only load present is the internal resistance of the contact surfaces and the inner gas. In extension (positive speeds), there are two differentiated areas with different damping coefficients. The blue curve is the linear approximation that was used in ADAMS/Car to avoid errors. It must be noted that the values in the Y axis are normalized for confidentiality reasons.

3.5.4. Bushing characteristics

The bushings are the topic of study in this thesis. To evaluate their impact, it is necessary to obtain their characteristic curves in order to be able to modify them later. There are three types of silentblocks in the Opel Astra: two in the front suspension, and one in the rear.

From this moment onwards, they will be referred to as front-front silentblock, rear-front silentblock, and rear silentblock, as shown in Figure 31.

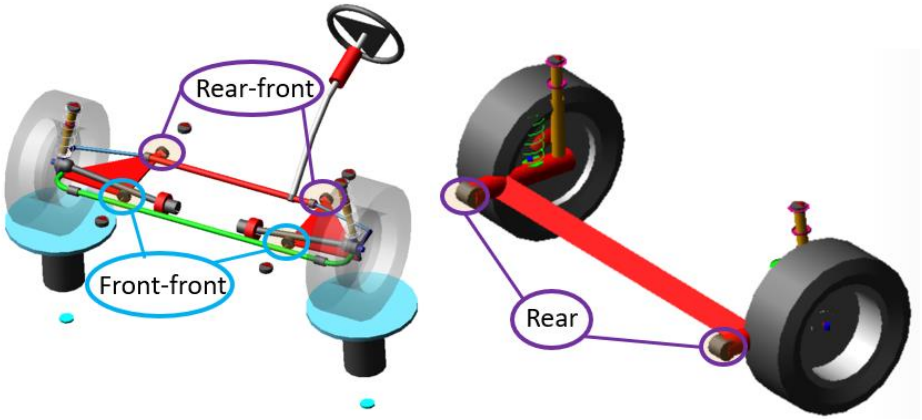

Figure 31: Opel Astra silentblock's names

As in was previously explained, these cylindrical silentblocks have 4 deformation modes. However, due to technical limitations, it was impossible to test them in the conical behavior. This case was, thus, approximated with default values.

All three silentblocks were tested in radial and axial tension, and in torsion. It is important that, even if the radial deformation mode is called radial in both X and Y directions (Figure 19), the rigidities of each bushing in both of the directions do not have to be equal. In fact, in the rear silentblocks, it was seen that the rigidity was greater in one of them, as it will be shown later.

Figure 32: Opel Astra real silentblocks

The three silentblocks analyzed can be seen in Figure 32 From left to right: Rear, front-front, and rear-front silentblocks. For the torsional test, the outer skin of the silentblock was fixed, and a torsional torque was applied. The deformation angle was then measured.

From the angle and the applied torque, the characteristics curve for the torsional stiffness were obtained. The real behavior has a hysteresis effect. However, due to software limitations, only the ideal curve could be implemented in ADAMS/Car. Figure 34 shows the disposition used for the torsional test. The torque wrench was attached to the inner layer of the bushing. The vertical displacement was measured in the ruler and later converted into degrees. Figure 33 shows the tooling used for the test. In black, the iron structure where the silentblocks were mounted; in red, the wrench.

The following parameters in the image were known:

$$a = 276mm$$

$$r = 45.5mm$$

$$l = 29mm$$

$$w = 28mm$$

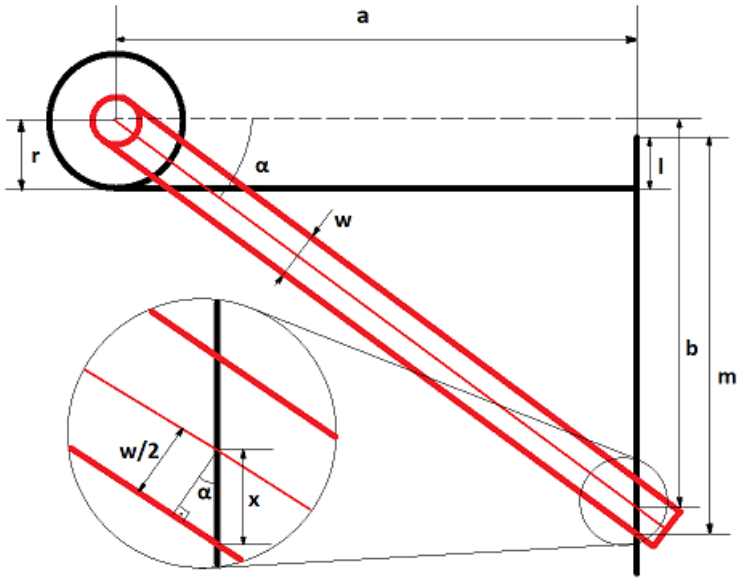

Figure 33: Torsional test tooling

From these parameters, the value of α as a function of the known parameters and m (measurement) was obtained:

$$\cos(\propto) = \frac{w/2}{x} \quad \rightarrow \quad x = \frac{w}{2 \cdot \cos(\propto)}$$

$$b = (r - l) + (m - x) = r - l + m - \frac{w}{2 \cdot \cos(\propto)}$$

$$tg(\propto) = \frac{b}{a} = \frac{r - l + m - \frac{w}{2 \cdot \cos(\propto)}}{a} \quad \rightarrow \quad a \cdot tg(\propto) + \frac{w}{2 \cdot \cos(\propto)} = r - l + m$$

$$\frac{2 \cdot a \cdot \sin(\propto) + w}{2 \cdot \cos(\propto)} = r - l + m \quad \rightarrow \quad a \cdot \sin(\propto) - (r - l + m) \cdot \cos(\propto) = -\frac{w}{2} \qquad (1)$$

If we consider the property of the cosine of the addition:

$$\mathrm{Q} \cdot \cos(n + m) = \mathrm{Q} \cdot \cos(n) \cdot \cos(m) - \mathrm{Q} \cdot \sin(n) \cdot \sin(m) \qquad (2)$$

Joining equivalent components from (1) and (2), we have that:

$$m = \propto$$

$$a = Q \cdot \sin(n)$$

$$r - l + m = -Q \cdot \cos(n)$$

Solving the equations, we obtain:

$$a^2 + (r - l + m)^2 = Q^2 \quad \rightarrow \quad Q = \sqrt{a^2 + (r - l + m)^2}$$

$$n = \arcsin\left(\frac{a}{Q}\right) \quad \rightarrow \quad n = \arcsin\left(\frac{a}{\sqrt{a^2 + (r - l + m)^2}}\right)$$

Joining this equivalences and equation (1), we can obtain the expression for ∝:

$$(r - l + m) \cdot \cos(\propto) - a \cdot \sin(\propto) = Q \cdot \cos(n + m) =$$

$$= \sqrt{a^2 + (r - l + m)^2} \cdot \cos\left(\propto + arcsin\left(\frac{a}{\sqrt{a^2 + (r - l + m)^2}}\right)\right) = \frac{w}{2}$$

$$\propto = arccos\left(\frac{w}{2 \cdot \sqrt{a^2 + (r - l + m)^2}}\right) - arcsin\left(\frac{a}{\sqrt{a^2 + (r - l + m)^2}}\right)$$

Figure 34: Torsional test disposition

After this test, the radial and axial rigidities were measured. For this means, a compression machine was used, positioning the bushings in different positions for the axial, radial x, and radial y deformations tests. The disposition for these tests can be seen in Figure 35. As happened with the torsional response, the silentblocks present a hysteresis effect, that had to be neglected afterwards due to software limitations.

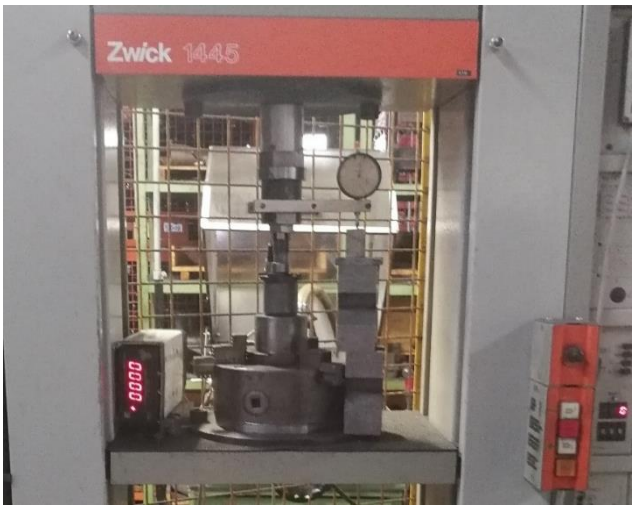

Figure 35: Axial and Radial tests disposition

Figure 36 to Figure 38 show the characteristics of the tested silentblocks. Note that the values have been normalized, and the hysteresis effect neglected for simplification

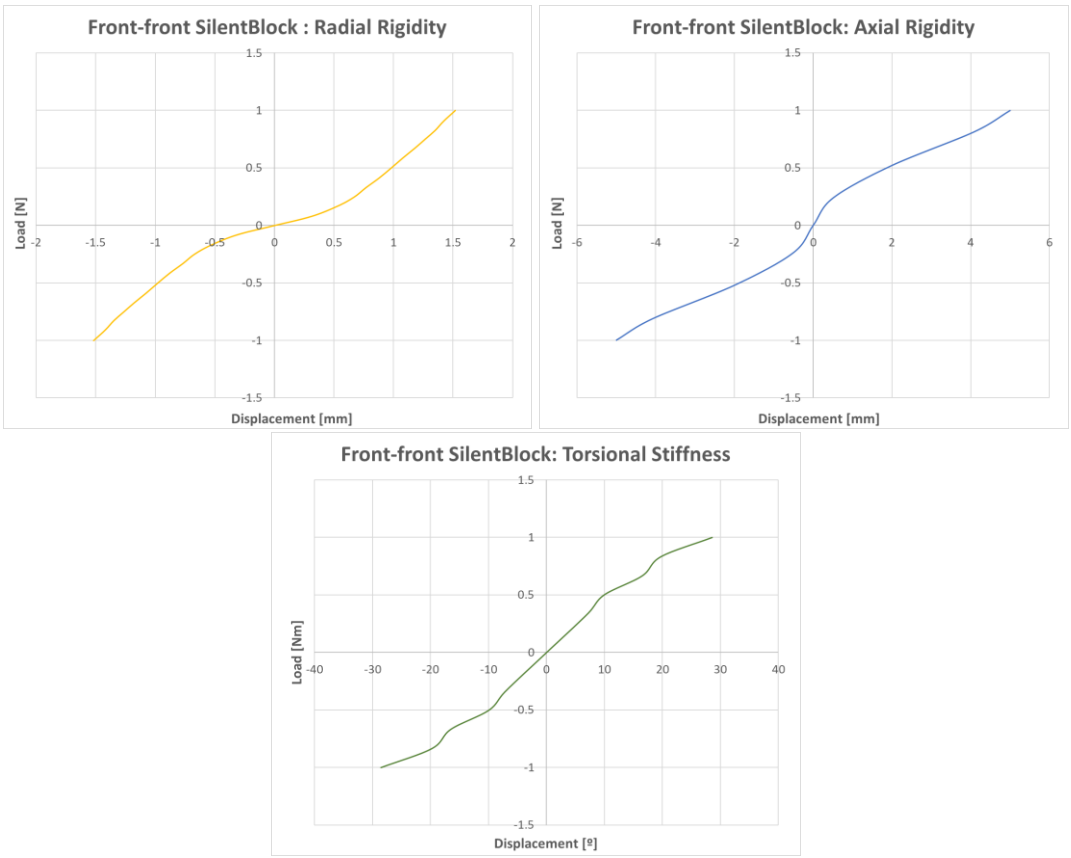

Figure 36: Front-front silentblock characteristics

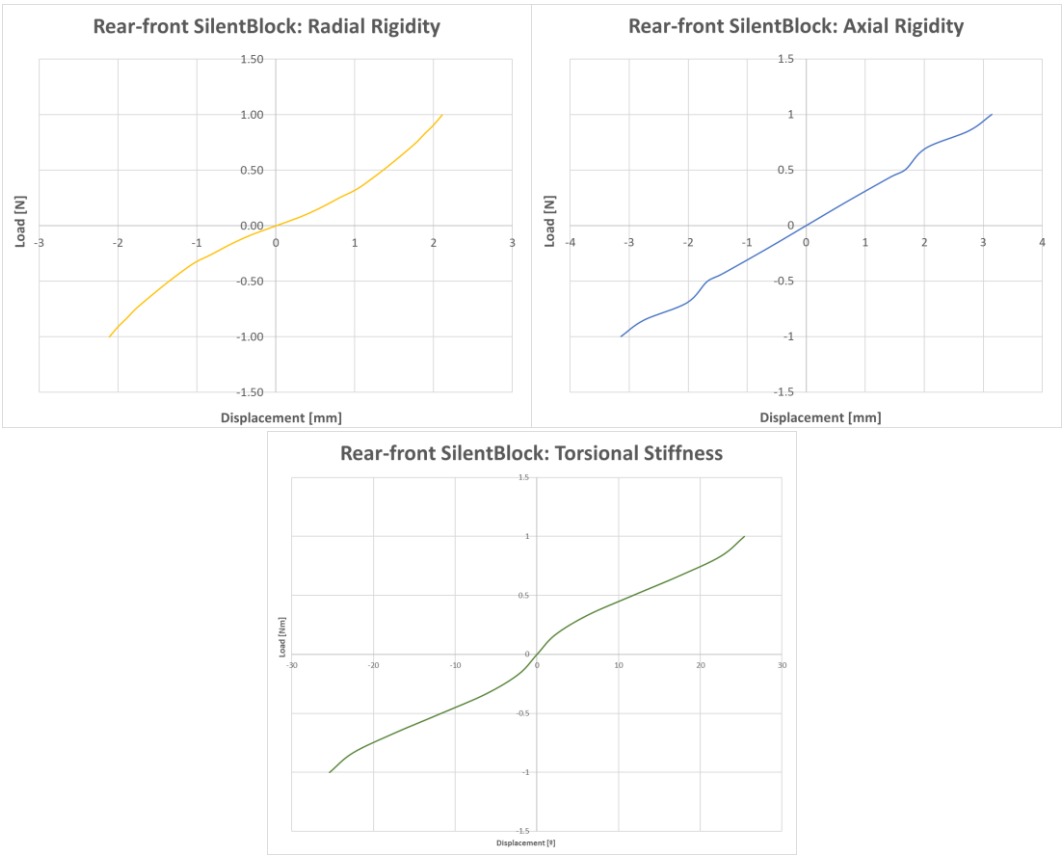

Figure 37: Rear-front silentblock characteristics

The two radial rigidities for both front silentblocks were equal, and thus, were simply named radial rigidity. However, this does not occur in the rear silentblock, where the difference was too big to be neglected and, therefore, the radial rigidities in the two directions. X (vertical) and Y (horizontal) were represented.

It is also important to note that the stiffness factor for the radial and axial directions were assumed to be 0.01, while it was set to zero for the torsional rotation.

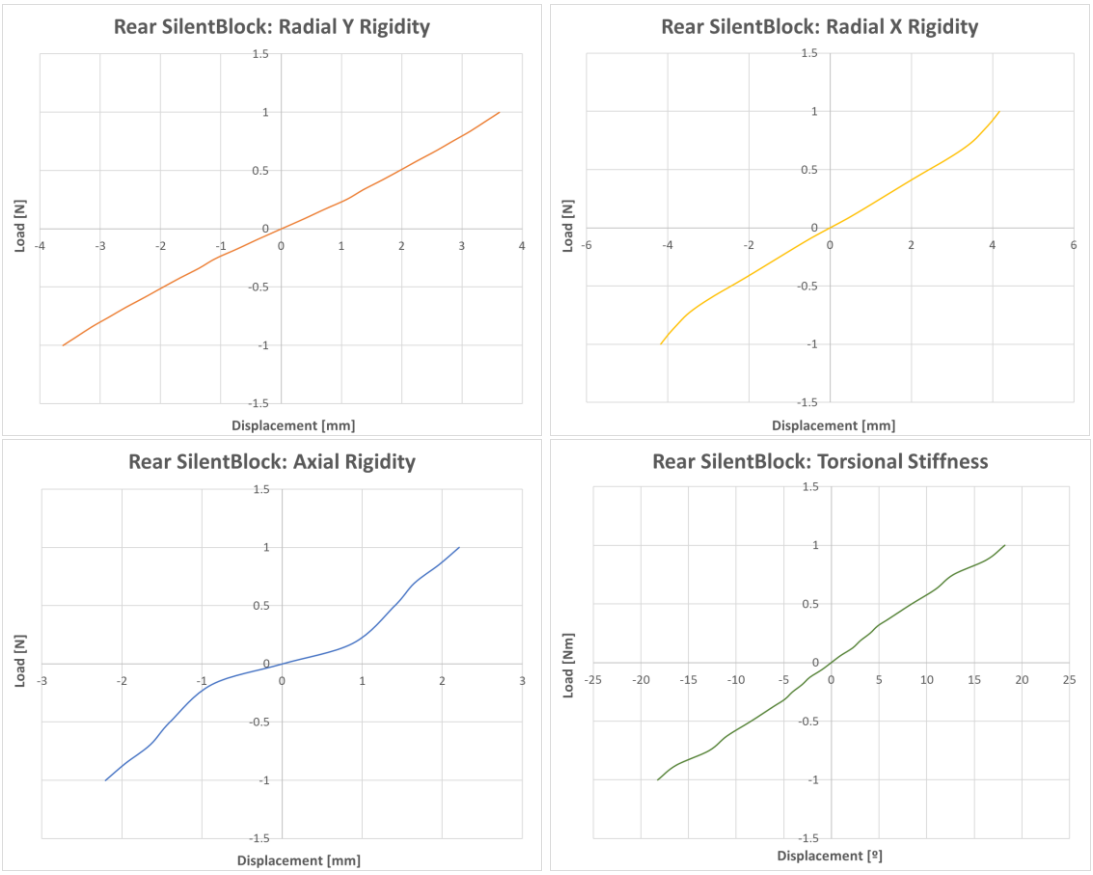

Figure 38: Rear silentblock characteristics

3.1. Full assembly

After obtaining all this data and inputting it into ADAMS/Car, the full model of the vehicle could be assembled. In order to join different subsystems in an assembly in ADAMS/Car, it is necessary to employ certain connection points that attach one component to the other. These points, called communicators, must have a coincident name, set as input/output, each in one of the two subsystems to join. The communicator with the output configuration will impose a certain motion to the input communicator. This motion is dependent on the degree of freedom restricted. This degree of freedom can go from a single one (Ex: the rotation of the transmission shafts) to six degrees of freedom (Ex: engine attachment to the front/rear suspension frames).

After setting all these communicators, the full assembly for the Opel Astra Caravan 1999 was created. This assembly can be seen in Figure 39.

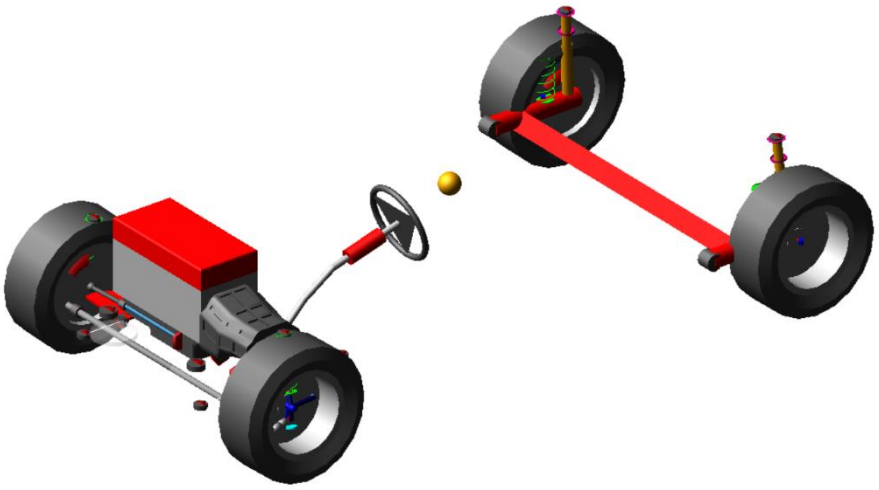

Figure 39: Opel Astra Caravan 1999 assembly

4. Driving conditions simulations

For the evaluation of the effect of the silentblocks characteristics in the dynamic behavior of the vehicle, two different types of tests were carried out. Since many simulations were done, this chapter serves as an introduction to present these tests, the geometries of the roads and the inputs, in order to avoid repetitions in following chapters.

4.1. Vehicle riding over bumps

The first test type is a scenario where the vehicle rides, at constant speed over a succession of ten bumps set alternatively to the left and to the right to produce a rolling effect in the vehicle. The geometry of the road is now explained.

The road is 200m long, and it has a sequence of ten bumps, five in each side of the road (left and right), set alternatively. The following image, from [6] shows the general geometry of the bumps:

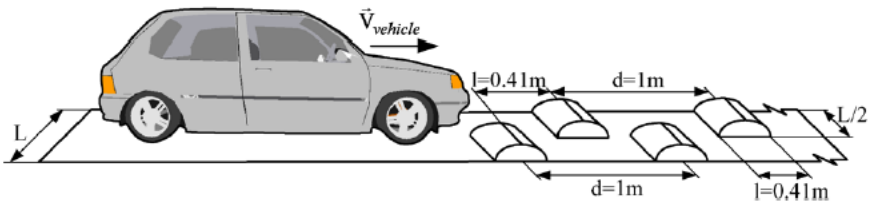

Figure 40: Bumped road geometry

The road has a width of 3 meters, and the bumps, as of Figure 40, are 1.5 meters wide. They are 0.1 meters high and have a sinusoidal shape with a period of 0.82. Therefore, the length of the bumps is 0.41m, the same as the distance from one bump to the one in the other side. Finally, the distance between two bumps in the same roadside is of 1m.

This type of analysis is made at constant speed. They were carried out at three different speeds: 60, 90 and 120km/h. The duration of the analyses is 6 seconds, the time needed for the car to travel the full length of the road at 120km/h.

4.2. Single lane change

The second analysis type developed is a single lane change. Since the response is symmetrical under a lane change of different direction, it was decided to do a lane change turning the vehicle to the right (Figure 41).

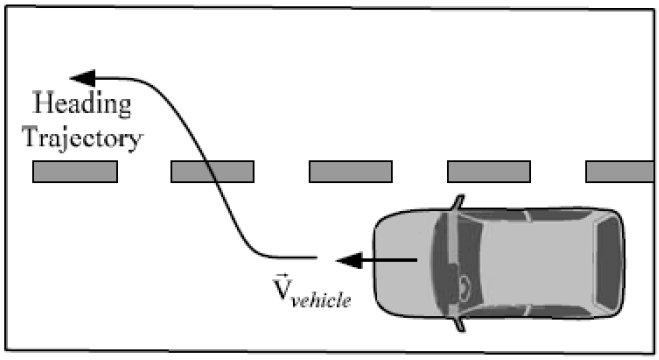

Figure 41: Single lane change maneuver
Image from [6]

Through this maneuver, the lateral stability and acceleration on the body of the vehicle will be evaluated. Evidently, aside from being wide enough to perform a lane change maneuver, the geometry of the road, in this case, is not so important.

As in the previous test, this driving condition was evaluated at three different speeds: 60, 90 and 120km/h. The desired response of the vehicle is a lateral displacement of 3.5m over 3 seconds. In order to obtain this response, the input in the vehicle was a sinusoidal steering angle with a period of three seconds, and a certain amplitude. This amplitude was obtained through iteration until the desired lateral displacement was obtained for each different velocity for the reference values of the silentblock rigidities (the real values in Figure 36 to Figure 38.

The steering inputs for the lane change maneuver at each speed are shown in the following graph:

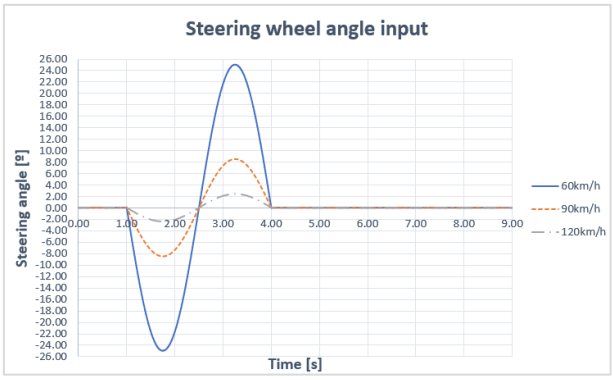

Figure 42: Single lane change steering angle input

5. Model validation

After building the full model of the vehicle, the first step is to validate said model. To do this, some analyses will be carried out to analyze the overall behavior of the car and compare it to other studies. The analyses taken as reference are the results from [2] and [6].

5.1. Validation model

There are several differences between our vehicle and the one used by J. Ambrósio and P. Verissimo in their study. For this reason, a second car model was built in ADAMS/Car. Most of the model is equal to the Opel Astra model, only some parameters were modified. The considerations made for this model will be explained in this chapter.

The geometry and mass distribution of the assembly was kept equal to that of the Opel Astra, since it is the object of study.

However, the properties of the dampers and springs were modified. This modification was done so that the suspension itself was much more rigid, and with a more predictable behavior, so that it was easier to understand the effect of the bushing characteristics. For this reason, the damper was considered as lineal. The rigidities and damping coefficients can be seen in the following table:

Component	Property	Units	Value
Front spring	Rigidity	N/m	59190
Rear spring	Rigidity	N/m	59190 *
Front damper	Damping coefficient	N·s/m	7917
Rear damper	Damping coefficient	N·s/m	7917 *

Table 10: Validation model parameters

For this validation, a comparison between the response with real bushings and the response with ideal bushings (rigid joint) will be done. However, the bushing characteristics in [2] and [6] are completely different to the ones tested, being, in their case, the rear bushings more rigid than the front ones. For this reason, another set of bushing properties was created, where the rigidity of the rear silentblocks in the radial and axial direction was multiplied by a factor of 4.

* The rear spring and dampers could only be set vertically due to software limitations. For this reason, their parameters were approximated to those of the front suspension.

5.2. Dynamic response validation

The analyses explained in chapter 4 will be done for the validation model with three different silenblock configurations:

- Real bushing characteristics
- Increased rigidity in the rear bushings.
- Ideal joint: fully rigid bushings.

In this chapter, the response of the vehicle in these three configurations will be shown, analyzed, and compared with the results in [2] and [6].

5.2.1. Vehicle riding over bumps

The behavior of the validation model riding over the et of bumps described in chapter 4 at 60, 90 and 120 km/h is now presented

5.2.1.1. Vertical displacement

The vehicle starts moving from a static condition. Once it hits the first bump, the body of the car should have a positive vertical displacement and, after some time, stabilize at the initial height. Figure 43 to Figure 45 show the output of the analyses.

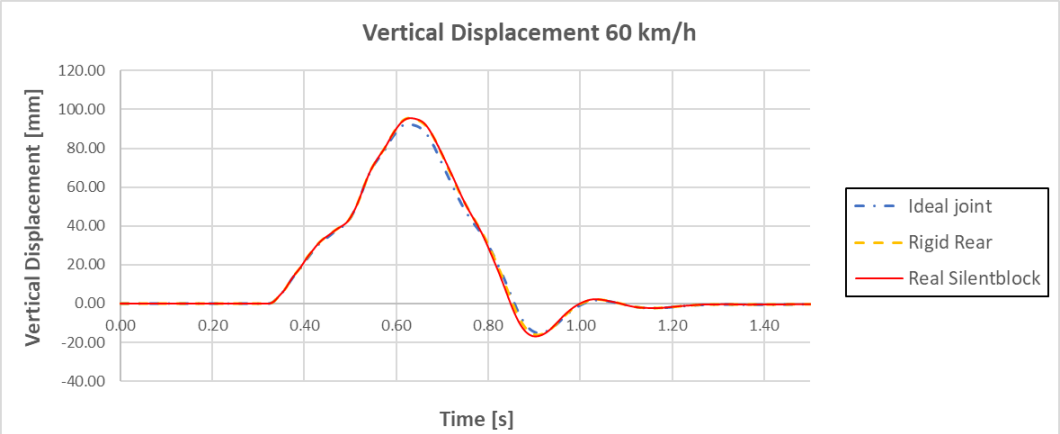

Figure 43: Validation model vertical displacement. 60km/h

It can be seen that the vehicle behaves as expected. The point in the timeline when the vertical displacement starts to increase is reduced in each graph due to the increase in speed.

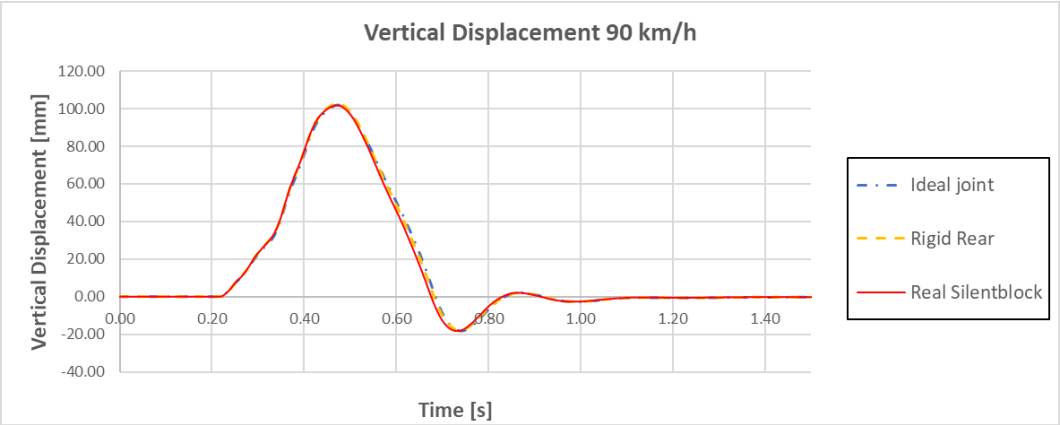

Figure 44: Validation model vertical displacement. 90km/h

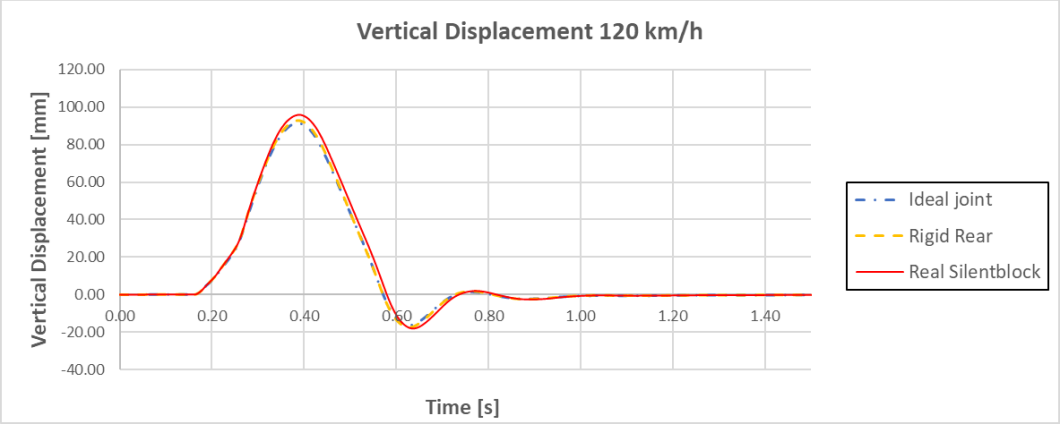

Figure 45: Validation model vertical displacement. 120km/h

If we compare these results to those in [6], shown in Figure 46 we see that, with the exception of the initial seconds where in their case there is a drop in height due to the vehicle not departing from the resting height, the overall behavior of the car is similar.

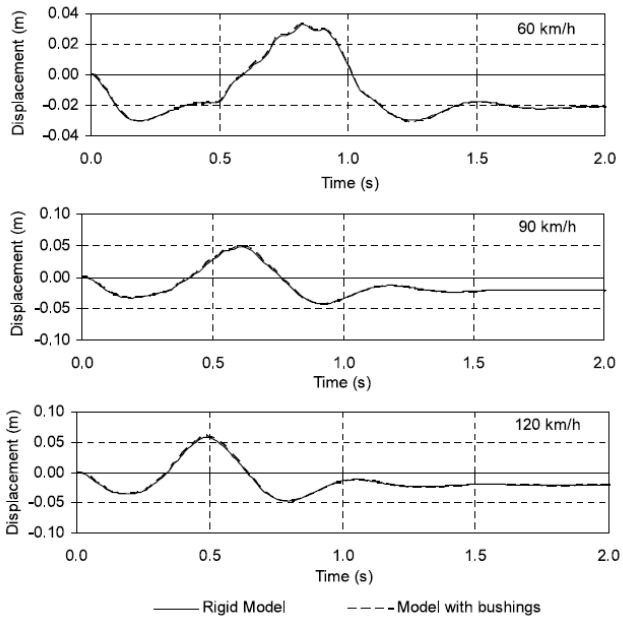

Figure 46: Reference vertical displacement from [6]

The absolute values of the output are not equal since the vehicle geometry and masses are different. It is noticeable that, in both cases, the ideal joint produces a slightly lower maximum vertical displacement under the same perturbation.

5.2.1.2. Vertical acceleration

The vertical acceleration was not analyzed in [6]. However, it is considered relevant and thus, in will also be studied for the model validation

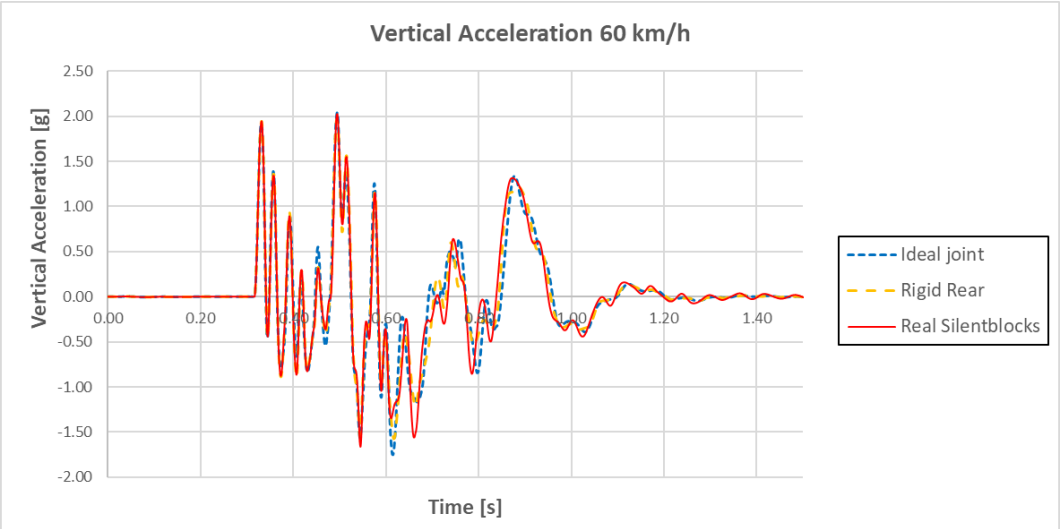

Figure 47: Validation model vertical acceleration. 60km/h

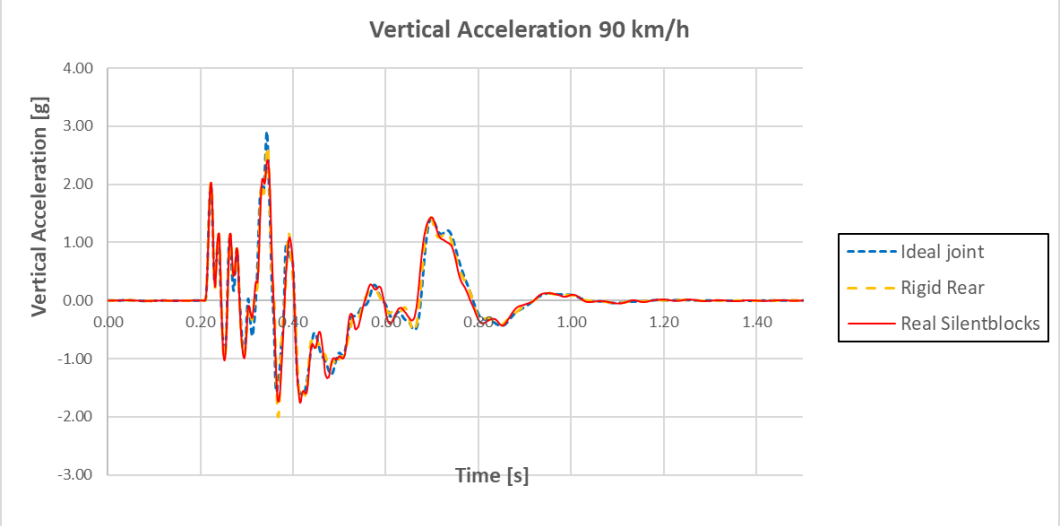

Figure 48: Validation model vertical acceleration. 90km/h

As happened before, the first contact time varies from graph to graph due to the change in speed. The highest peak of the vertical acceleration for real silentblocks increases with speed as expected. It is noticeable that overall, the vertical acceleration is the same in all three configurations. The biggest difference is in areas of low acceleration peaks. The reason for this is that the silentblocks mitigate low amplitude vibrations by absorbing them in the elastic

material. Therefore, when the acceleration is low, the peaks are mitigated with non-ideal joints.

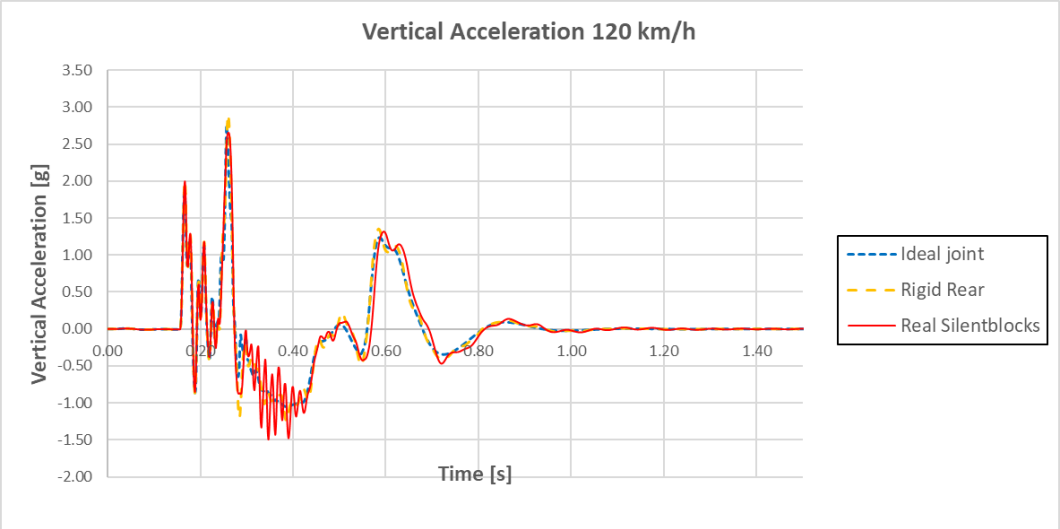

Figure 49: Validation model vertical acceleration. 120km/h

5.2.1.3. Roll acceleration

Due to the bumps being placed alternatively, a rolling motion is produced in the cabin of the vehicle. This motion will be now analyzed by means of the roll acceleration of the CoG of the vehicle.

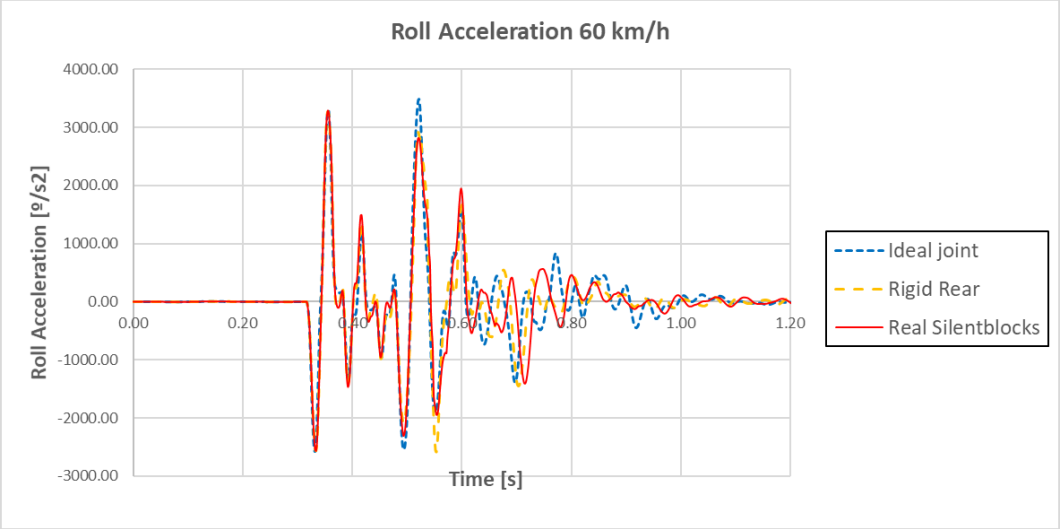

Figure 50: Validation model roll acceleration. 60km/h

In line with what happened with the vertical acceleration, it is expected that the low value peaks of acceleration are mitigated with elastic joints. This effect can be clearly seen in Figure 50 to Figure 52, where with the exception of the first and fastest peaks, the rest are all mitigated.

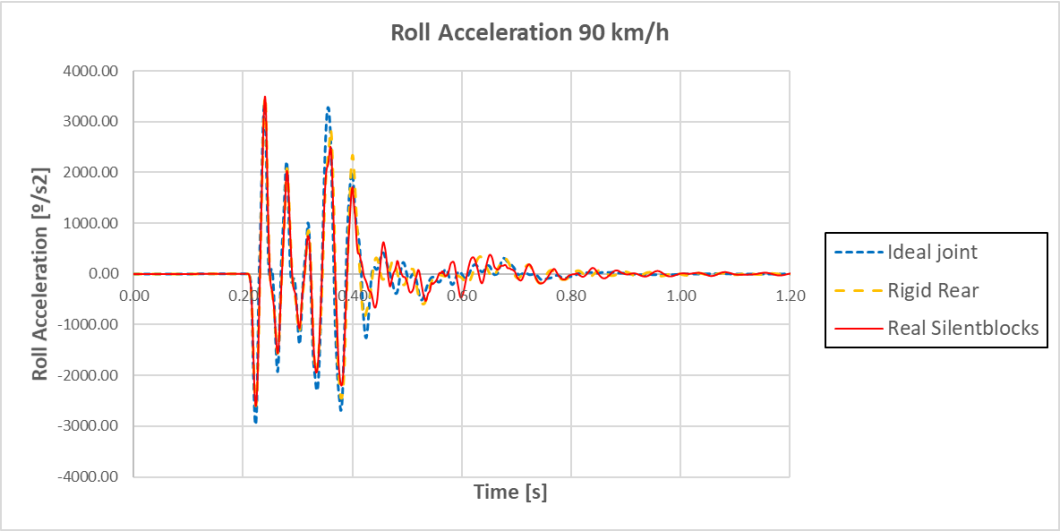

Figure 51: Validation model roll acceleration. 90km/h

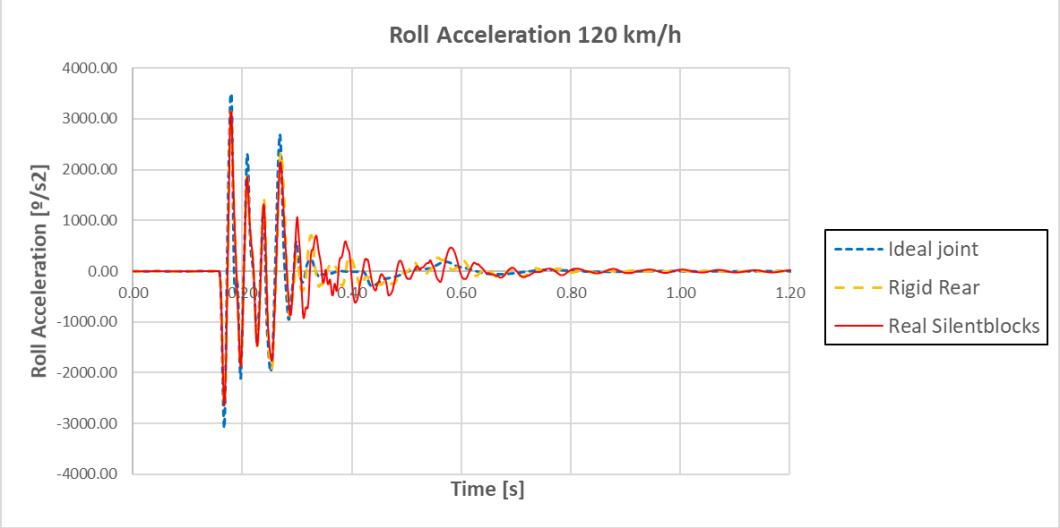

Figure 52: Validation model roll acceleration. 120km/h

Comparing these results to those in [6] (Figure 53), many similarities in the shape of the acceleration can be seen:

- The rolling motion fluctuates from one side to the other, being more or less symmetrical.
- Ideal joints produce slightly higher acceleration values.
- After a certain point, the different acceleration peaks are faster (higher frequency) with ideal joints, producing a misalignment between the different curves.

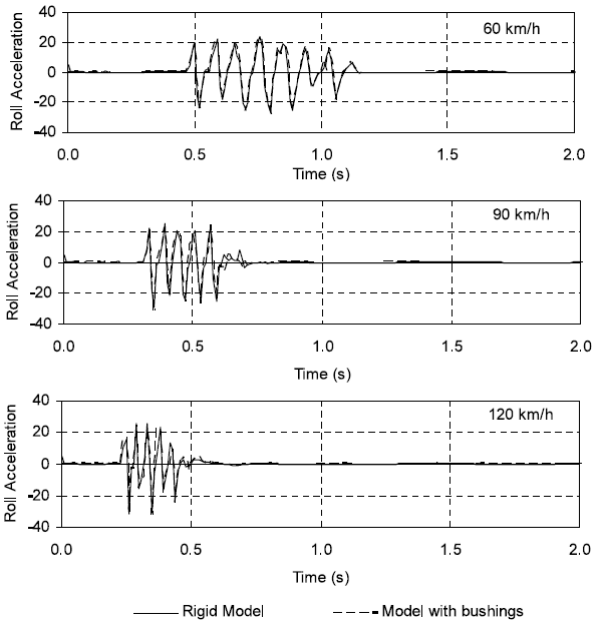

Figure 53: Reference roll acceleration from [6]

As in previous cases, the actual acceleration values are not comparable since the specifications of the two vehicles are different.

5.2.2. Single lane change

In this chapter, the lateral response of the vehicle in a lane change maneuver will be presented. The maneuver will be performed at 60, 90 and 120km/h. The input for these speeds was show in Figure 42.

5.2.2.1. Lateral displacement

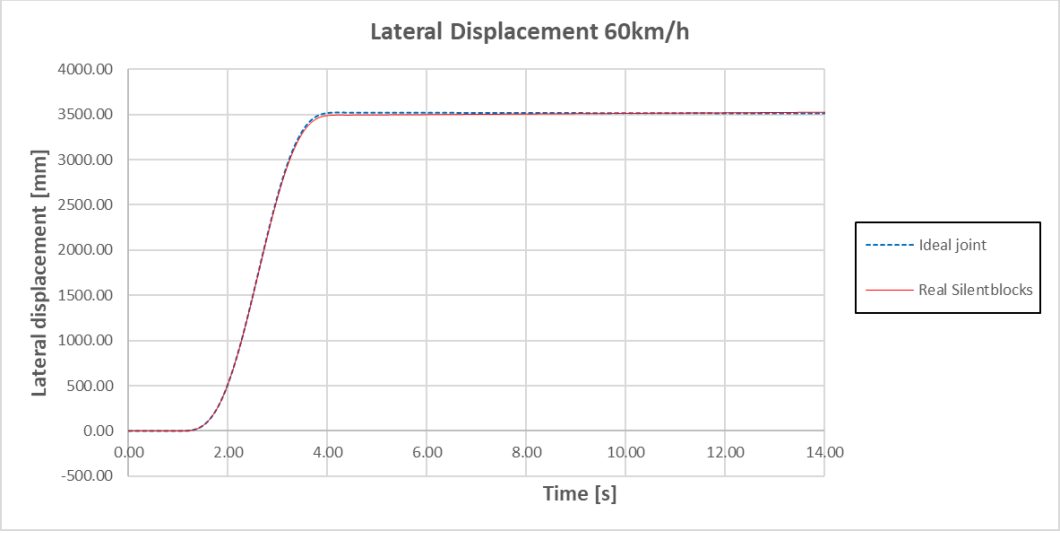

Figure 54: Validation model lateral displacement. 60km/h

The first variable to be analyzed in this driving condition is the lateral displacement. The analysis was design to, ideally, produce a 3.5m displacement over three seconds. Therefore, this trajectory is expected in the ideal situation, and a more unstable behavior with the rubber bushings. In Figure 54 to Figure 56 the results obtained for these tests at the three different speeds are shown.

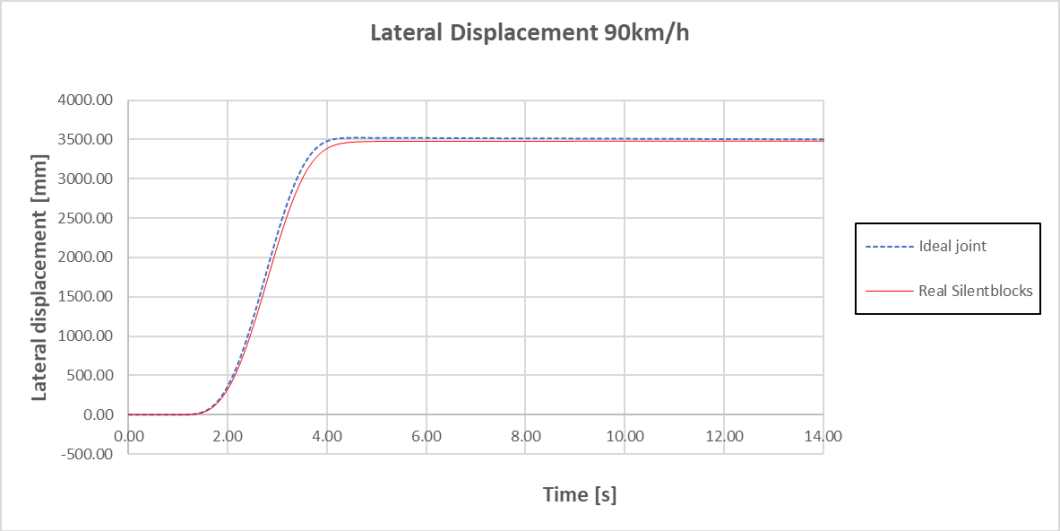

Figure 55: Validation model lateral displacement. 90km/h

At lower speeds the differences are less noticeable. However, if we take a look at the graph of 90 and 120km/h it is clear that in the situation with real bushings, the vehicle need more time to perform the maneuver, and the final trajectory is not the expected one, but the direction of the vehicle does not end up in a straight line. This means that, with softer silentblocks, the vehicle becomes more unstable laterally.

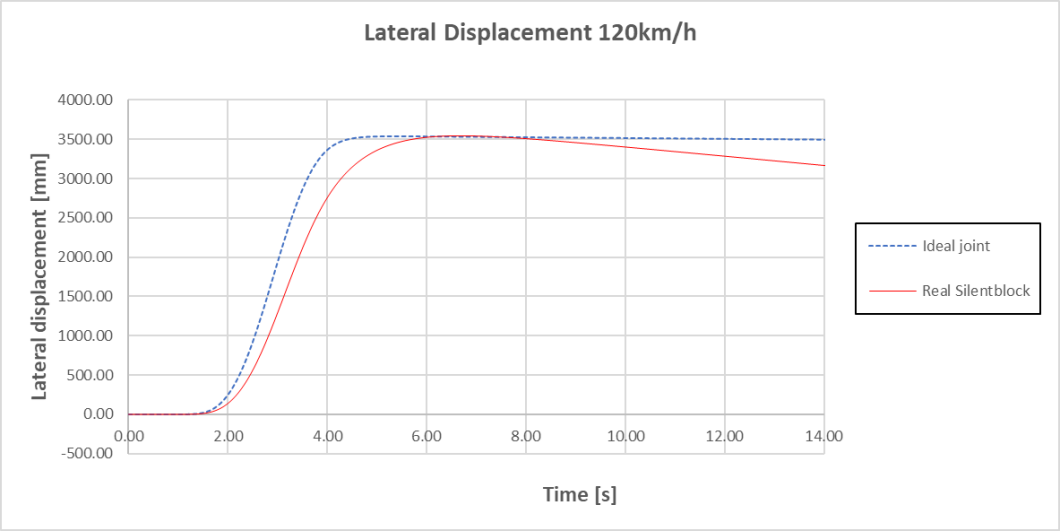

Figure 56: Validation model lateral displacement. 120km/h

Taking a look at the results obtained in [6], shown in Figure 57, we see that even if with a more marked tendency, this same effect of the elastic silentblock is clearly seen. The trajectory of the real vehicle becomes more unstable that in the ideal scenario.

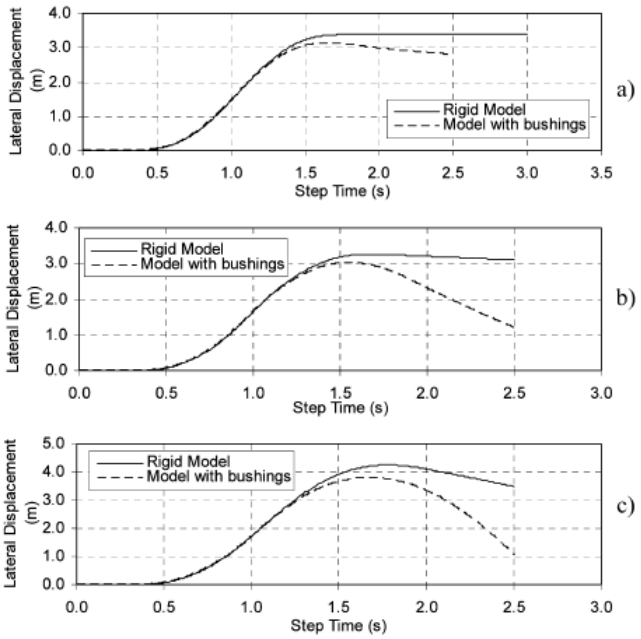

Figure 57: Reference lateral displacement from [6]

5.2.2.2. Lateral acceleration

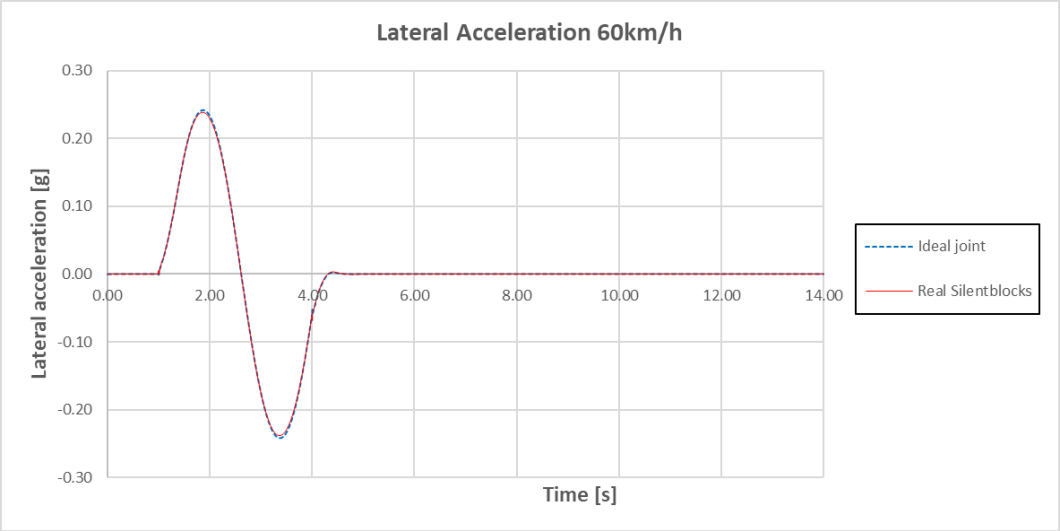

Figure 58: Validation model lateral acceleration. 60km/h

Lateral acceleration is directly related to the lateral displacement. Therefore, the expected output should be in line with what was explained in that situation. Analyzing Figure 58 to Figure 60, we see that this is, indeed, the case, as the acceleration is decreased and delayed in time with respect to the ideal situation. The difference seen between the positive and negative acceleration in the real case is what makes the final trajectory not to be the desired one.

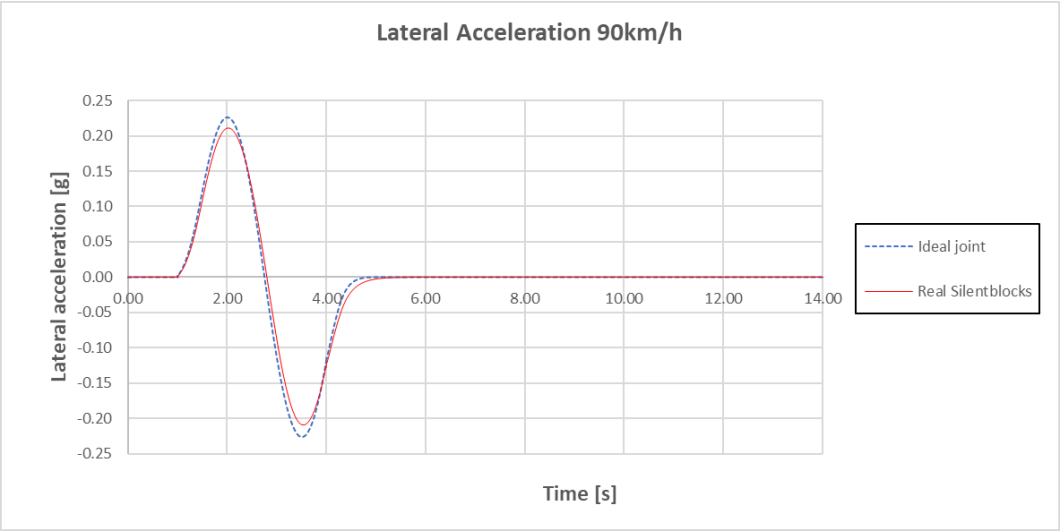

Figure 59: Validation model lateral acceleration. 90km/h

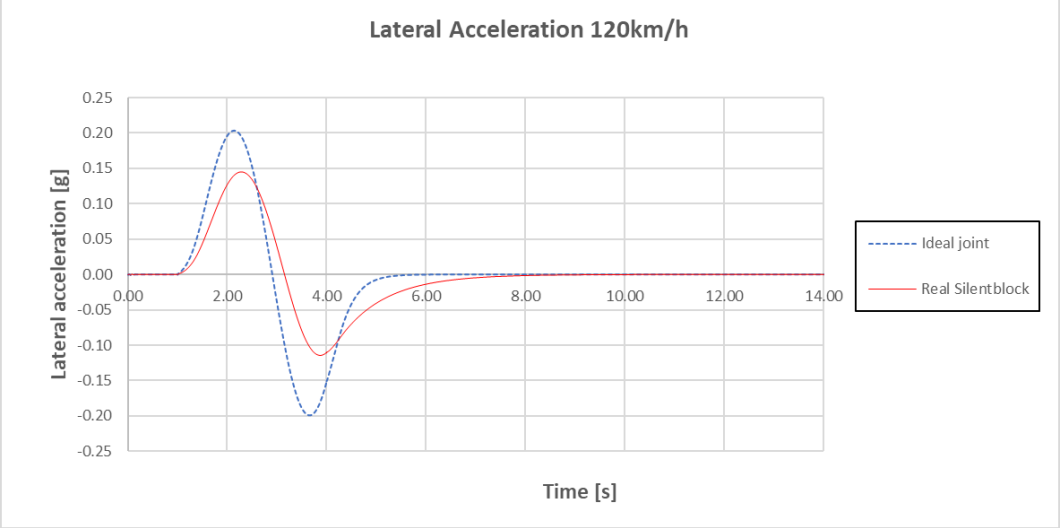

Figure 60: Validation model lateral acceleration. 120km/h

In Figure 61 we see that, the reference results from [6] show the same delay in the real accelerations, increasing the instability in that case.

The difference in the shape of the acceleration, and also of the bigger directional instability in their tests is due the difference in the input between the analyses in that work and in this one.

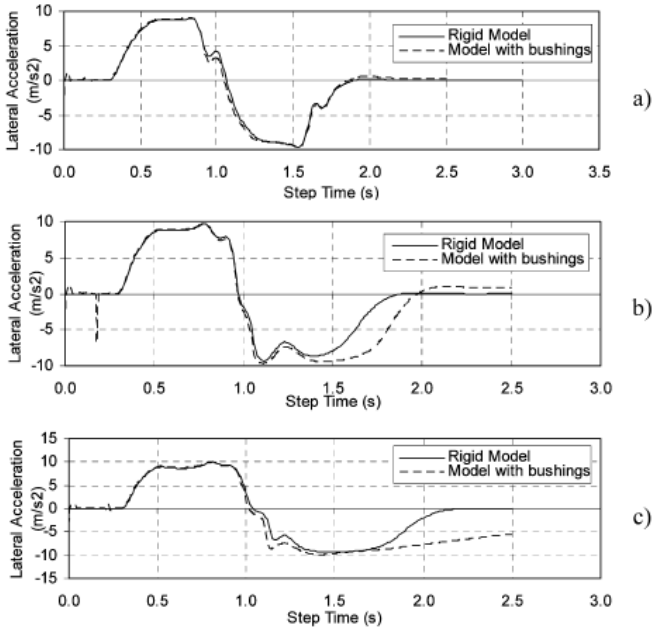

Figure 61: Reference lateral displacement from [6]

From all these analyses, it can be seen that, even if the actual values and the inputs in the lane change maneuver are a bit difference, the general response of the vehicles under the same driving situations are equivalent. Therefore, the vehicle behaves as expected.

5.3. Sensitivity validation

A sensitivity analysis is used to understand the influence of a variation of certain parameters on the global performance of the full system. There are several ways to perform sensitivity analyses. In this work, it is going to be used the finite difference method explained by Haftka, R. T., & Adelman, H. M. in [8].

The modified parameters of these sensitivity analyses are the different rigidities of the bushings. An increment of a 1% was applied to the different rigidities from the real values, taken as the reference for the analysis.

To obtain the sensitivity values, the difference between the response of the reference model, and the response of the model with the modified characteristic is divided by the variation of the parameter, 0.01 in this case.

For the validation of the sensitivity, two simplifications are made:

- The two front silentblocks are modified at the same time, so there is only difference between front and rear bushings.
- The two radial rigidities are modified together as one.

5.3.1. Vehicle riding over bumps

In this chapter, the sensitivity of the vertical displacement, and vertical and roll accelerations to the rigidities of the bushings is presented.

5.3.1.1. Vertical displacement

Figure 62 to Figure 64 show the sensitivity analysis results for the vertical displacement of the chassis at the three speeds of study: 60, 90 and 120km/h.

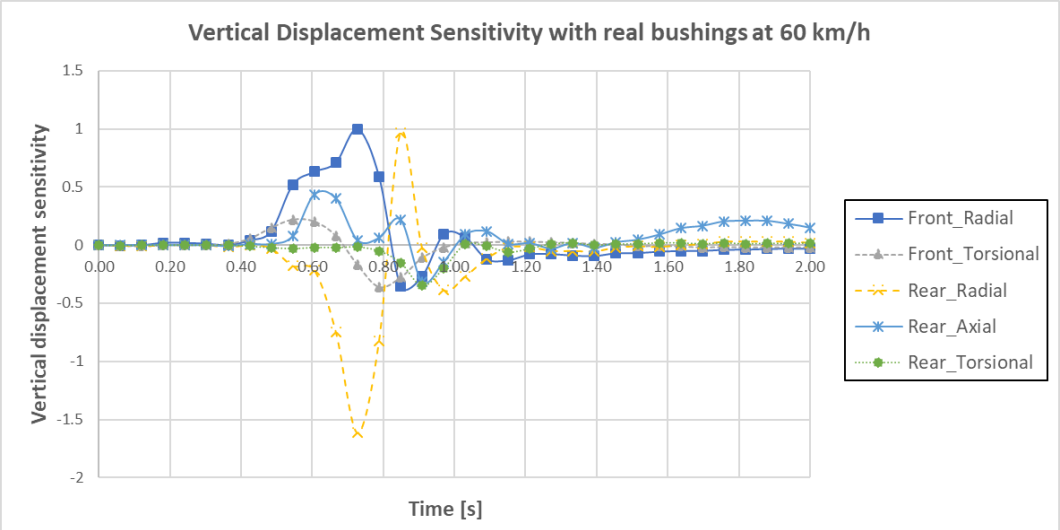

Figure 62: Validation model vertical displacement sensitivity. 60km/h

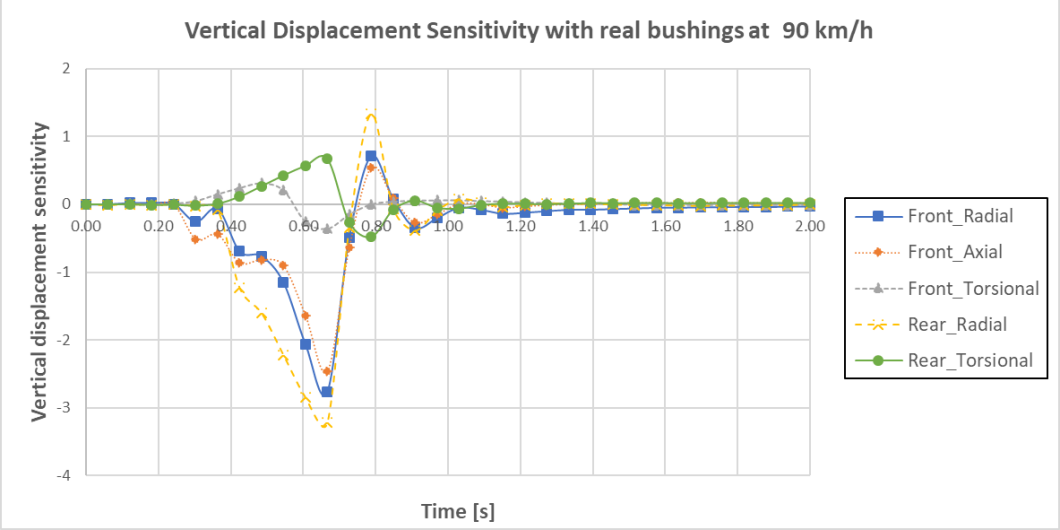

Figure 63: Validation model vertical displacement sensitivity. 90km/h

It can be seen from the graphs that the radial rigidity of both the front and rear bushings have the biggest impacts at lower speeds. However, at higher speeds the impact of the front suspension gains more importance. The torsional stiffness of the rear bushings also gains

impact with speed. It is also noticeable the impact of the axial component of the rear suspension. Due to the roll movement, increasing the lateral rigidity of the rear wheels does not permit the car to absorb these stresses, producing a destabilizing effect.

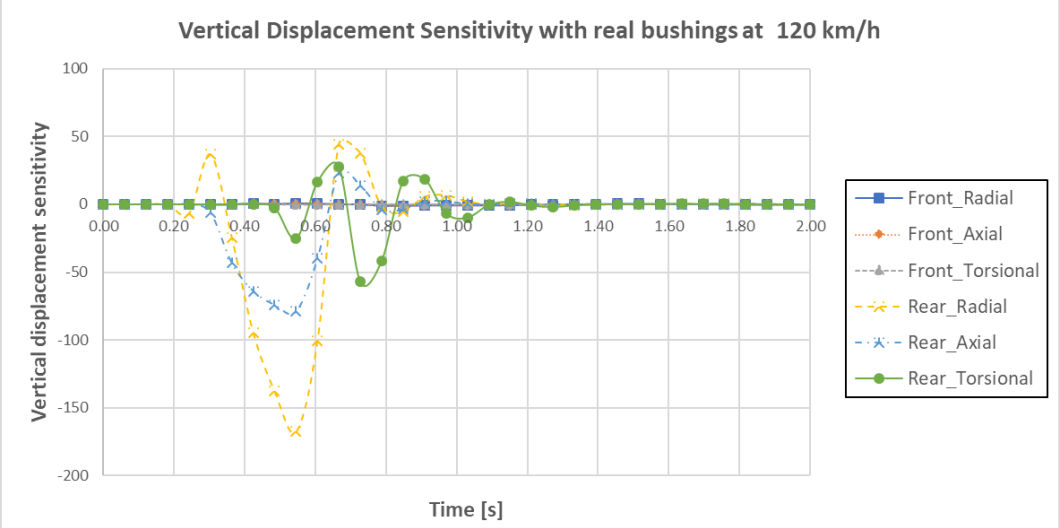

Figure 64: Validation model vertical displacement sensitivity. 120km/h

5.3.1.2. Vertical acceleration

Figure 65 to Figure 67 show the sensitivity analysis results for the vertical acceleration of the chassis at the three speeds of study: 60, 90 and 120km/h.

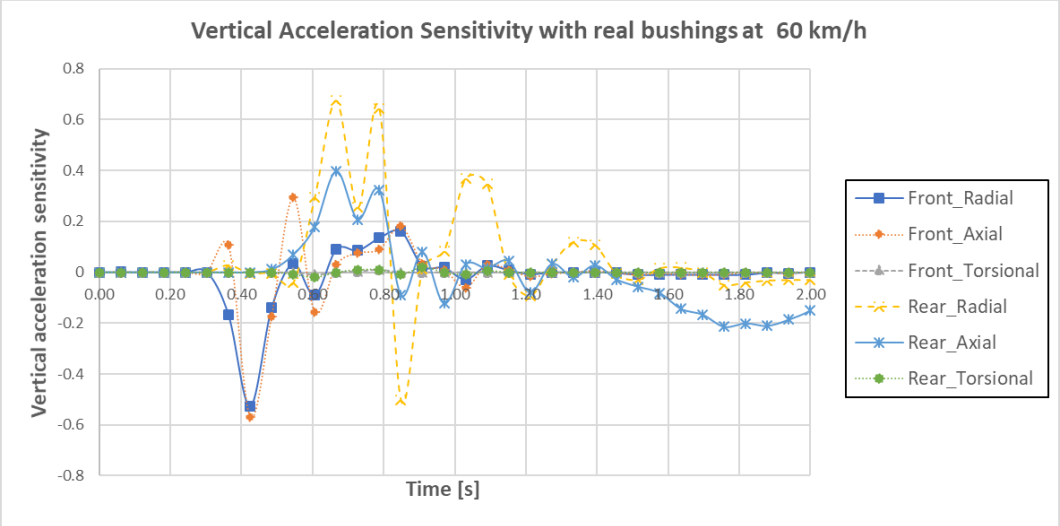

Figure 65: Validation model vertical acceleration sensitivity. 60km/h

In line with what was seen in the vertical displacement, the radial rigidity has the biggest influence in the accelerations. However, the axial rigidity of front silentblocks also has a similar effect in this case. At high speeds, the rear torsional components gain importance.

Finally, as expected from the previous chapter, the instability of the output with respect to the reference with an increase of the rear axial rigidity is noticeable.

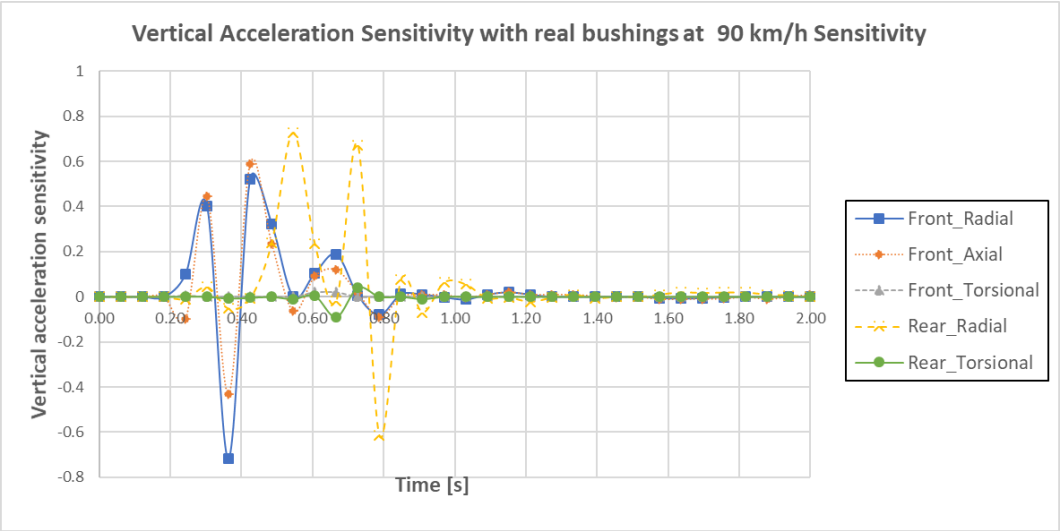

Figure 66: Validation model vertical acceleration sensitivity. 90km/h

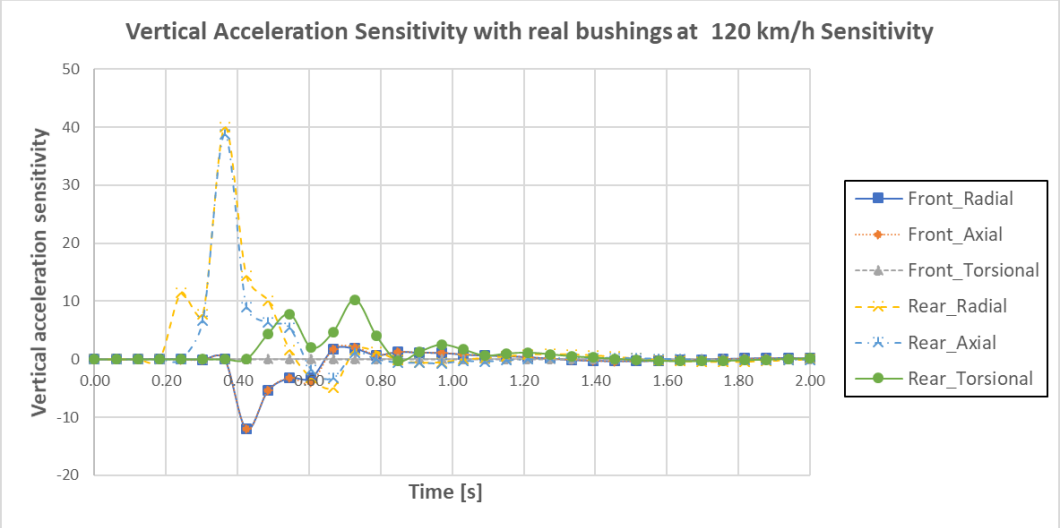

Figure 67: Validation model vertical acceleration sensitivity. 120km/h

5.3.1.3. Roll acceleration

Figure 68 to Figure 70 represent the sensitivity of the roll acceleration in the cabin of the validation model to a variation of a 1% in the different rigidities of the silentblocks at three different speeds: 60, 90 and 120km/h.

The effect of the radial component of the bushings is predominant at lower speeds, decreasing, specially the effect of the front bushings' radial stiffness at higher speeds, and increasing the impact of the torsional stiffness at the rear.

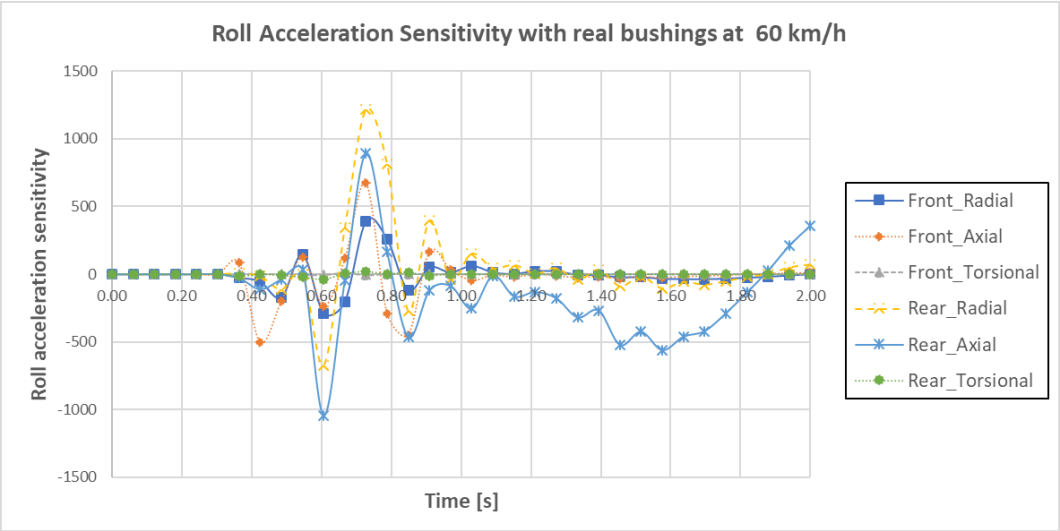

Figure 68: Validation model roll acceleration sensitivity. 60km/h

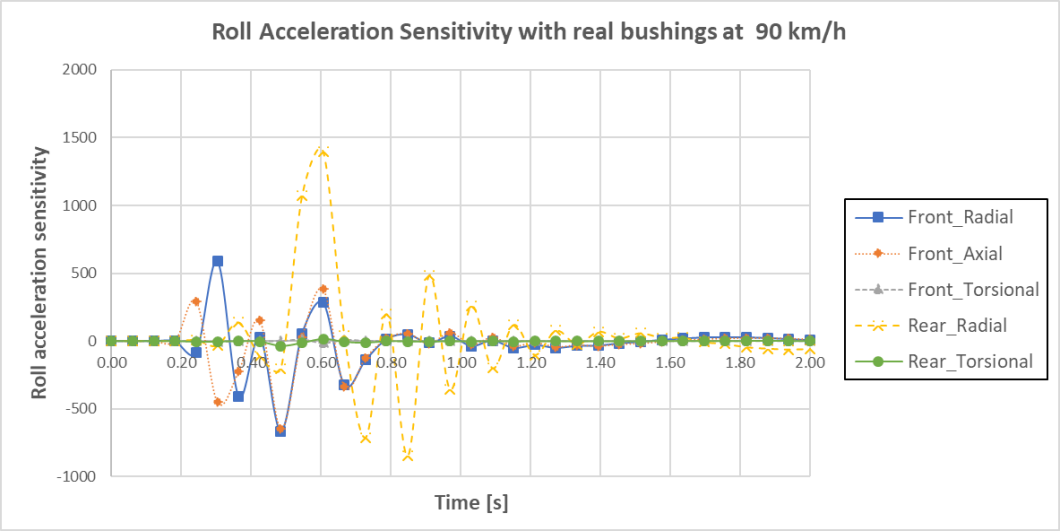

Figure 69: Validation model roll acceleration sensitivity. 90km/h

Once again, it is visible the destabilizing effect of the axial component of the rear suspension cylindrical bushings. This was to be expected considering that these results belong to the same analyses as the vertical displacement and acceleration.

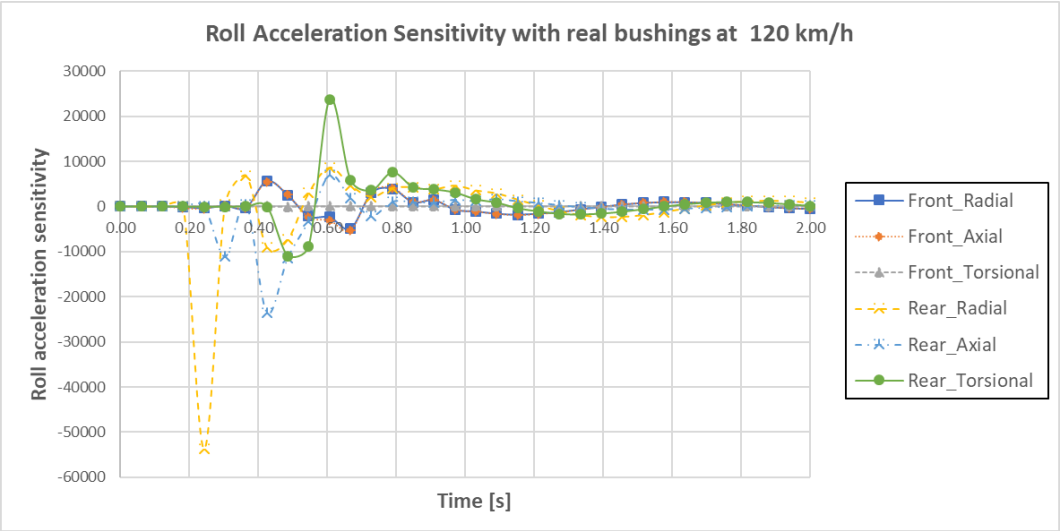

Figure 70: Validation model roll acceleration sensitivity. 120km/h

5.3.2. Single lane change

In this chapter, the sensitivity of the lateral displacement and acceleration to the rigidities of the bushings is presented.

5.3.2.1. Lateral displacement

Figure 71 to Figure 73 show the influence of the studied parameters in the lateral displacement of the vehicle after performing a lane change maneuver.

The sensitivity results in this situation are much clearer, since the same behavior is clearly seen at each of the three speeds.

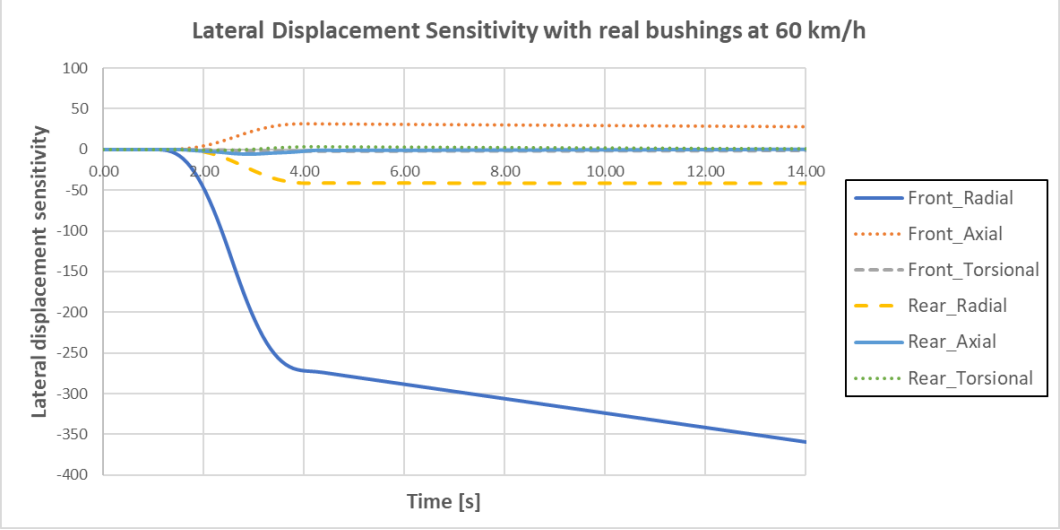

Figure 71: Validation model lateral displacement sensitivity. 60km/h

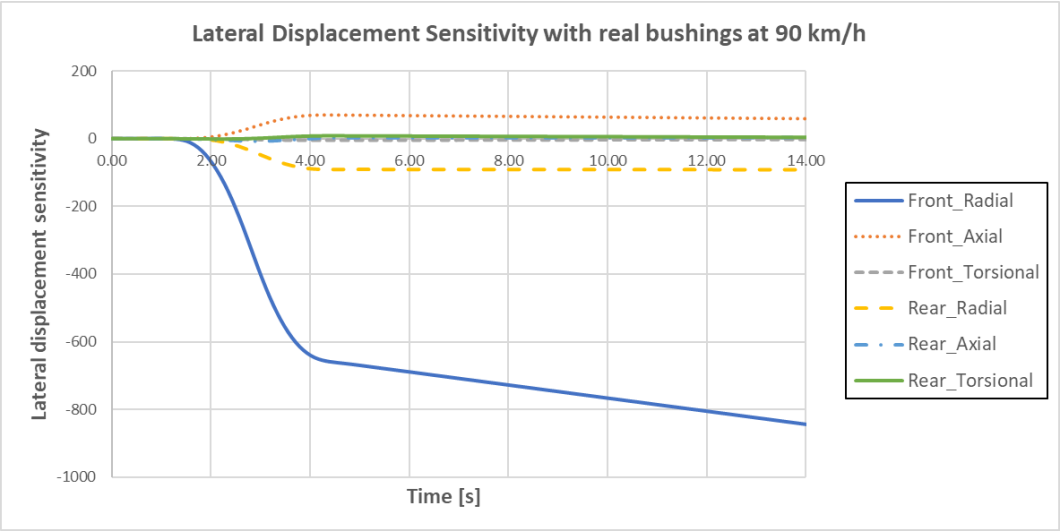

Figure 72: Validation model lateral displacement sensitivity. 90km/h

There is an evident and very important impact of the radial rigidity of the front bushings on the lateral displacement of the vehicle. An increase on this rigidity results in a smaller lateral step performed by the vehicle, and a more stable trajectory after the maneuver.

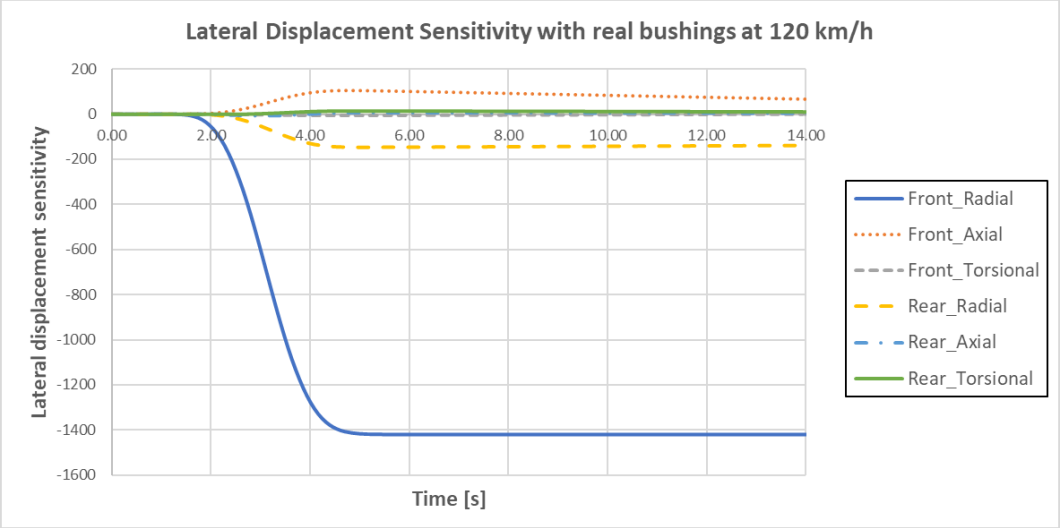

Figure 73: Validation model lateral displacement sensitivity. 120km/h

The other two parameters that also influence this lateral displacement are the real radial and the front axial rigidities. The first produces a similar effect as the front radial rigidity, but with a smaller impact. The later has the opposite effect: an increase in said parameter results in a larger lateral offset of the vehicle, but with a more stable trajectory. The rest of the parameters have a neglectable impact.

5.3.2.2. Lateral acceleration

Finally, Figure 74 to Figure 76 show the lateral accelerations observed in these simulations.

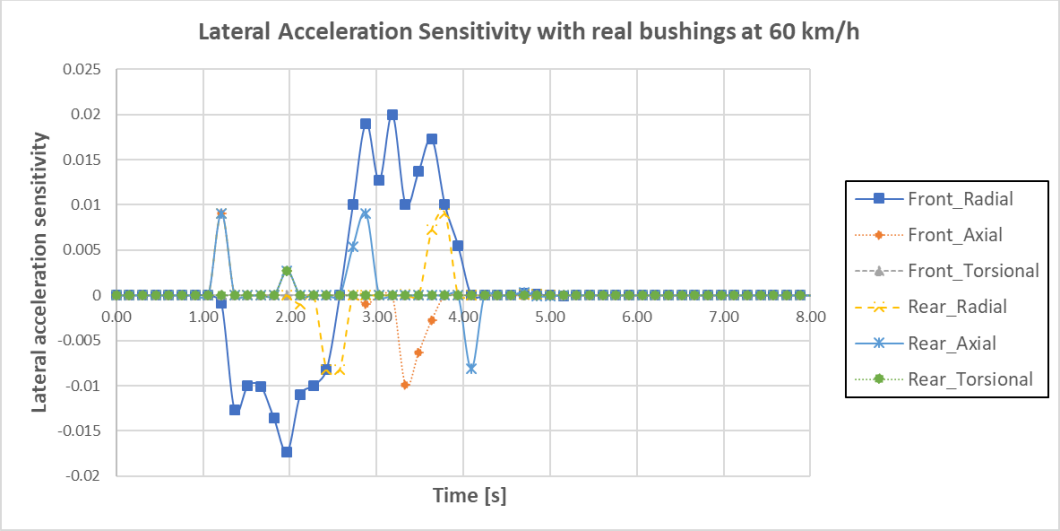

Figure 74: Validation model lateral acceleration sensitivity. 60km/h

These graphs are closely related to the lateral displacement. For this reason, the influencing variables are the same. It is seen a predominance of the effect of the front radial parameter over the rest, being also observable the impact of the front axial and rear radial rigidities.

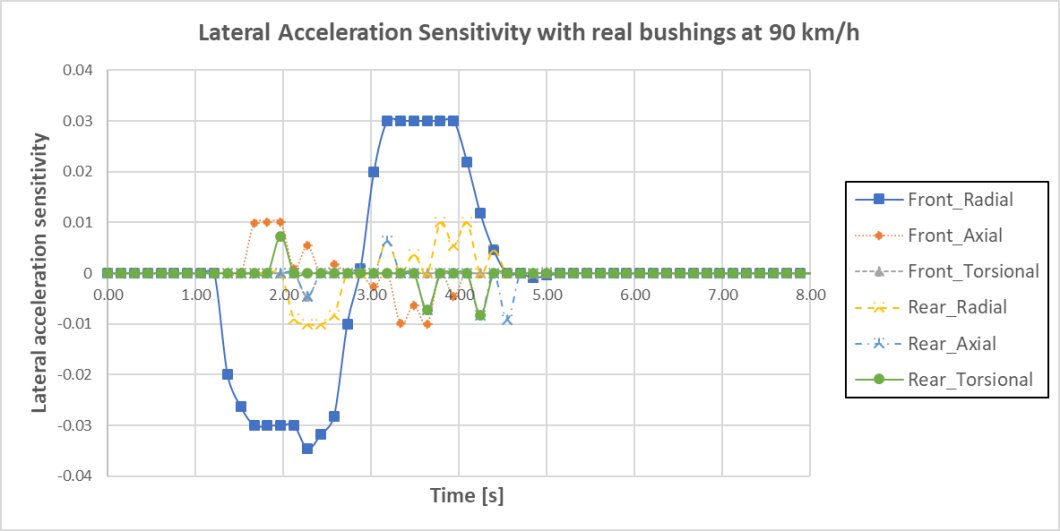

Figure 75: Validation model lateral acceleration sensitivity. 90km/h

It is, however, also visible a variation in the lateral acceleration after an increase in the rear axial rigidity. Nevertheless, it does not have an actual impact in the lateral displacement of the vehicle.

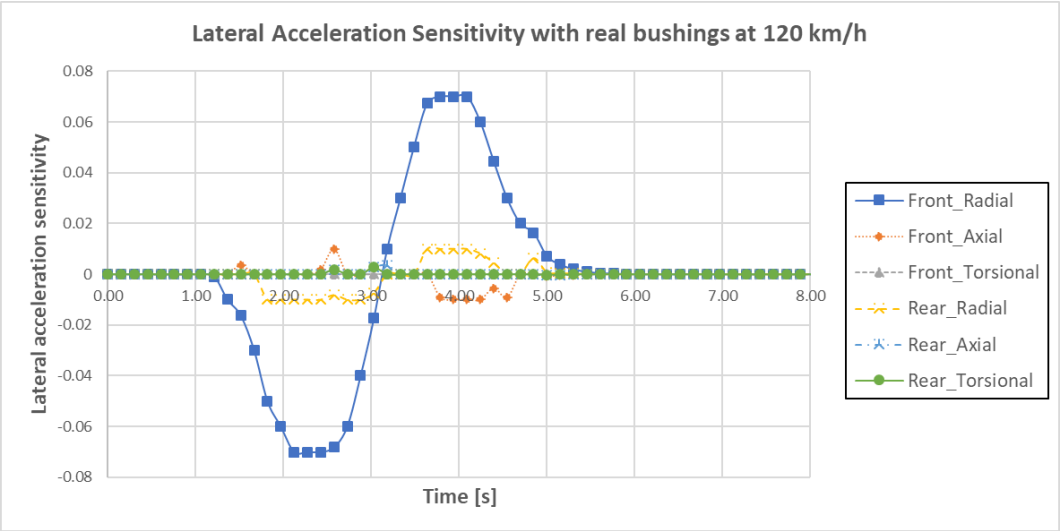

Figure 76: Validation model lateral acceleration sensitivity. 120km/h

6. Results

After analyzing the validation model, and seeing that it is behaving as expected, it is time to implement all the real components of the Opel Astra Caravan 1999 explained in chapter 3.

In this chapter, the results of the analyses performed with the full car model will be presented.

Summarizing the analyzed parameters, the effect of the radial rigidities in X and Y directions, the axial and the torsional stiffnesses for the front-front, rear-front and rear bushings were tested.

6.1. Dynamic response

In order to analyze the response of the full model, and the impact of the rigidity of the bushings, a great number of analyses were performed for different percentual variations of each of the analyzed parameters.

In order to try to see the effect of an increase/decrease on the rigidity of different parameters, a great number of analyses were performed. The full summary of performed analyses and results obtained is shown in Table 11.

		Affected bushing					
		Front front bushing		Rear front bushing		Rear bushing	
		Analyses	Parameters	Analyses	Parameters	Analyses	Parameters
Modified Parameter	Radial X stiffness	Bumped road	Vertical displacement	Bumped road	Vertical displacement	Bumped road	Vertical displacement
			Vertical acceleration		Vertical acceleration		Vertical acceleration
			Roll acceleration		Roll acceleration		Roll acceleration
		Lane change	Lateral displacement	Lane change	Lateral displacement	Lane change	Lateral displacement
			Lateral acceleration		Lateral acceleration		Lateral acceleration
	Radial Y stiffness	Bumped road	Vertical displacement	Bumped road	Vertical displacement	Bumped road	Vertical displacement
			Vertical acceleration		Vertical acceleration		Vertical acceleration
			Roll acceleration		Roll acceleration		Roll acceleration
		Lane change	Lateral displacement	Lane change	Lateral displacement	Lane change	Lateral displacement
			Lateral acceleration		Lateral acceleration		Lateral acceleration
	Axial stiffness	Bumped road	Vertical displacement	Bumped road	Vertical displacement	Bumped road	Vertical displacement
			Vertical acceleration		Vertical acceleration		Vertical acceleration
			Roll acceleration		Roll acceleration		Roll acceleration
		Lane change	Lateral displacement	Lane change	Lateral displacement	Lane change	Lateral displacement
			Lateral acceleration		Lateral acceleration		Lateral acceleration

		Affected bushing					
		Front front bushing		Rear front bushing		Rear bushing	
		Analyses	Parameters	Analyses	Parameters	Analyses	Parameters
Modified Parameter	Torsional stiffness	Bumped road	Vertical displacement	Bumped road	Vertical displacement	Bumped road	Vertical displacement
			Vertical acceleration		Vertical acceleration		Vertical acceleration
			Roll acceleration		Roll acceleration		Roll acceleration
		Lane change	Lateral displacement	Lane change	Lateral displacement	Lane change	Lateral displacement
			Lateral acceleration		Lateral acceleration		Lateral acceleration

Table 11: Performed analyses for Opel Astra model

This makes 24 different analyses types. Each of these analysis types was performed at three different speeds: 60, 90 and 120km/h. Also, in order to show the impact of rigidity variation, several analyses in each category were carried out for different rigidities configurations. The employed rigidities variations were:

- For radial and axial rigidities, a variation of ±10% on the bushing rigidity was tested, evaluated every 2% of variation. This makes up to 11 configurations considering the reference value.

- For torsional rigidity, since the rotation around the z axis is the DoF of the joint, the it was considered that the ideal joint opposed no resistance. This means a -100% applied to the torsional rigidity. Therefore, the tested configurations go from -100% to the reference one, making up to 15 different configurations considering the reference case.

With all these considerations, a total of 860 analyses were performed, and 2160 results files were obtained. All the analyses for the same results variable, and the same modified rigidity of a specific bushing at a certain speed were graphed together to see the variation. In total, 180 graphs were made. Due to the excessive amount of data obtained, not all can be shown in this work.

Since the realistic model of the Opel Astra is really complex, small variations in different parameters results in a variation in almost every output. For this reason, it is, in some cases, hard to interpret the effect of the parameters in these graphs.

For these two reasons, only those results where the effect is clearer will be now shown.

Due to the high number of curves, for an easier understanding, the following representation methodology was implemented: the reference configuration curve is always represented in red. For the radial and axial rigidities, an increase in the rigidity is represented in blue, a decrease in green. For the torsional rigidity, the greener the curves, the closer to the ideal joint, the bluer, the closer to the reference configuration.

- **Effect of front front silentblock's radial Y rigidity variation on the lateral displacement.**

In the real model results, the tendency seen in the validation model also applies: the outputs for the lane change are more easily understood.

As it was seen in the validation model, the biggest impact on the lateral displacement is due to the front silentblocks' radial rigidity. However, after this more in-depth analyses, it is seen that most of this effect is due to the front front silentblocks' radial Y rigidity.

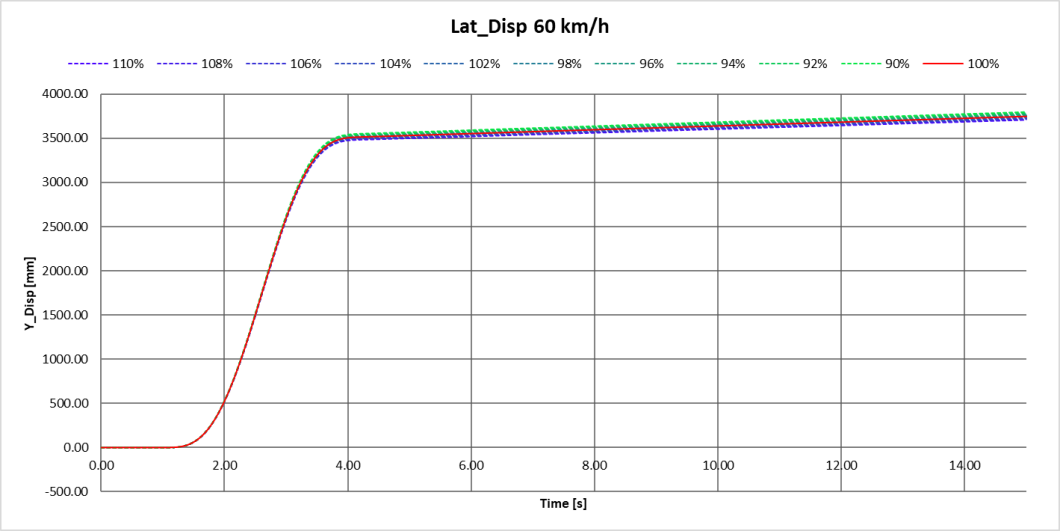

Figure 77: Real model lateral displacement. 60km/h. Front front bushing's radialY rigidity

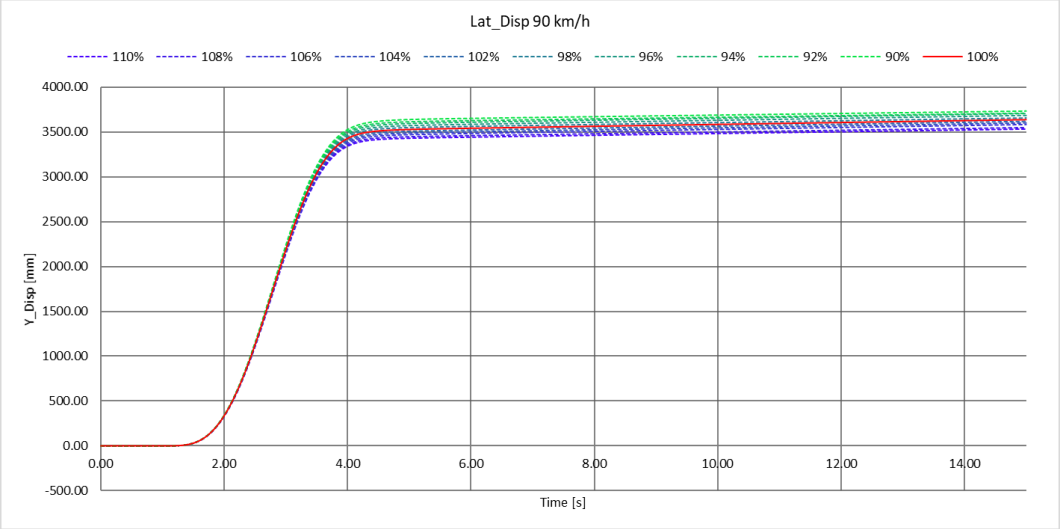

Figure 78: Real model lateral displacement. 90km/h. Front front bushing's radialY rigidity

In Figure 77 to Figure 79, this effect is shown. It is clearly seen that, with more rigid components in said direction, the vehicle becomes more stable, resulting in a smaller lateral step but with a straighter final direction. This effect is more clearly seen at higher speeds, where the effect is very relevant in the vehicle response.

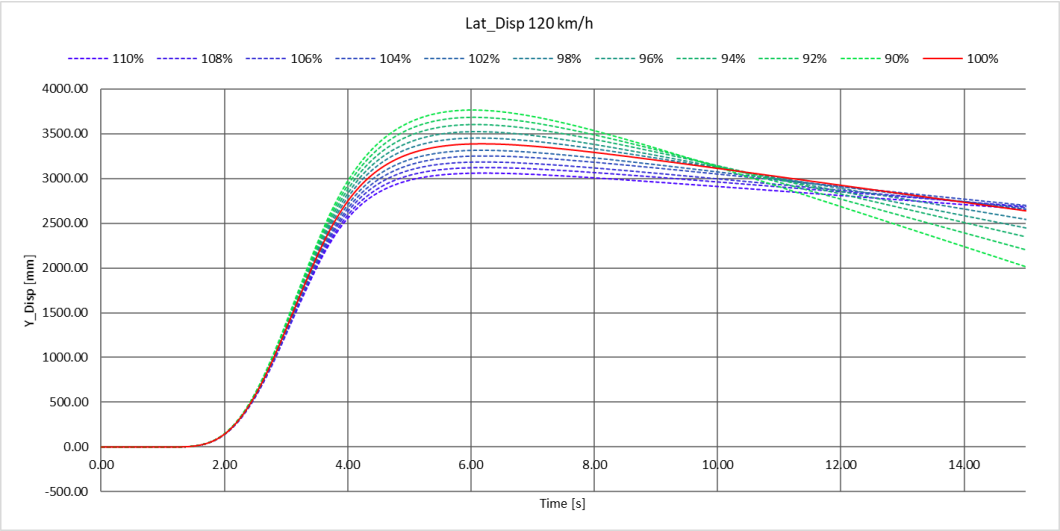

Figure 79: Real model lateral displacement. 120km/h. Front front bushing's radialY rigidity

- **Effect of front front silentblock's radial Y rigidity variation on the lateral acceleration.**

Evidently, after having seen the results for the lateral displacement, it was expected a similar impact in the lateral acceleration, since both parameters are closely related to each other.

These results are shown in Figure 80 to Figure 82. In line with the previous results, the effect is more clearly seen at higher speeds, where the acceleration, at lower rigidity values is increased and the return to zero value is delayed in time, producing the previously observed destabilizing effect. For higher rigidity values, the opposite effect is observed: lower acceleration peak with a faster return to the initial value.

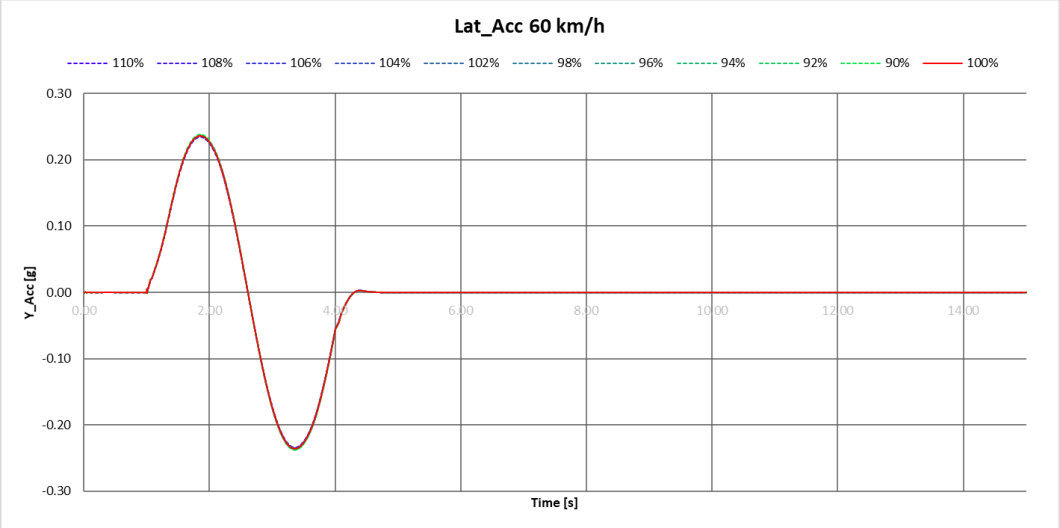

Figure 80: Real model lateral acceleration. 60km/h. Front front bushing's radialY rigidity

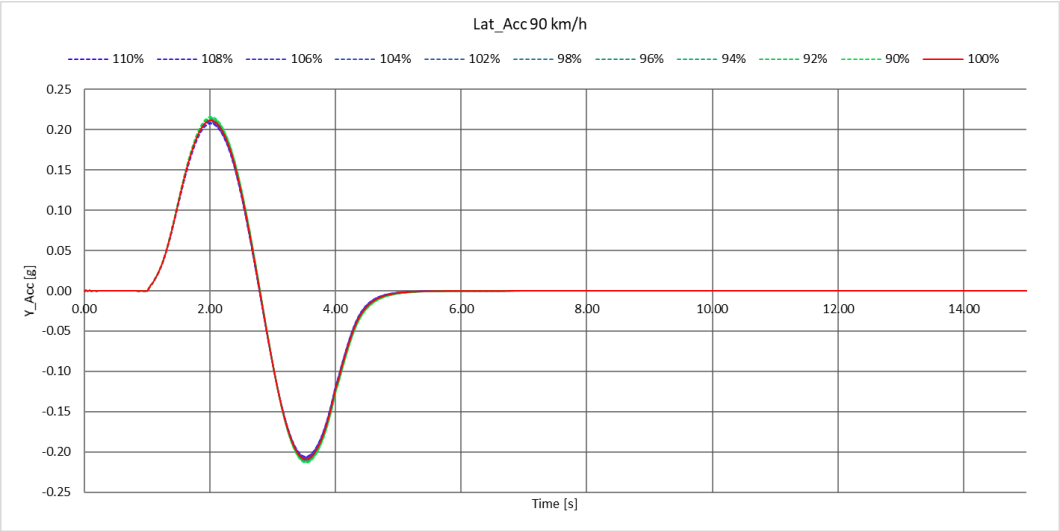

Figure 81: Real model lateral acceleration. 90km/h. Front front bushing's radialY rigidity

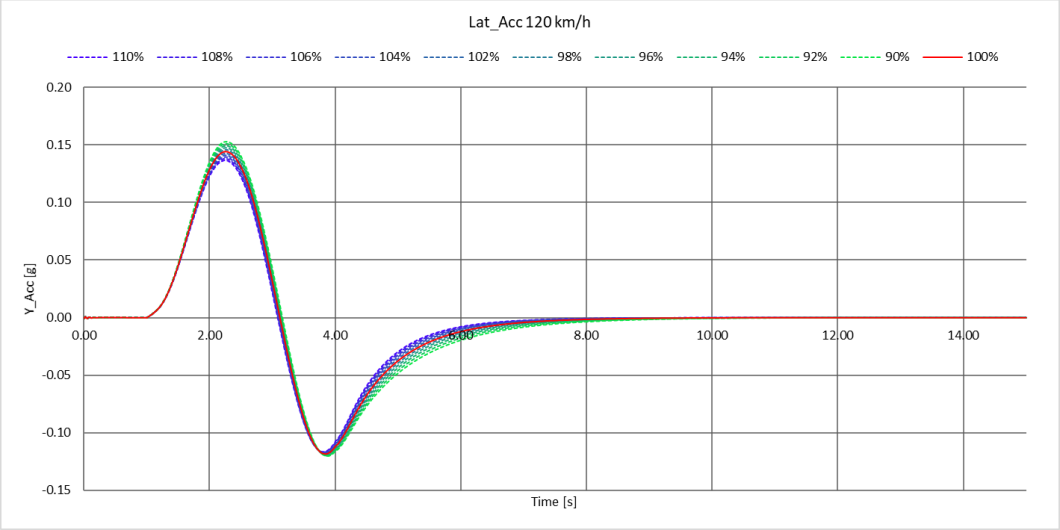

Figure 82: Real model lateral acceleration. 90km/h. Front front bushing's radialY rigidity

- **Effect of rear front silentblock's radial X rigidity variation on the roll acceleration.**

As it was explained in previous chapters, the main purpose of the silentblocks is the absorption of high vibrations. This effect should be seen in the effect on the accelerations. Theoretically, higher accelerations, specially at higher frequencies and lower peaks should be seen when the bushings are more rigid, and they should decrease when the bushings are softer, since the absorption is bigger

The parameter more related to the roll acceleration is the radial X rigidity, since it is the one working in this direction. The effect of this parameter in the rear front silentblock is the best example of this situation

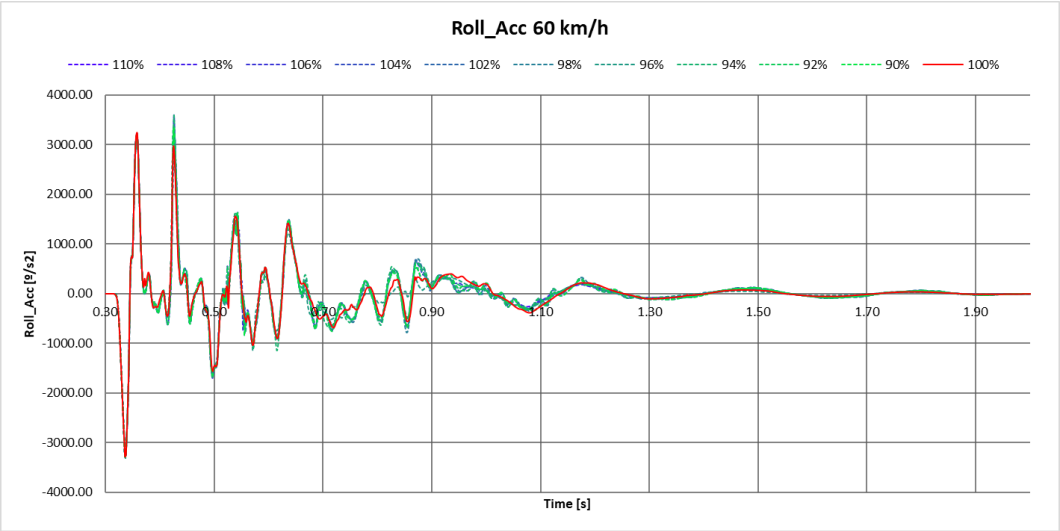

Figure 83: Real model roll acceleration. 60km/h. Rear front bushing's radialX rigidity

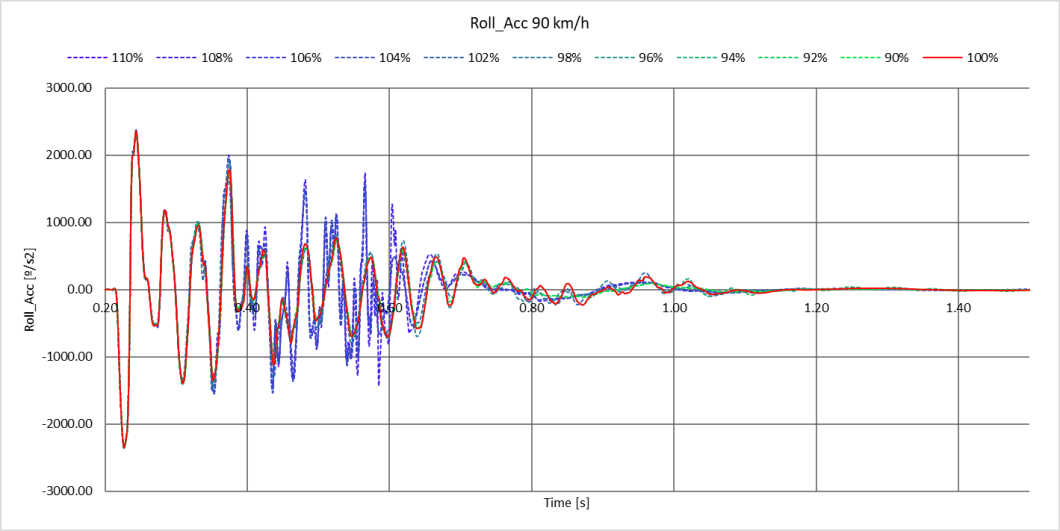

Figure 84: Real model roll acceleration. 90km/h. Rear front bushing's radialX rigidity

Figure 83 to Figure 85 show the output of the roll acceleration in this situation. At lower speeds, the roll oscillations are more extended in time. For this reason, the frequency of the oscillations is lower, and the outputs with different configurations are similar.

However, looking at the graphs of higher speeds, specially at 90 km/h, it is seen a remarkable increase in the acceleration peaks for higher rigidities (blue). At 90km/h it is also seen an almost full cancellation of the roll acceleration for peaks after second 0.8 for lower rigidity values.

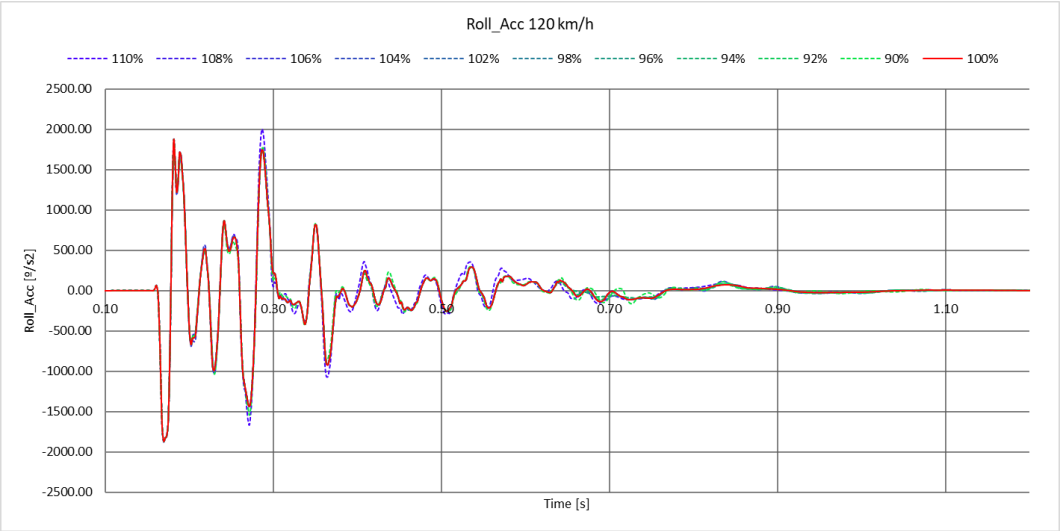

Figure 85: Real model roll acceleration. 120km/h. Rear front bushing's radialX rigidity

- **Effect of rear front silentblock's radial Y rigidity variation on the lateral displacement.**

There are several parameters that have a lineal impact in the lateral behavior. Some interesting ones are the effect of the radial Y and axial rigidity of the rear front silentblocks in this output. This influence is very similar for both parameters.

It was previously stated that, in the validation model it was seen that the radial rigidity of the front silentblocks resulted in a more stable output. However, having a look at Figure 86 to Figure 88, we see that the radial rigidity of the rear front silentblocks in the Y direction shows the opposite tendency.

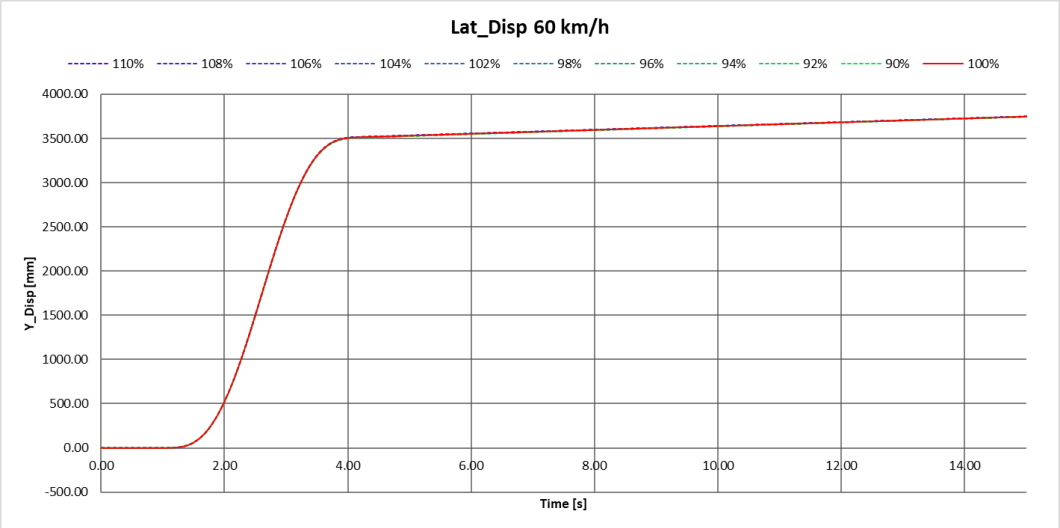

Figure 86: Real model lateral displacement. 60km/h. Rear front bushing's radialY rigidity

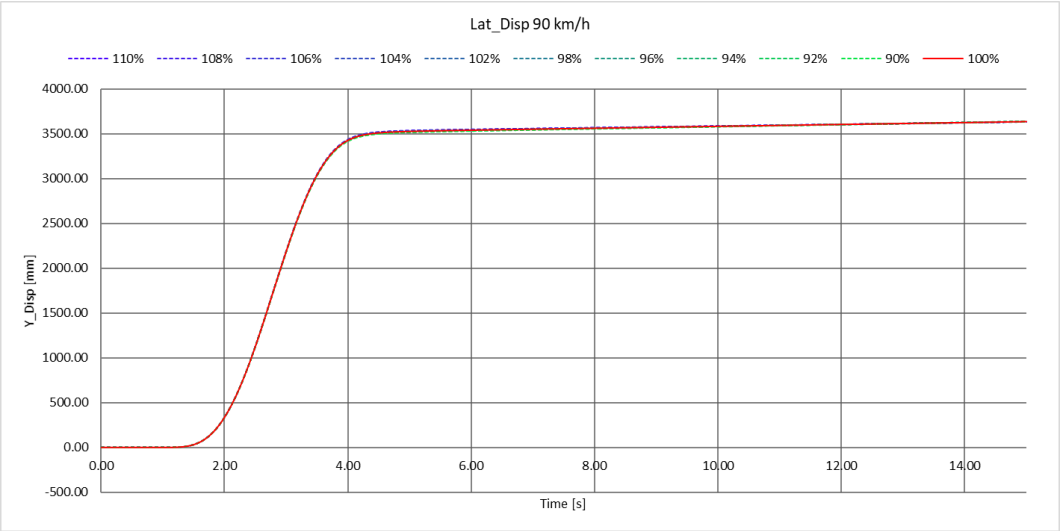

Figure 87: Real model lateral displacement. 90km/h. Rear front bushing's radialY rigidity

In these figures it can be seen, specially at higher speeds, that more rigid rear front silentblocks result in a less stable lateral displacement. However, since this effect is much smaller than the one seen in Figure 77 to Figure 79, if we increase the rigidity in both front silentblocks, this undesired effect is compensated, and the final output is more stable.

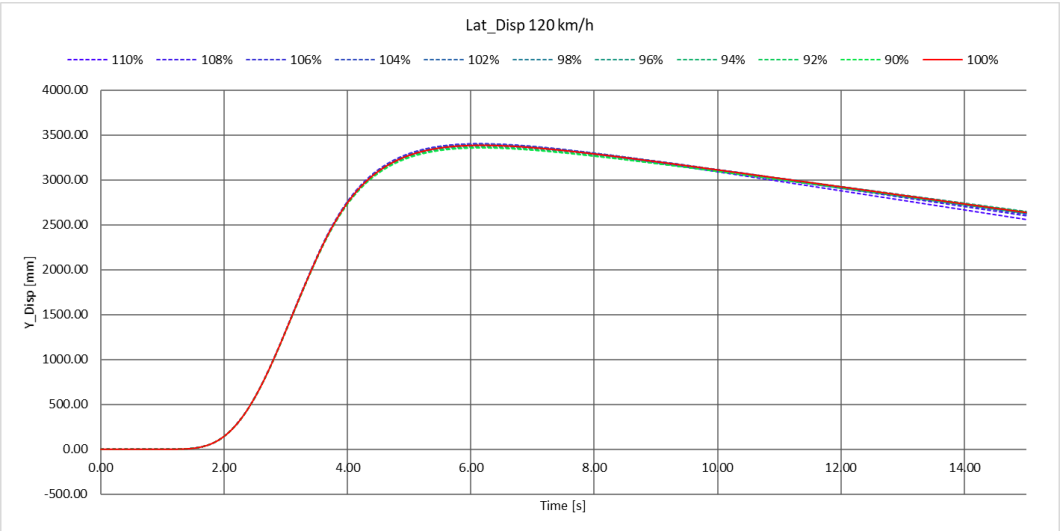

Figure 88: Real model lateral displacement. 120km/h. Rear front bushing's radialY rigidity

- **Effect of rear silentblock's torsional rigidity variation on the vertical displacement.**

The most evident lineal effect on the vertical displacement of the chassis, is the impact of the torsional stiffness of the rear silentblocks.

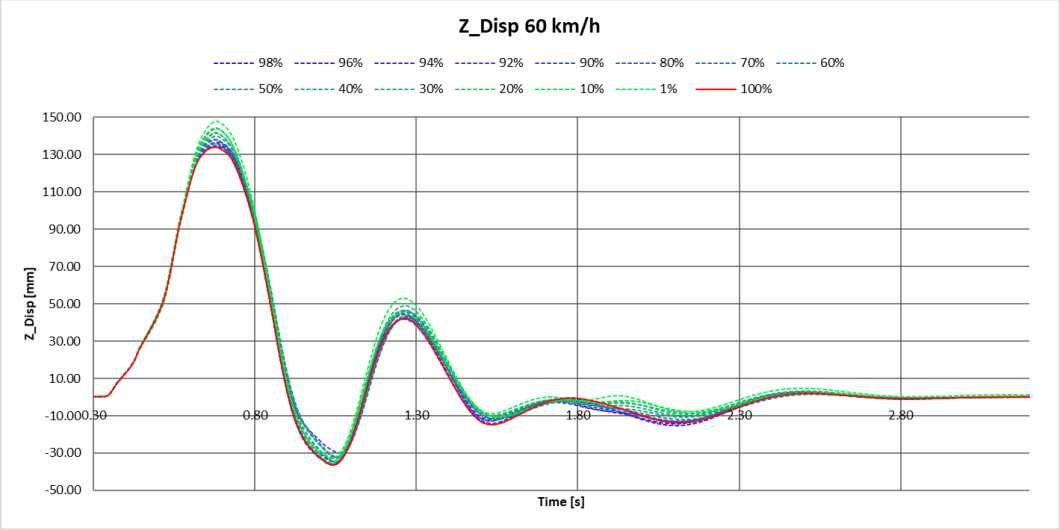

Figure 89: Real model vertical displacement. 60km/h. Rear bushing's torsional rigidity

Figure 89 to Figure 91 show this effect. It can be seen that the vertical displacement is bigger when the silentblocks are more similar to the ideal configuration (in green). This effect is remarkable at every speed.

An ideal rotation around the z axis of the bushing allows the chassis to raise more when the front wheels collide with the bumps, since there is a lesser opposition from the rear axis. Due to this increase in the vertical displacement, the peaks seen in the graphs are delayed in time.

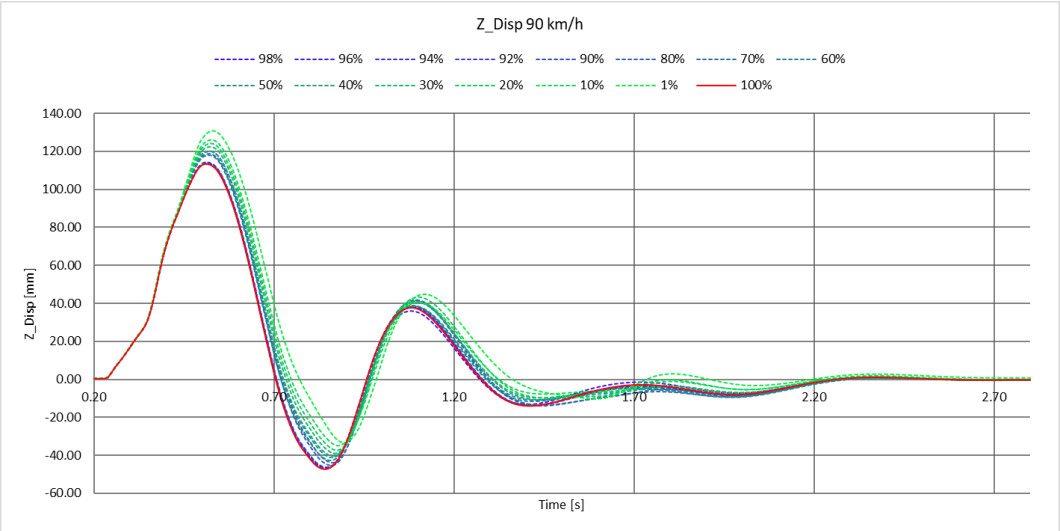

Figure 90: Real model vertical displacement. 90km/h. Rear bushing's torsional rigidity

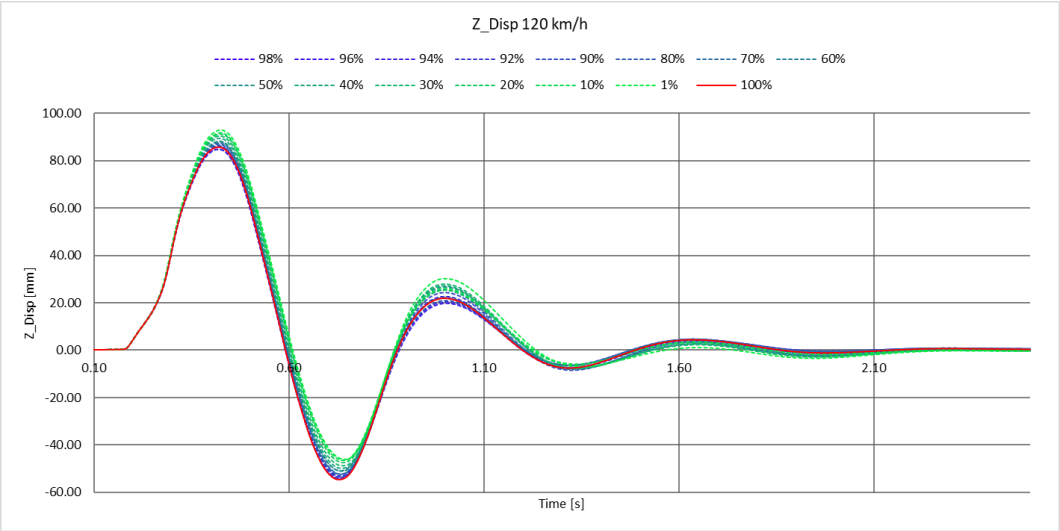

Figure 91: Real model vertical displacement. 120km/h. Rear bushing's torsional rigidity

- **Effect of rear silentblock's torsional rigidity variation on the vertical acceleration.**

Having this big impact on the vertical displacement, it is interesting to analyze what is happening to the vertical acceleration during these analyses.

This is what is shown in Figure 92 to Figure 94. Most of the higher peaks seen in these graphs come from the green lines, associated to the ideal scenario. The red curve, which represent the reference case and, in this case, the softer configuration of bushings, is located as the central line of all the curves.

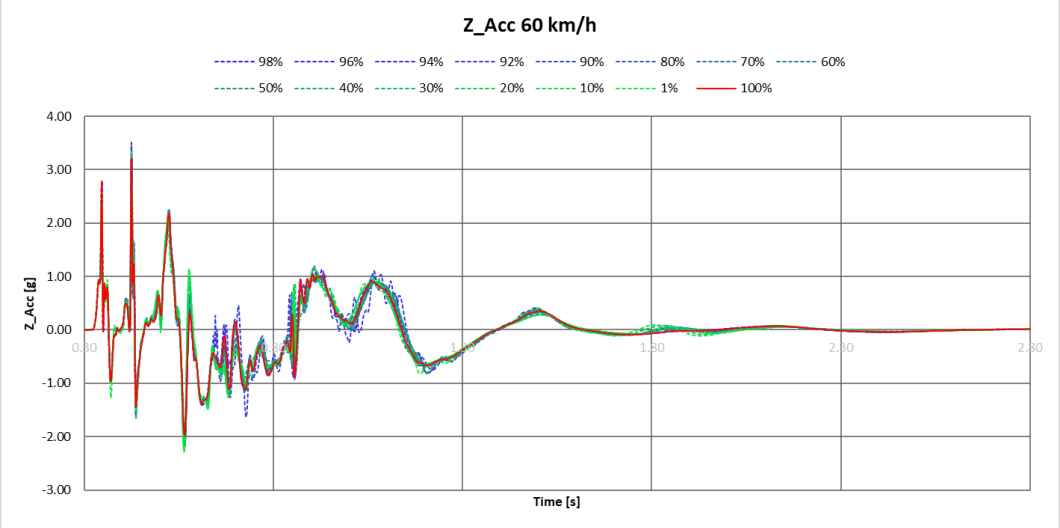

Figure 92: Real model vertical acceleration. 60km/h. Rear bushing's torsional rigidity

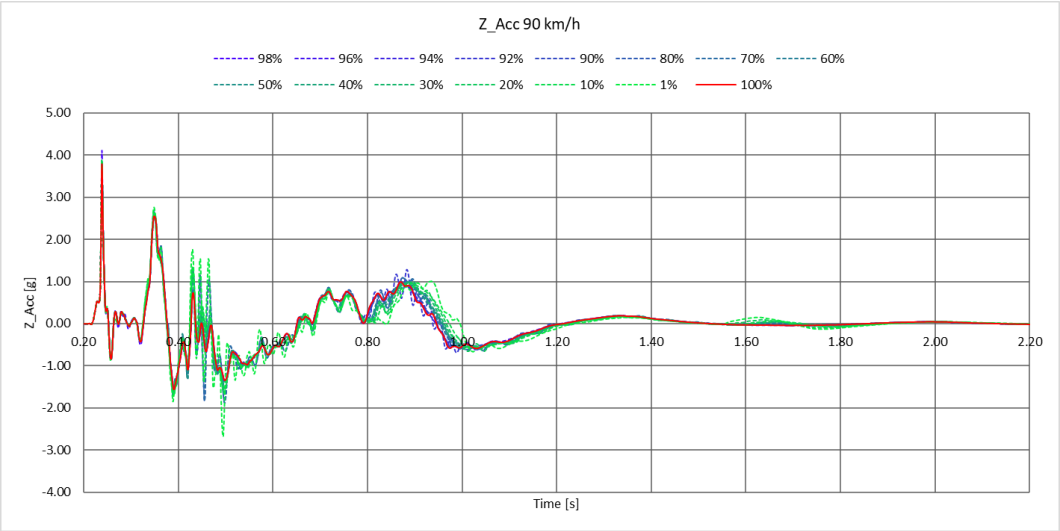

Figure 93: Real model vertical acceleration. 90km/h. Rear bushing's torsional rigidity

Once again, the biggest increase in the maximum absolute values of the acceleration due to an increase in the rigidity is seen at 90km/h. This may be due to resonant phenomena at this specific speed for this vehicle and obstacle geometry.

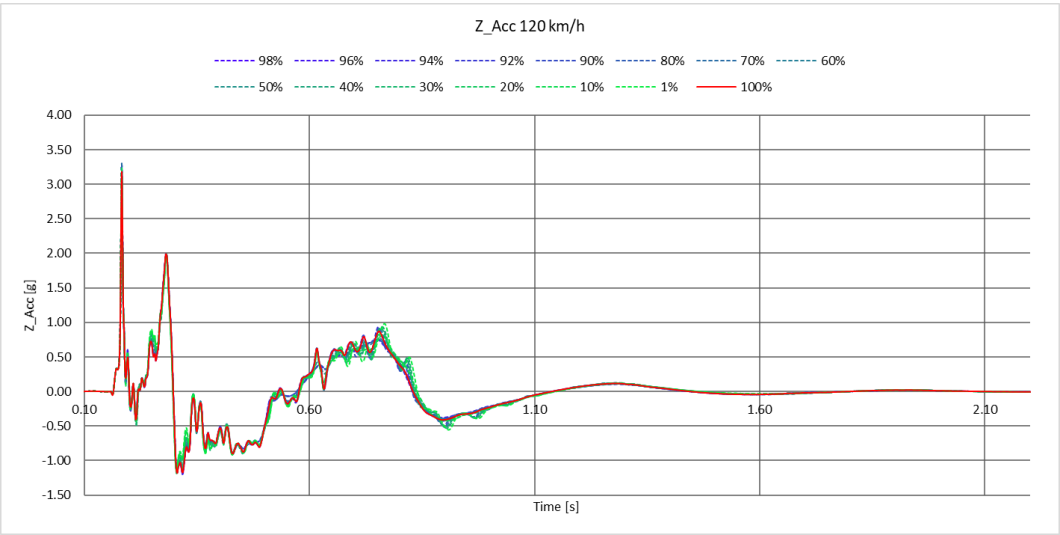

Figure 94: Real model vertical acceleration. 120km/h. Rear bushing's torsional rigidity

At 120km/h, even if the damping effect of the bushings is not so prominent, it is observable that all the small salient values are from the more rigid configurations.

- **Effect of rear silentblock's torsional rigidity variation on the lateral displacement.**

The las analyses that are going to be shown are the results of the influence of the rear silentblocks' torsional rigidity variation on the lateral displacement.

Together with the radial Y rigidity of the front front silentblocks, this is the parameter that has the biggest impact in this response of the vehicle.

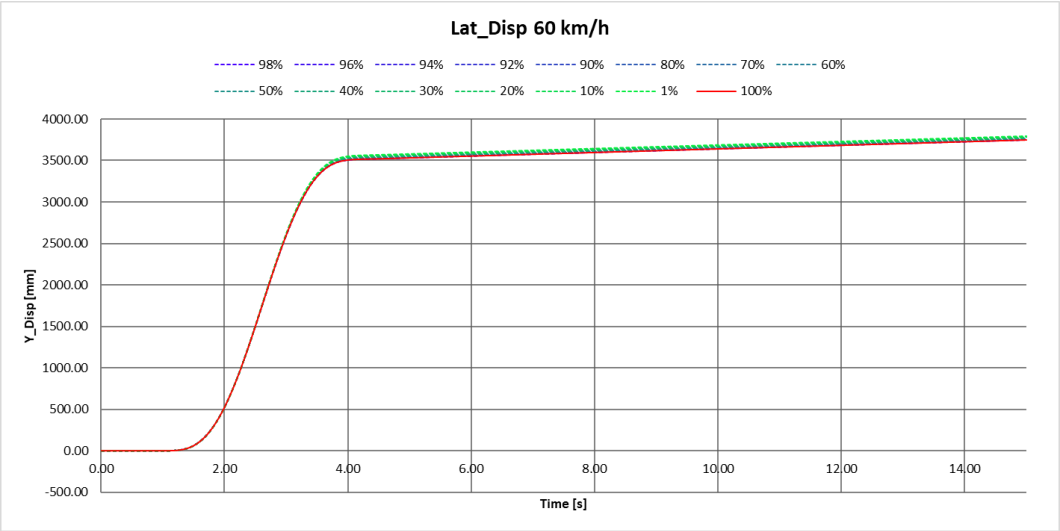

Figure 95: Real model lateral displacement. 60km/h. Rear bushing's torsional rigidity

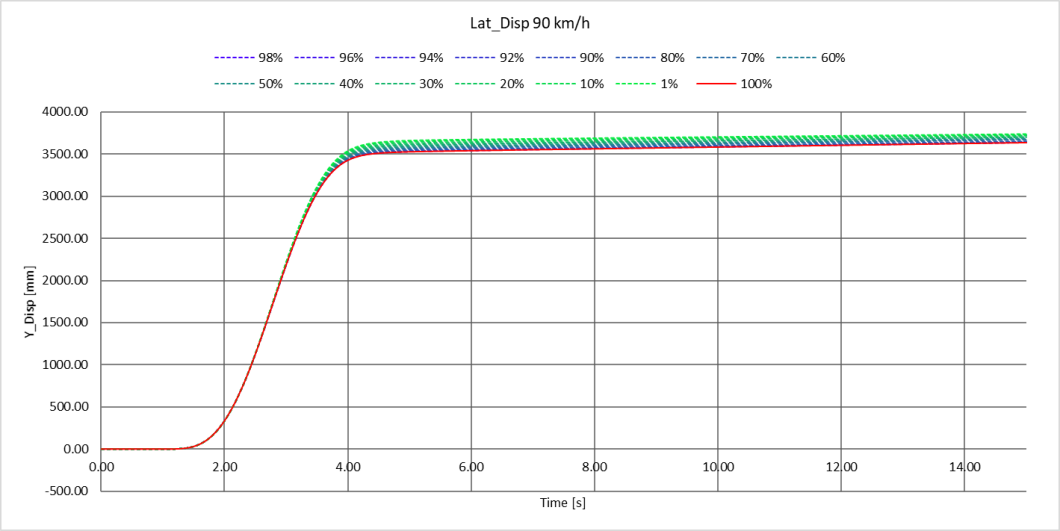

Figure 96: Real model lateral displacement. 90km/h. Rear bushing's torsional rigidity

Figure 95 to Figure 97 show these results. It can be seen that ideal joint results in an output that shows a bigger lateral step and a more unstable trajectory. Once again, the effect is more noticeable at higher speeds.

This repercussion is opposite to the impact of the radial Y rigidity of the front front silentblocks. The more rigid in the torsional DoF, the more unstable the car becomes after a lane change.

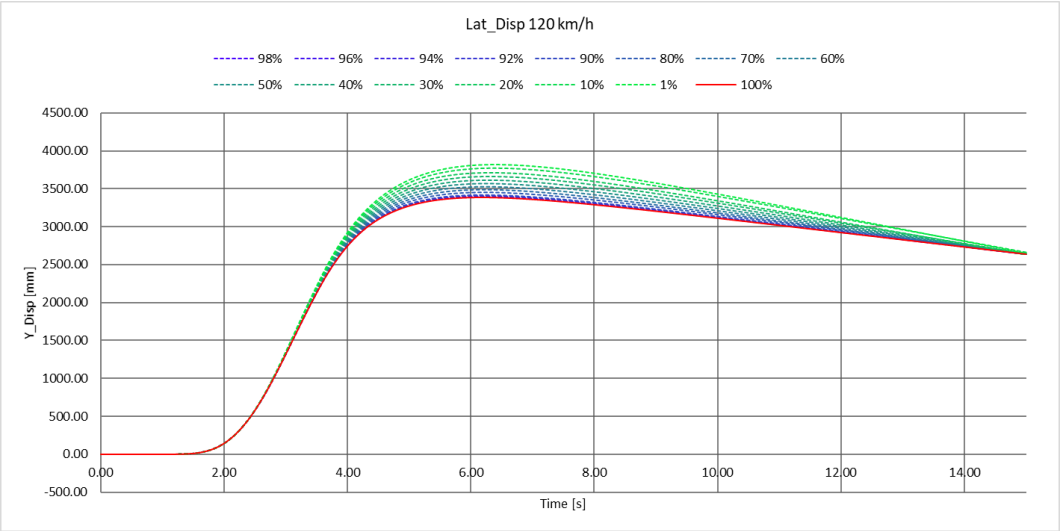

Figure 97: Real model lateral displacement. 120km/h. Rear bushing's torsional rigidity

6.2. Sensitivity

In this chapter, the sensitivity analyses results performed for the Opel Astra Caravan 1999 will be shown.

The employed methodology is the finite differences method, from [8], as explained in chapter 5.3. There are, however, some differences. The first difference is that the rigidity step used for the calculations is, in this case, a 2% increase. The second difference is that in these analyses, the sensitivity for each individual parameter of each bushing was analyzed separately.

Due to the last difference explained, there are to many curves for a proper understanding of the graphs. For this reason, the sensitivity curves from the front and rear bushings will be plotted separately for a better understanding.

6.2.1. Vehicle riding over bumps

In this chapter, the sensitivity graphs of the vertical displacement, and vertical and roll accelerations to the rigidities of the bushings are presented.

6.2.1.1. Vertical displacement

From the rest of analyses in this work, it is expected that the results for the vehicle riding over bumps tests are harder to interpret. This is what happens in this situation, but the effect is increased. Due to the complexity of the model, any change in any parameter has an impact in the outputs.

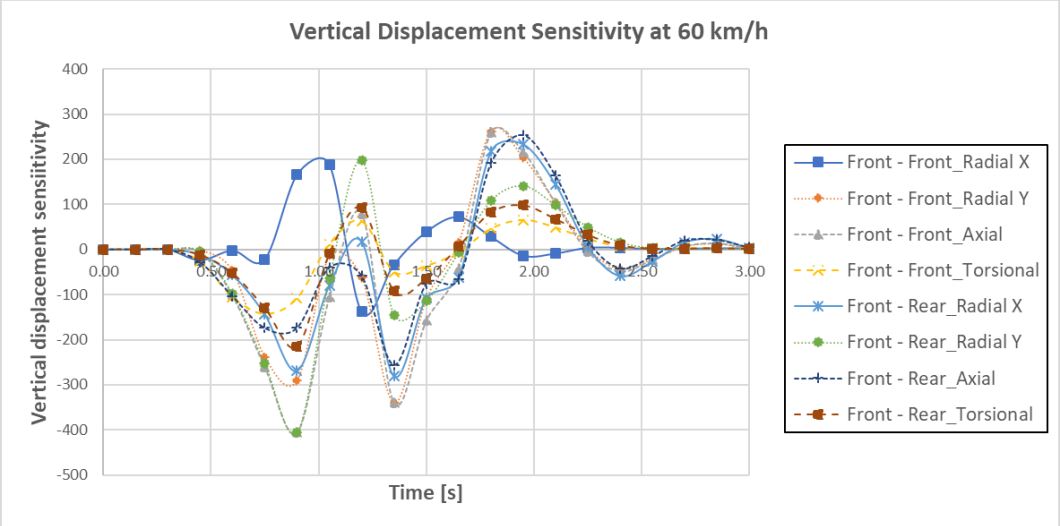

Figure 98: Real model vertical displacement sensitivity. 60km/h. Front bushings

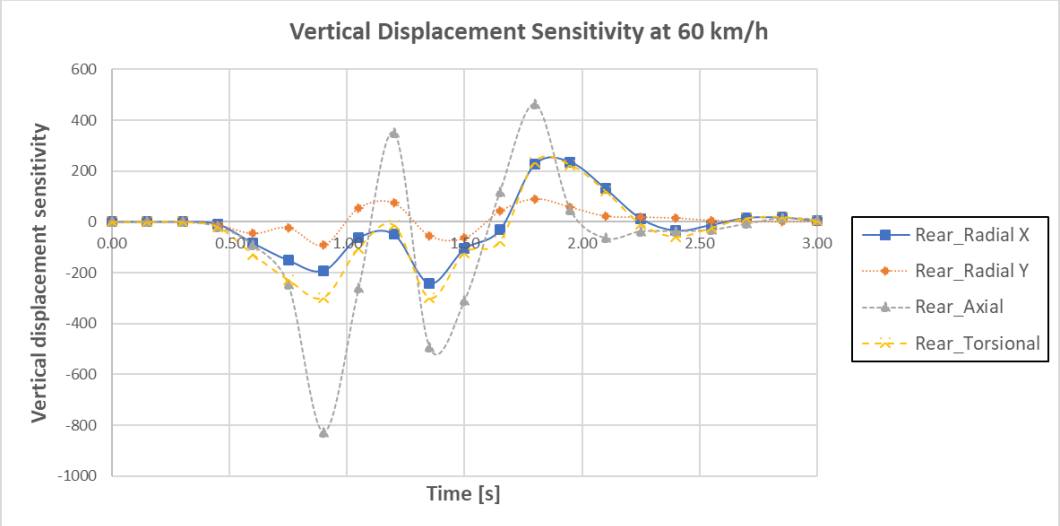

Figure 99: Real model vertical displacement sensitivity. 60km/h. Rear bushings

Not only this happens, but we can also see that certain parameters have a huge impact at a certain speed. This is due to specific resonant phenomena at specific speeds. For this reason, it is more important to pay attention to those parameters that have a continuous impact at every speed.

While almost all parameters have some degree of impact on the vertical displacement, it can be seen, for example, that while the axial component of the front front bushings appear as one of the most important at lower speeds, its effect is much lower at higher speed ranges. The same happens with various parameters.

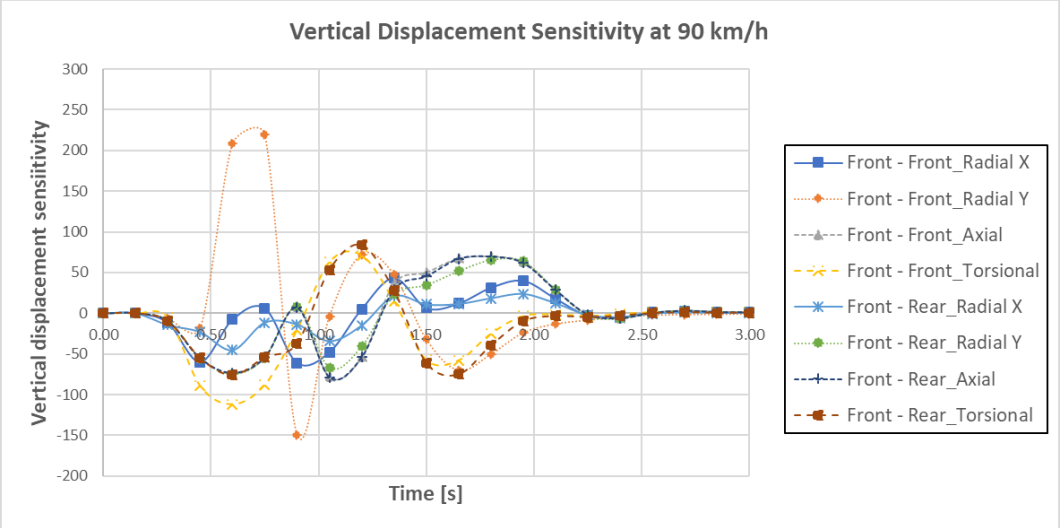

Figure 100: Real model vertical displacement sensitivity. 90km/h. Front bushings

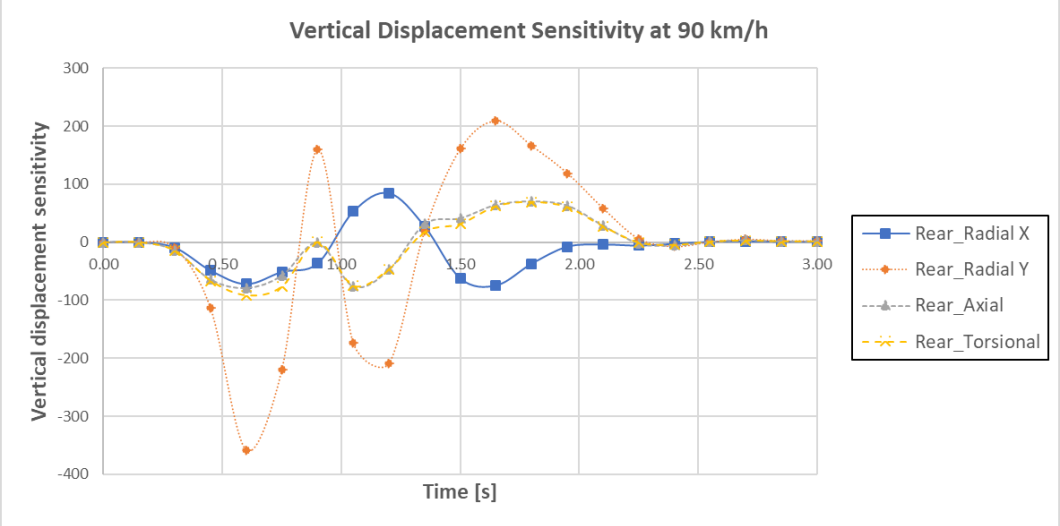

Figure 101: Real model vertical displacement sensitivity. 90km/h. Rear bushings

The parameters that seem to provide a more continuous effect at every speed are the radial rigidities in the X (vertical) direction of all three silentblocks. These three parameters have almost the same impact in all the graphs, increasing the maximum achieved displacement and the settling time.

Other parameters, such as the torsional and radial rigidities in the Y direction of the rear silentblock seem to gain more importance at higher speeds.

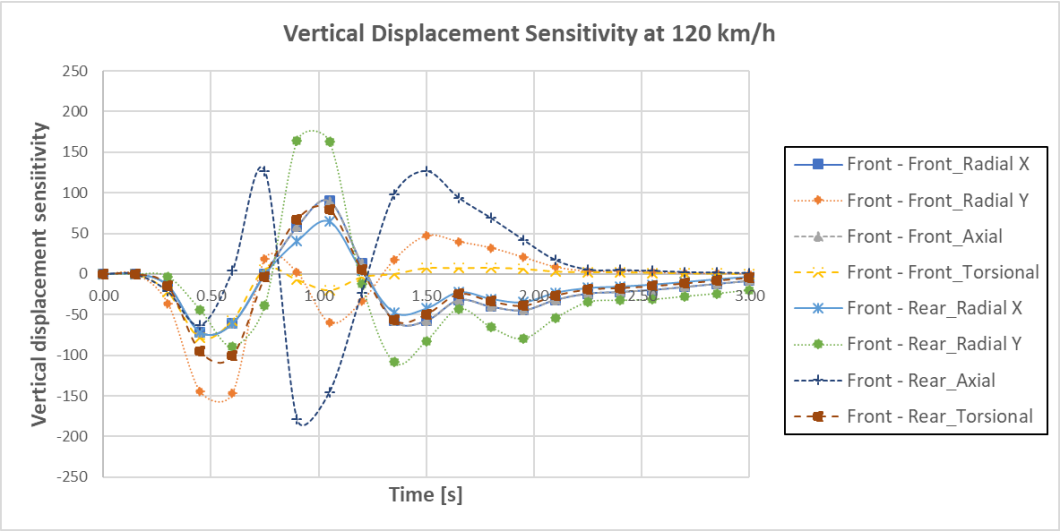

Figure 102: Real model vertical displacement sensitivity. 120km/h. Front bushings

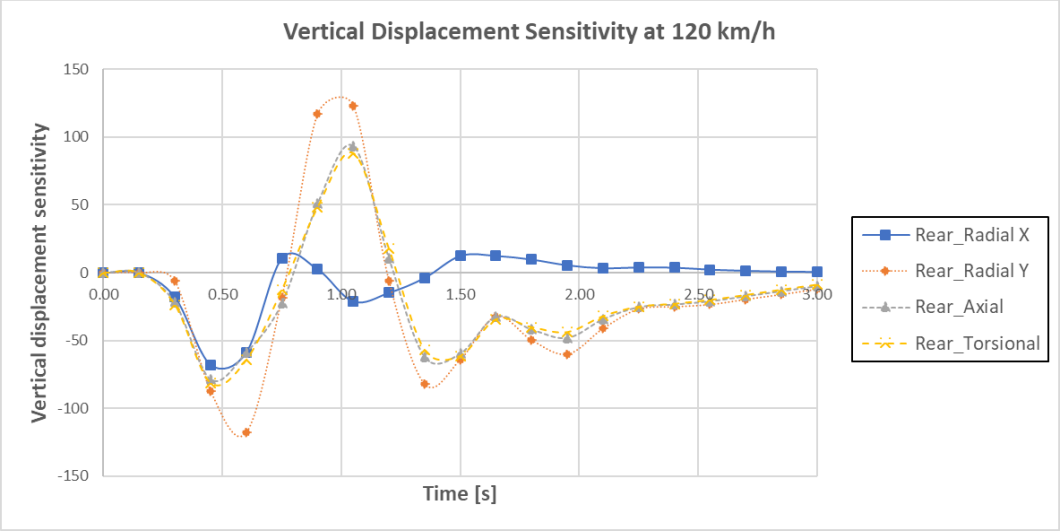

Figure 103: Real model vertical displacement sensitivity. 120km/h. Rear bushings

6.2.1.2. Vertical acceleration

Since the vertical acceleration is closely related to the vertical displacement, it is expected to have a similar behavior. Figure 104, Figure 106 and Figure 108 show the sensitivity of the vertical acceleration to a 2% increase in the rigidity of the front bushing rigidities. Figure 105, Figure 107 and Figure 109 show the sensitivity to this increase on the rear bushings.

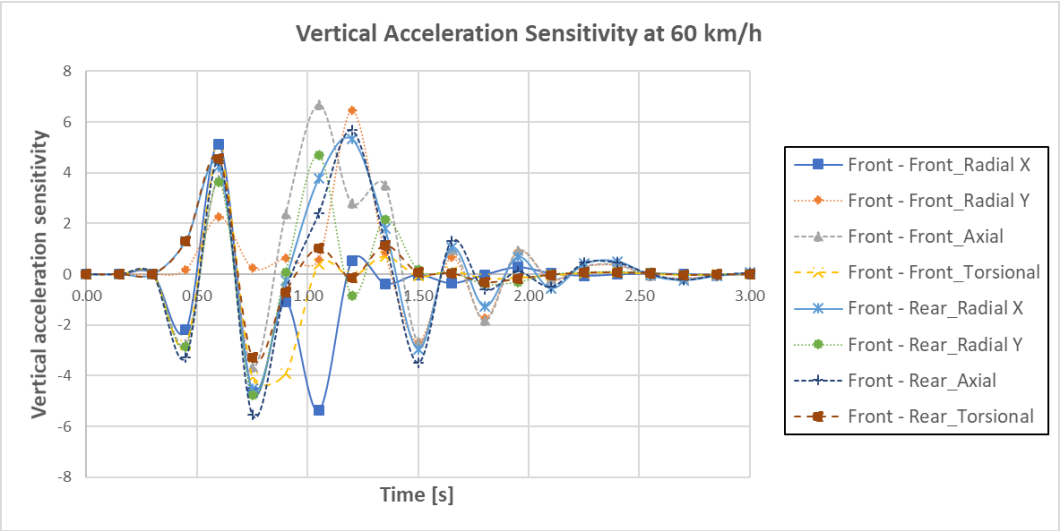

Figure 104: Real model vertical acceleration sensitivity. 60km/h. Front bushings

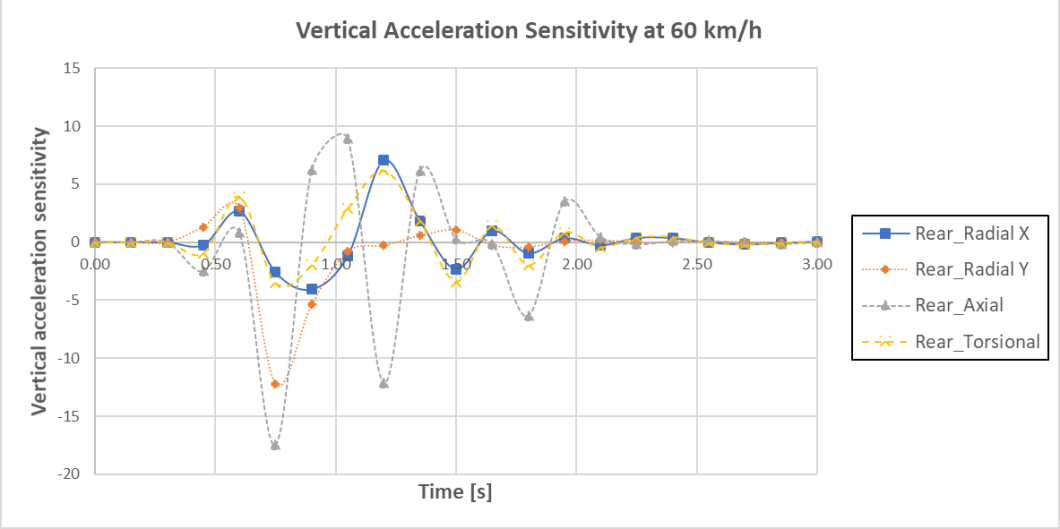

Figure 105: Real model vertical acceleration sensitivity. 60km/h. Rear bushings

Once again, instead of paying attention to certain peaks at a specific speed, it is important to take into consideration those parameters that influence in the same manner the vertical acceleration response at every speed.

Like in the previous results, the parameters that show the most continuous effect in all the graphs are the radial rigidities in the X (vertical) direction of the three bushings.

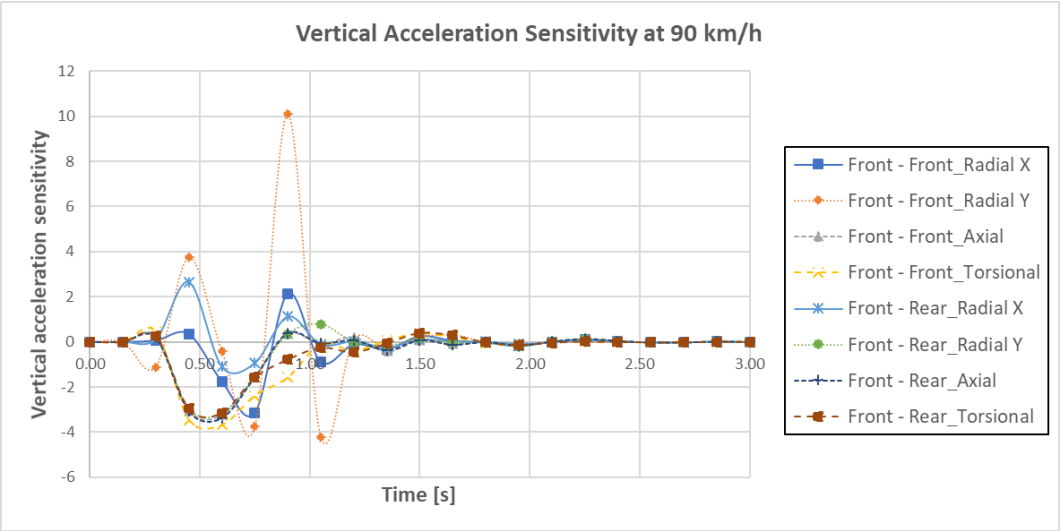

Figure 106: Real model vertical acceleration sensitivity. 90km/h. Front bushings

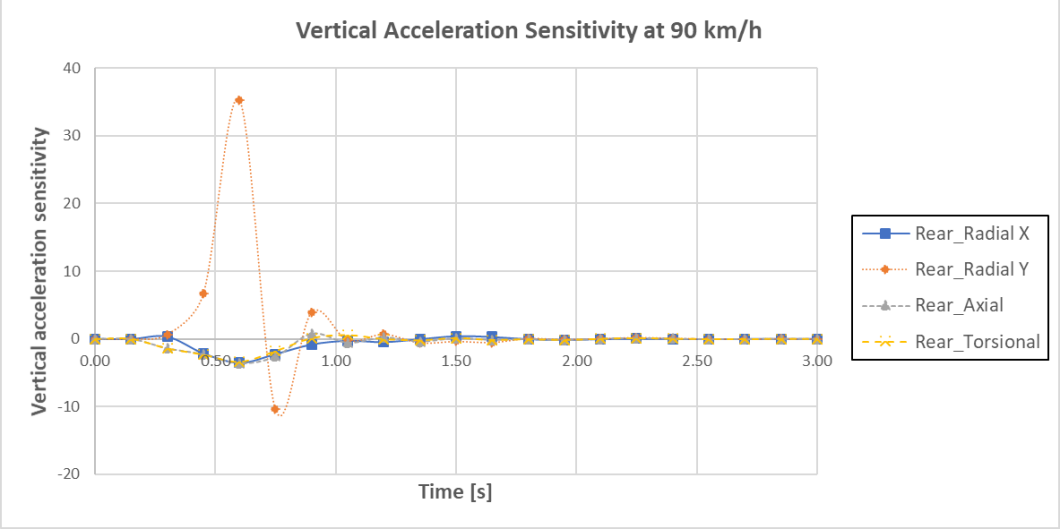

Figure 107: Real model vertical acceleration sensitivity. 90km/h. Rear bushings

It is also remarkable the increase in the impact of the torsional stiffness of the front silentblocks at high speeds, since this effect is not neglectable.

Lastly, the axial rigidity of the rear silentblocks seem to have e negative influence in the vertical acceleration, being especially remarkable at 60 and 120 km/h.

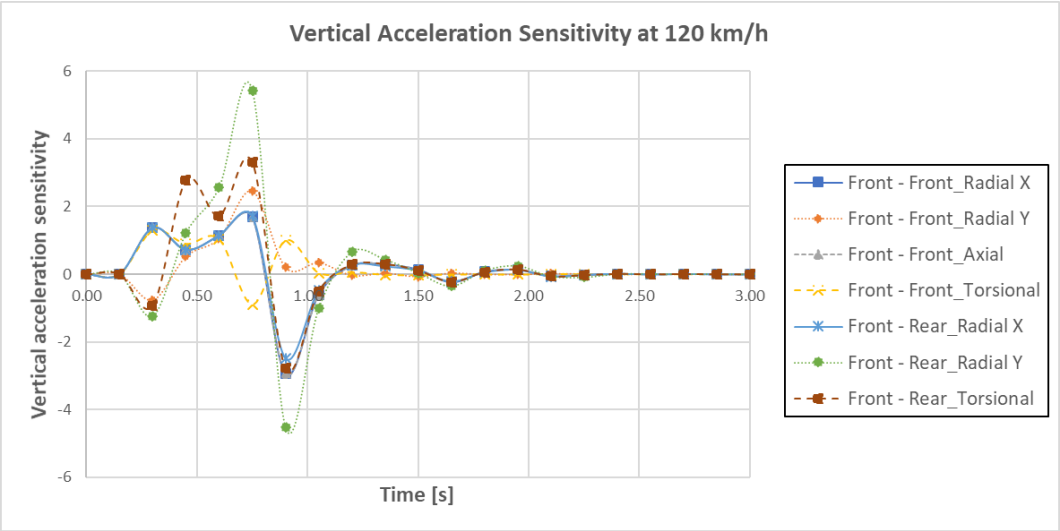

Figure 108: Real model vertical acceleration sensitivity. 120km/h. Front bushings

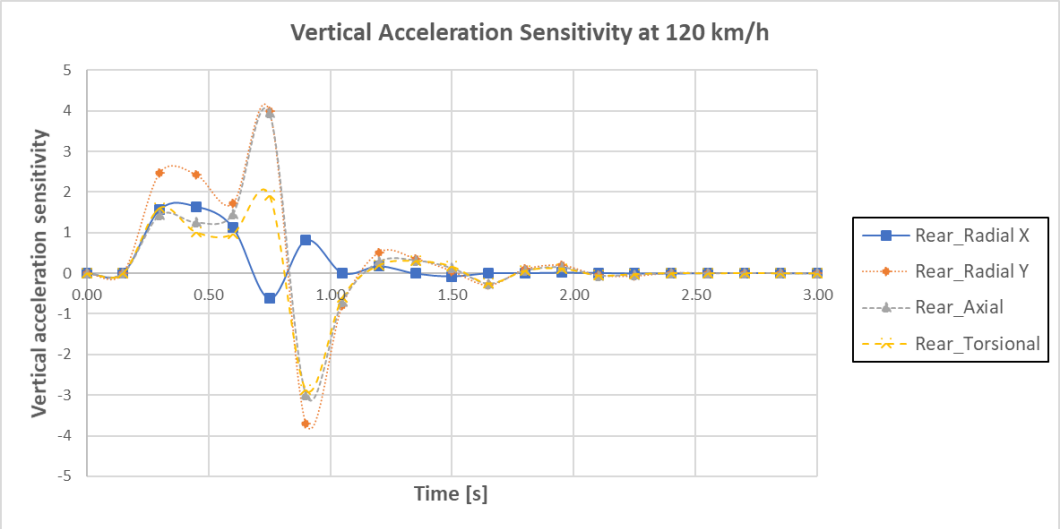

Figure 109: Real model vertical acceleration sensitivity. 120km/h. Rear bushings

6.2.1.3. Roll acceleration

Due to the fast changes in the curve of the roll acceleration, any small change results in an impact in these curves and, similarly to what happened with the vertical acceleration, the sensitivity curves will show a dependence on all the parameters to a certain extent.

Figure 110, Figure 112 and Figure 114 show the sensitivity of the roll acceleration to changes in the rigidities of the front silentblocks, while Figure 111, Figure 113 and Figure 115 show the sensitivity of this output to the variation on the rear silentblocks.

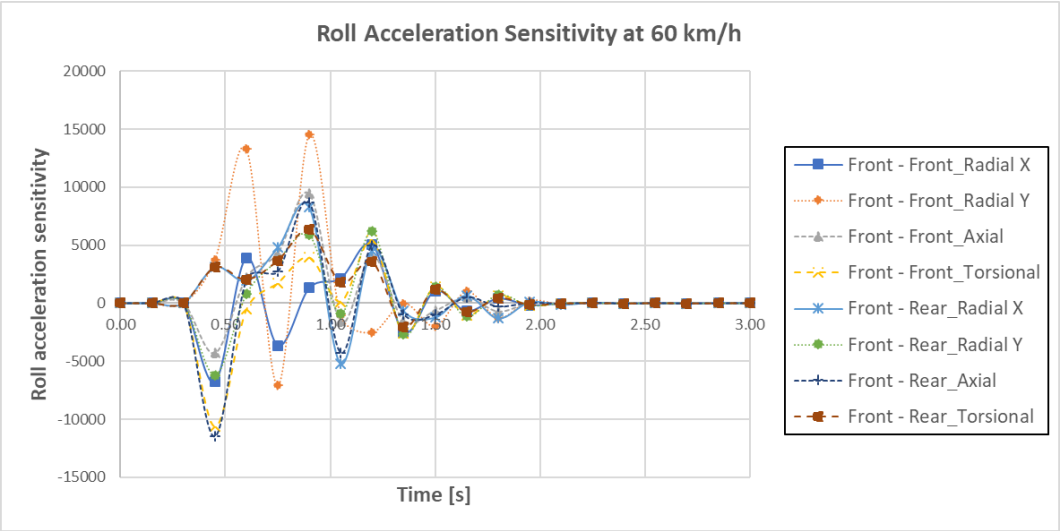

Figure 110: Real model roll acceleration sensitivity. 60km/h. Front bushings

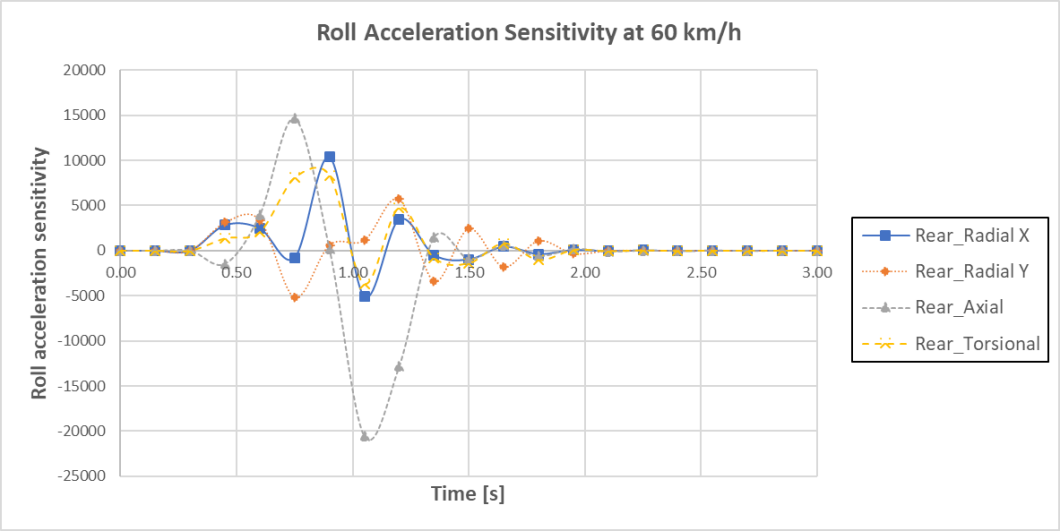

Figure 111: Real model roll acceleration sensitivity. 60km/h. Rear bushings

In these curves there is an important impact of the torsional stiffness of the fromt front bushing, that can be seen in all three of the graphs.

Some parameters that were expected to influence the roll acceleration and indeed do, are the radial X rigidity of the front front and rear front silentblocks. These rigidities work in the vertical direction of these bushings, which should be, in theory the more affected direction. The radial X rigidity of the rear bushings, however, seems to have a smaller importance than other parameters.

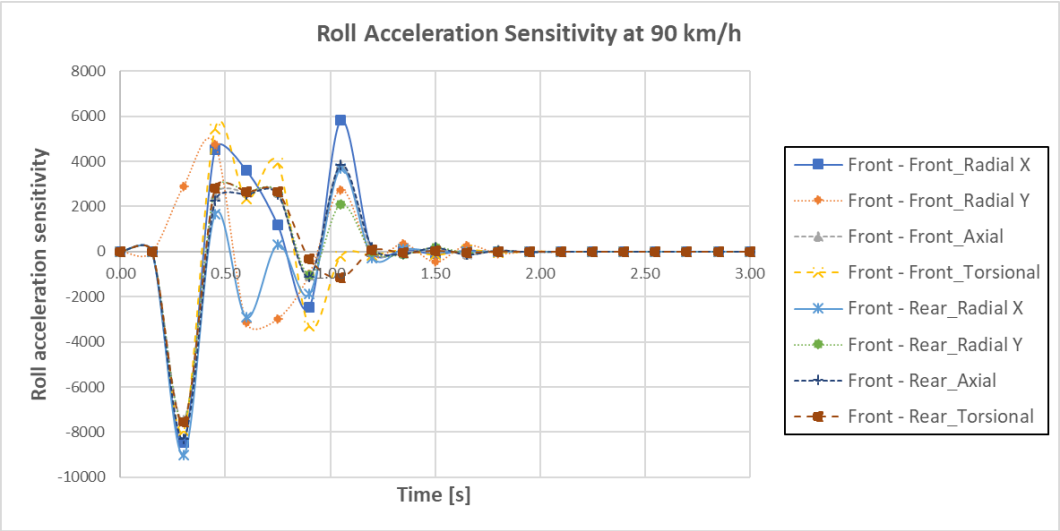

Figure 112: Real model roll acceleration sensitivity. 90km/h. Front bushings

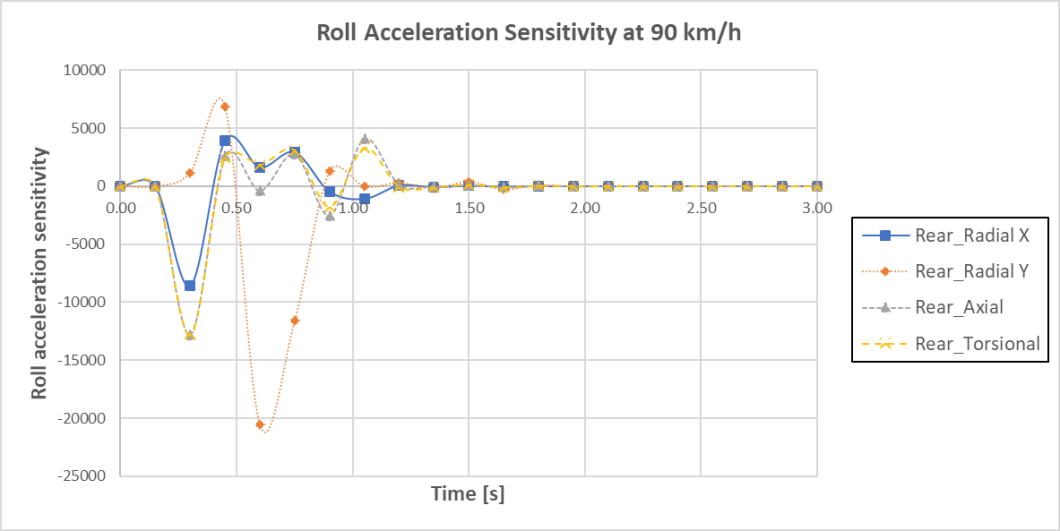

Figure 113: Real model roll acceleration sensitivity. 90km/h. Rear bushings

Finally, the axial rigidity of the rear front bushing was not expected to have a big impact in the roll acceleration. Nevertheless, it is clearly seen that is one of the parameters with the biggest repercussion, specially at higher speeds. The reason for this could be the destabilization of the vehicle due to the rolling motion, that makes this bushing work more in this direction.

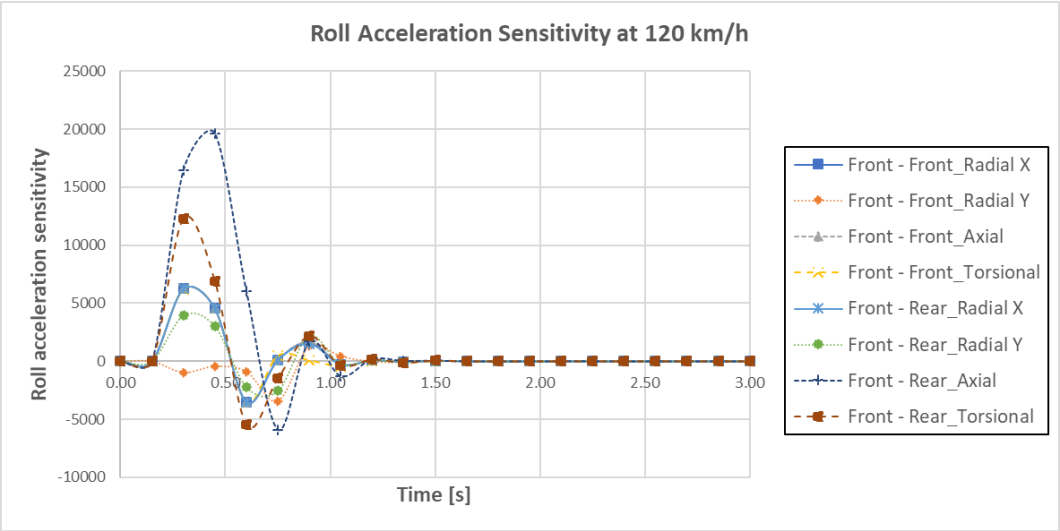

Figure 114: Real model roll acceleration sensitivity. 120km/h. Front bushings

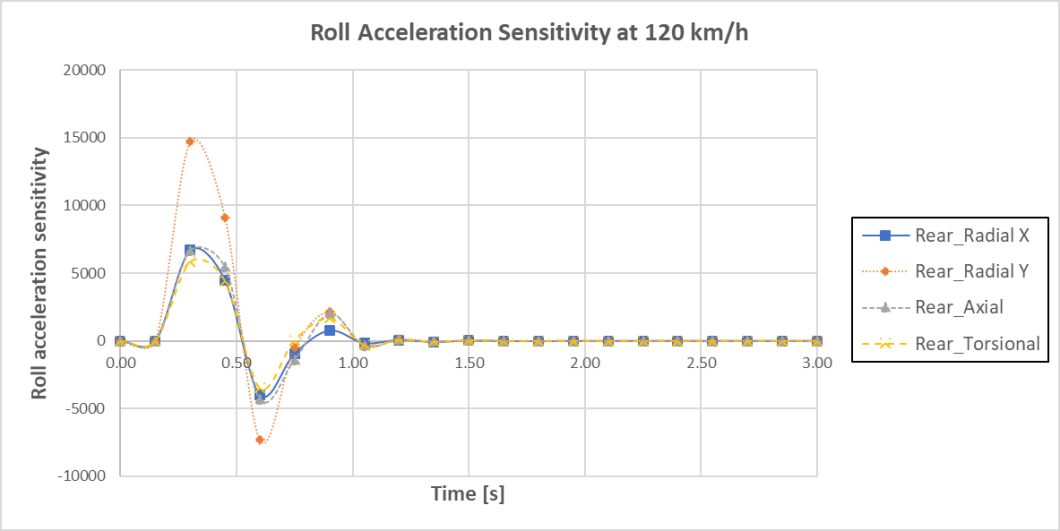

Figure 115: Real model roll acceleration sensitivity. 120km/h. Rear bushings

6.2.2. Single lane change

In this chapter, the sensitivity graphs of the lateral displacement and acceleration to the rigidities of the bushings are presented.

6.2.2.1. Lateral displacement

The outputs of the lane change maneuver are, once again, more continuous and easier to understand that the previous results. It is for this reason that these sensitivity graphs are much simpler.

Figure 116, Figure 118 and Figure 120 show the sensitivity graphs of the influence of front silentblocks rigidities in the lateral displacement. Figure 117, Figure 119 and Figure 121 show the influence of the rear silentblocks in this output.

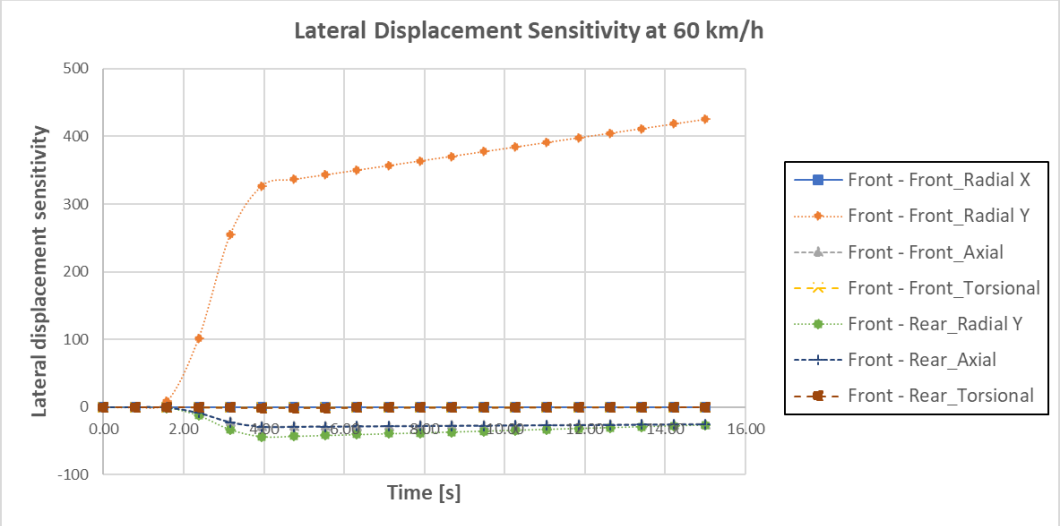

Figure 116: Real model lateral displacement sensitivity. 60km/h. Front bushings

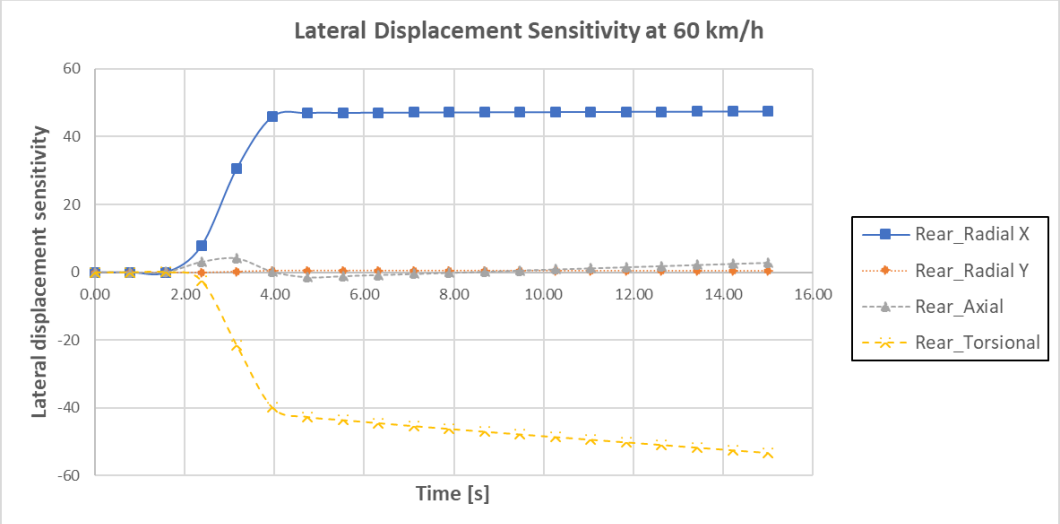

Figure 117: Real model lateral displacement sensitivity. 60km/h. Rear bushings

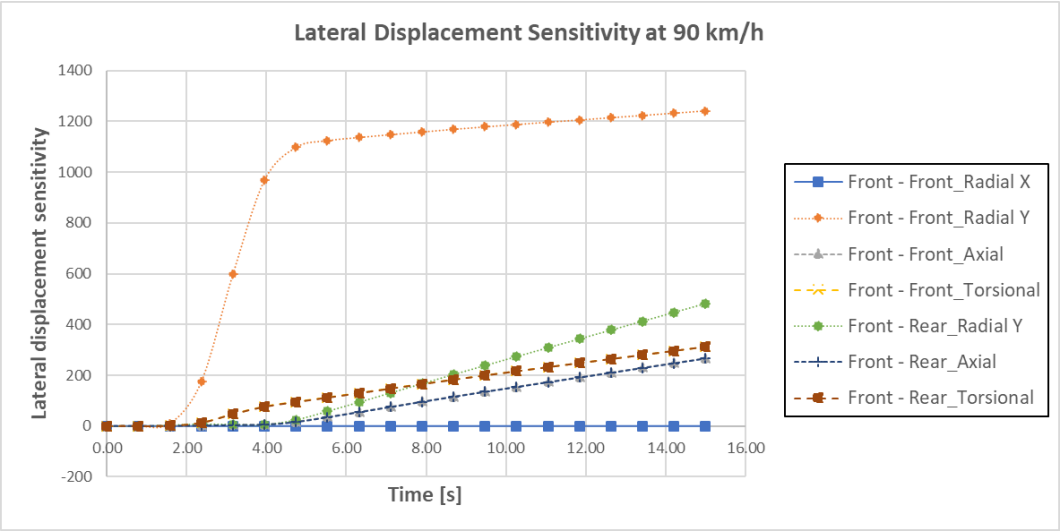

Figure 118: Real model lateral displacement sensitivity. 90km/h. Front bushings

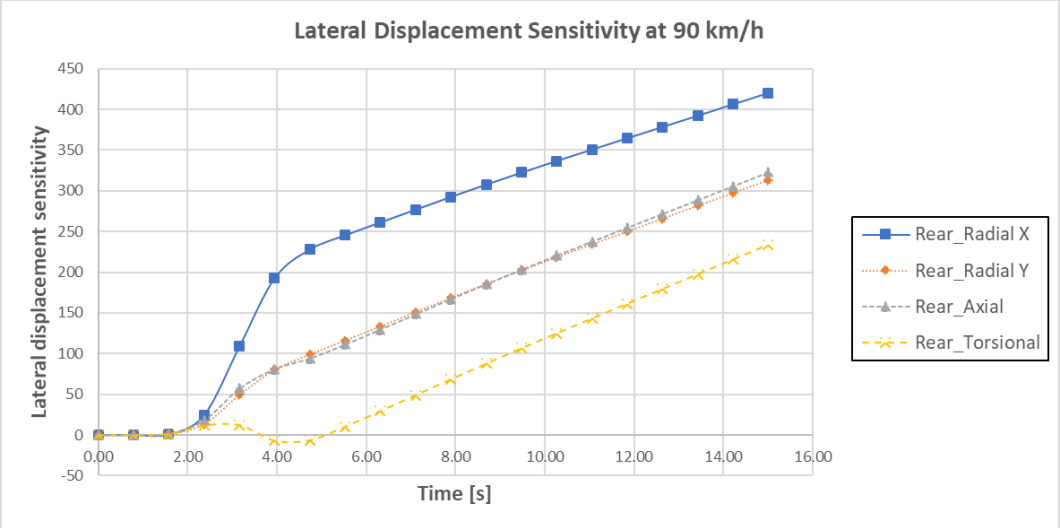

Figure 119: Real model lateral displacement sensitivity. 90km/h. Rear bushings

As it was expected from previous analyses, there is an evident predominance of the radial Y rigidity of the front front silentblock in the lateral displacement. An increase in the rigidity of this bushing in said direction results in a bigger and more instable lateral step at any speed.

The axial and radial Y rigidities of the rear front silentblock has, as explained before, a smaller but inverse effect on the lateral displacement.

Finally, the rear bushings radial X and torsional stiffnesses also have a remarkable influence, better seen at lower speeds.

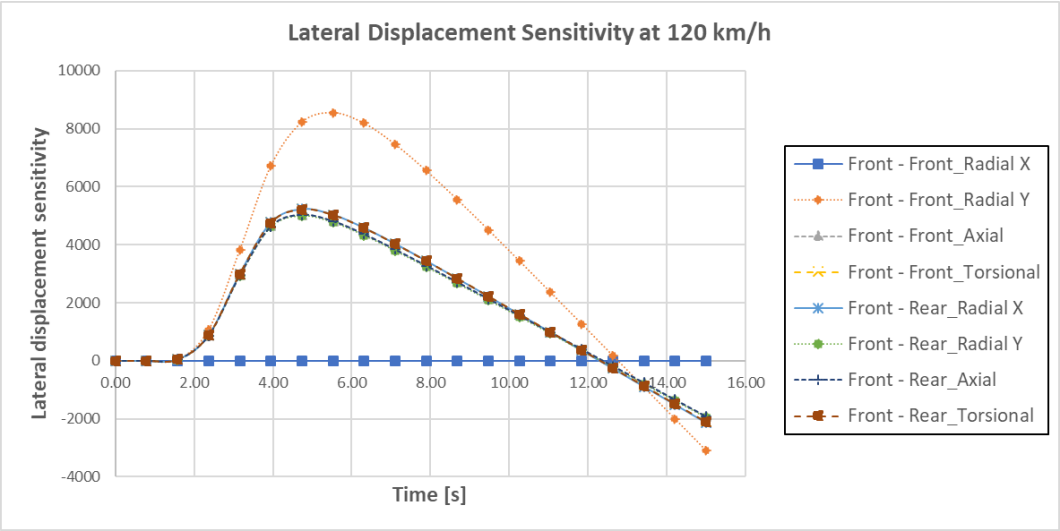

Figure 120: Real model lateral displacement sensitivity. 120km/h. Front bushings

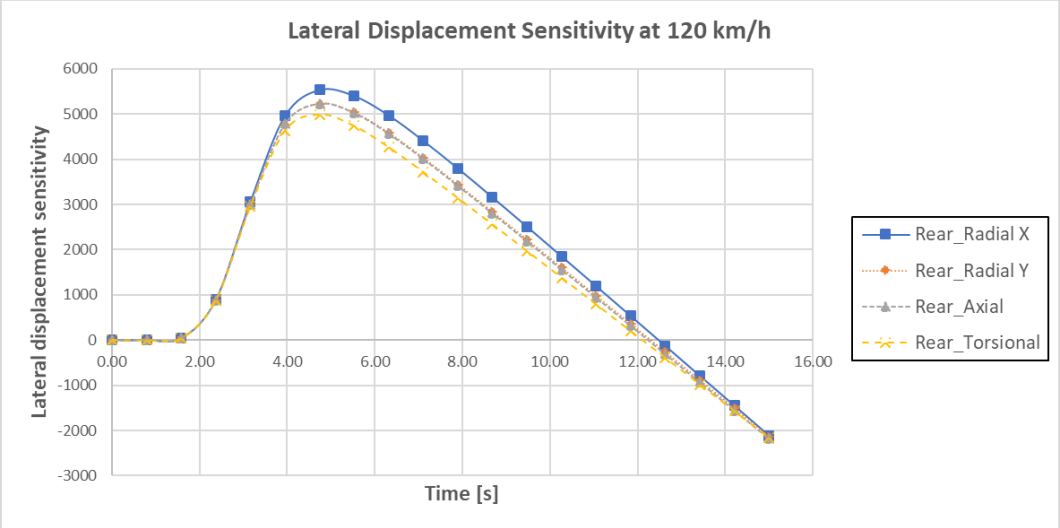

Figure 121: Real model lateral displacement sensitivity. 120km/h. Rear bushings

6.2.2.2. Lateral acceleration

The lateral acceleration is directly related to the lateral displacement. For this reason, the conclusions achieved should be similar.

On the one hand, Figure 122, Figure 124 and Figure 126, the effect of the front silentblocks' rigidities on the lateral acceleration is shown. As with the lateral displacement, the radial Y rigidity of the front front silentblocks is always predominant. The torsional stiffnesses and

the radial Y stiffness of the rear front silentblock also impact the lateral acceleration but with a smaller relevance.

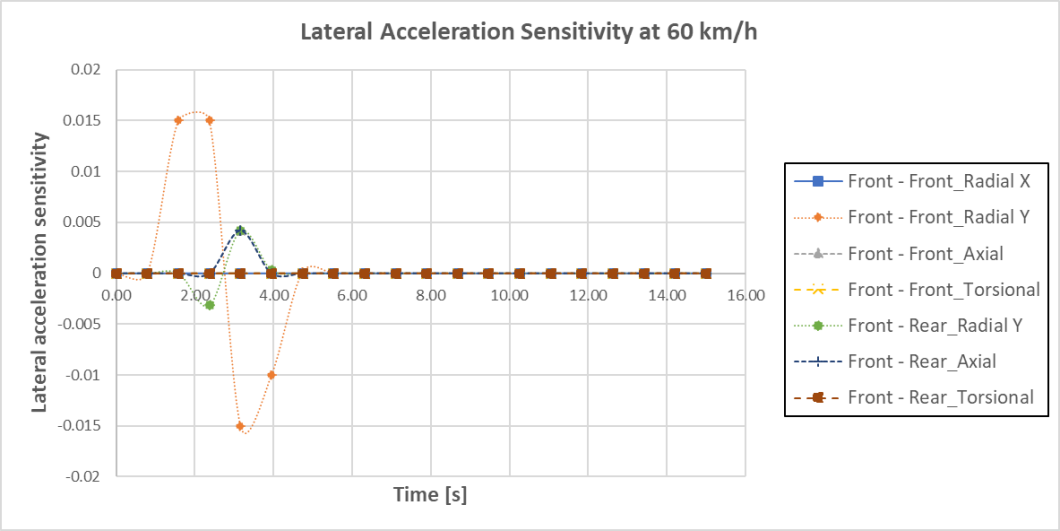

Figure 122: Real model lateral acceleration sensitivity. 60km/h. Front bushings

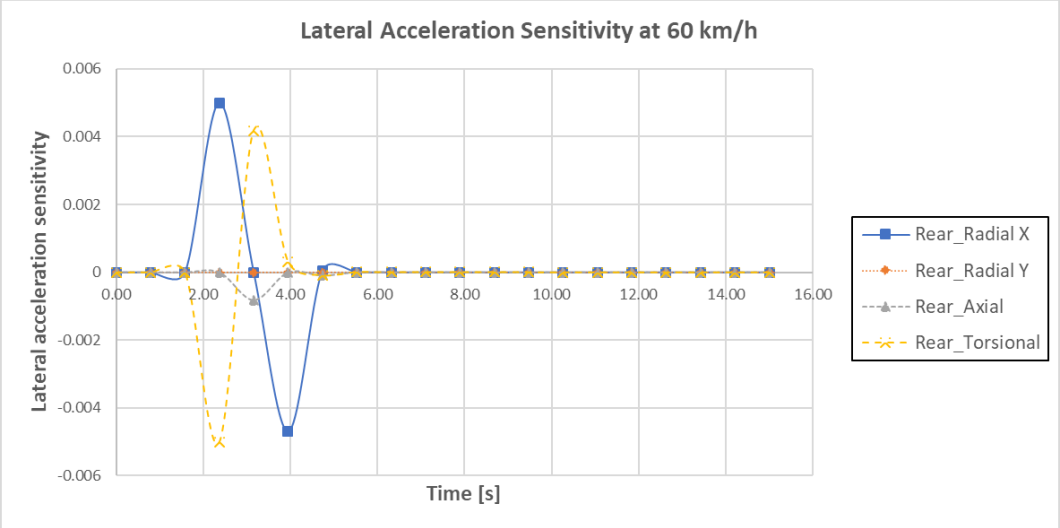

Figure 123: Real model lateral acceleration sensitivity. 60km/h. Rear bushings

On the other hand, Figure 123, Figure 125 and Figure 127 show the influence of the rigidities of the rear bushings in this output.

The radial X and the torsional stiffnesses of the rear bushings have the biggest importance out of the rear bushing parameters, influencing the lateral acceleration in opposite directions.

However, the impact of the radial X rigidity of rear bushings seems to increase with speed, while the torsional stiffness losses relevance.

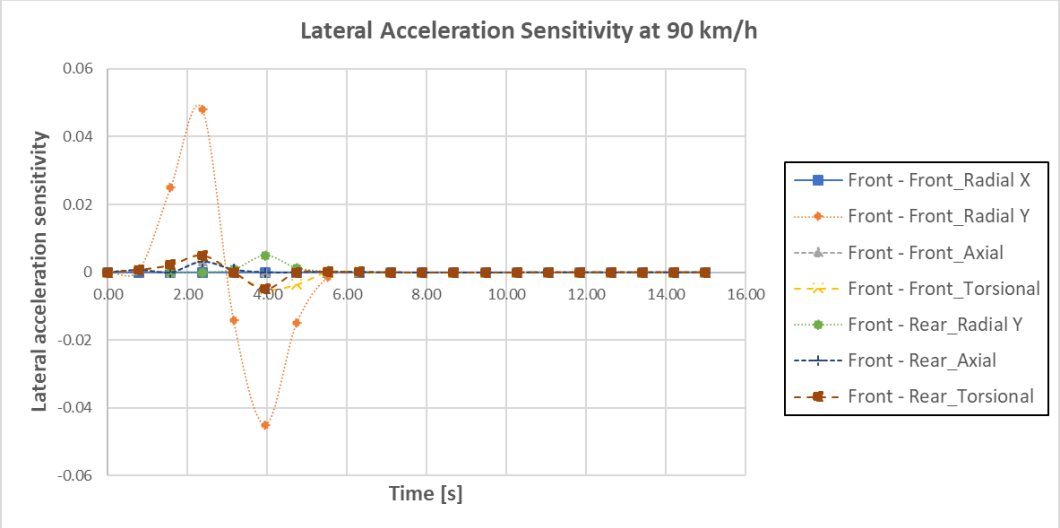

Figure 124: Real model lateral acceleration sensitivity. 90km/h. Front bushings

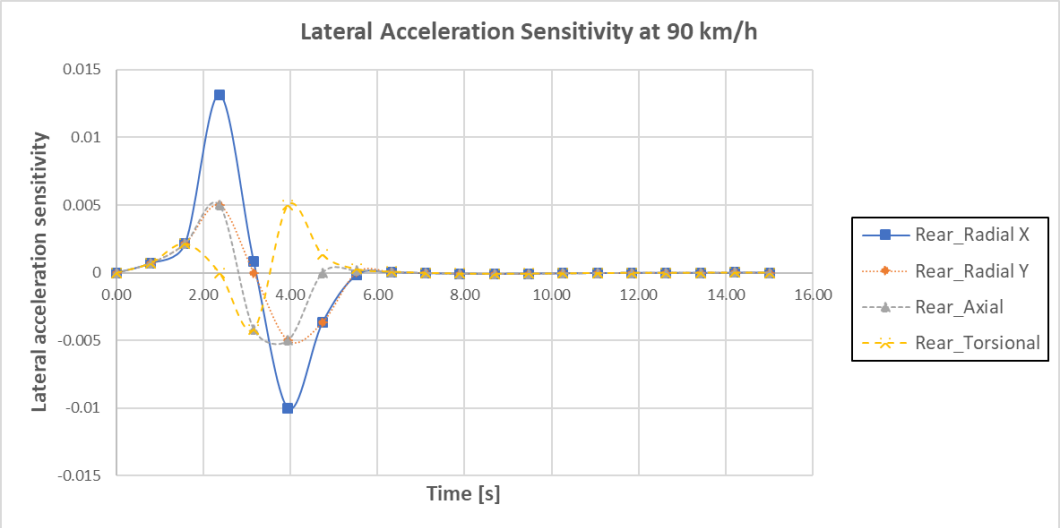

Figure 125: Real model lateral acceleration sensitivity. 90km/h. Rear bushings

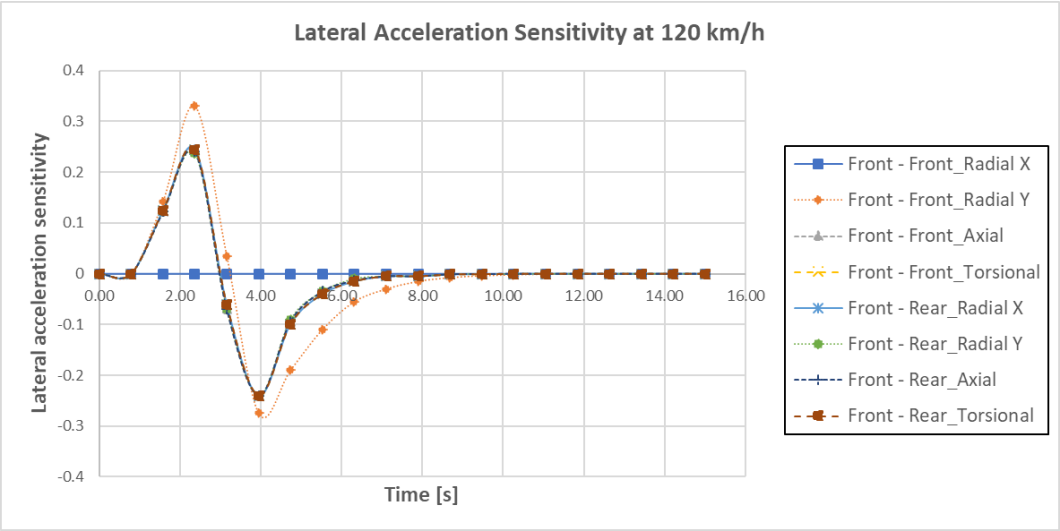

Figure 126: Real model lateral acceleration sensitivity. 120km/h. Front bushings

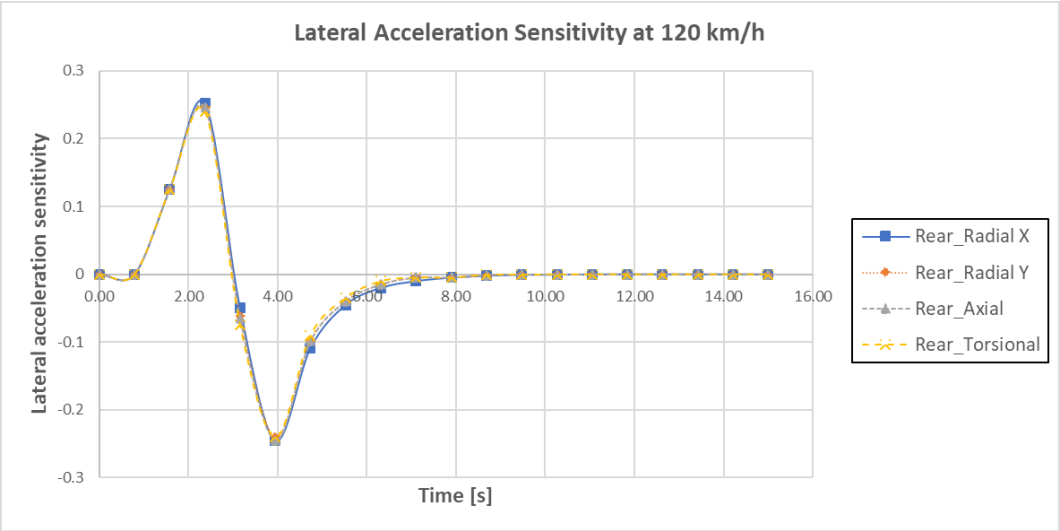

Figure 127: Real model lateral acceleration sensitivity. 120km/h. Rear bushings

7. Conclusions

7.1. Work conclusions

From all the work performed during this thesis, some conclusions can be reached. The first one is that, through the modification of the rigidities of the silentblocks, the alteration of the lateral response results much simpler that the alteration of the vertical and rolling behavior, where it was found a much more complex interconnection of all the parameters.

In other to improve de dynamic response of the Opel Astra Caravan 1999 and, in accordance with the results of this work, the following considerations should be taken:

- The radial Y rigidity of the front front silentblock has a huge influence on the lateral response, while not showing a remarkable impact on the bumped road maneuver. Therefore, this rigidity should be increased as much as possible in order to provide a better lateral stability.

- The radial X rigidity (vertical) of both front bushings don't show relevance in the lateral response while having a continuous and negative impact on the vertical response. This effect could be mitigated reducing these rigidities or increasing the damping coefficient in this direction.

- Torsional and radial X rigidity in rear bushings impact every output. Therefore, a variation in any direction would prejudice some output. The best course of action would be to increase the damping coefficient of this silentblock.

- A small decrease on the radial Y and axial rigidity of rear front silentblock would slightly improve the lateral response while reducing the acceleration peaks experienced in the cabin of the car.

- Softer front silentblocks in the torsional DoF would also slightly improve the satisfaction of the passengers in the body of the car.

7.2. Problems encountered

Throughout the development of this work, there were two main problems sources. The first had to be with the software and the second with the data of the work.

While ADAMS is a widely used software and there is plenty of information on it, it is not easy to find information and tutorials on the module ADAMS/Car. This made the project start later in tame than expected due to the learning period. However, the biggest problem came from limitations of the software. The available license in the Politecnico di Torino is a user license. This license allows the use and modification of premade templates but, unlike the template builder license, it does not allow to modify internal parameters of these templates. This made it impossible to achieve the real geometry of the rear suspension and thus, all of the parameters had to be approximated, resulting in not so realistic results for the rear bushings.

The second problem comes from the amount of data and parameters present in the work, what makes it difficult to comprehend and separate the effect of the different parameters even through sensitivity analyses.

7.3. Future lines

The main objective of this work was to analyze the influence of the four explained rigidities in the three silentblocks on the dynamic response of the vehicle in order to know the best way to proceed in order to improve these components.

A possible future line of work would be to test the bushings in the conical deformation mode in order to check the relevance of this parameters and improve the model by creating a rear suspension closer to the reality.

However, the most direct next step should be to develop silentblocks with the proposed improvements and simulate the model with those components in order to see the dynamic response of the car and whether it does indeed improve.

8. Bibliography

[1] BARTON, David C.; FIELDHOUSE, John D. Automotive Chassis Engineering. Springer, 2018.

[2] AMBRÓSIO, Jorge; VERISSIMO, Paulo. Sensitivity of a vehicle ride to the suspension bushing characteristics. Journal of Mechanical Science and Technology, 2009, vol. 23, no 4, p. 1075-1082.

[3] CAPUTO, Alessandro; SPINA, Michele; GUGLIELMINO, Eugenio. Sensitivity of Suspension System Performance to Bushing Stiffness Variation-An Evaluation Methodology. SAE transactions, 2003, p. 166-177.

[4] GOBBI, M., et al. Experimental Study and Numerical Modeling of the Dynamic Behaviour of Tyre/Suspension While Running Over an Obstacle. En ASME 2006 International Mechanical Engineering Congress and Exposition. American Society of Mechanical Engineers Digital Collection, 2006. p. 195-204.

[5] BLUNDELL, M. V. The influence of rubber bush compliance on vehicle suspension movement. Materials & design, 1998, vol. 19, no 1-2, p. 29-37.

[6] AMBRÓSIO, Jorge; VERISSIMO, Paulo. Improved bushing models for general multibody systems and vehicle dynamics. Multibody System Dynamics, 2009, vol. 22, no 4, p. 341.

[7] REIMPELL, Jornsen; STOLL, Helmut; BETZLER, Jurgen. The automotive chassis: engineering principles. Elsevier, 2001.

[8] HAFTKA, Raphael T.; ADELMAN, Howard M. Recent developments in structural sensitivity analysis. Structural optimization, 1989, vol. 1, no 3, p. 137-151.

[9] DE PAUW, Dirk JW; VANROLLEGHEM, Peter A. Practical aspects of sensitivity analysis for dynamic models. 2003.

[10] HERRANZ, EI Efler. Diseño de la suspensión trasera de un vehículo formula student. Tesis Doctoral. Tesis de grado. Universidad Politécnica de Madrid. España, 2016.[Online]. Available: https://goo. gl/YkgNnv.

[11] LEE, Hyun Seong, et al. Prediction of the dynamic equivalent stiffness for a rubber bushing using the finite element method and empirical modeling. International Journal of Mechanics and Materials in Design, 2019, vol. 15, no 1, p. 77-91.

[12] DZIERŻEK, Sławomir. Experiment-based modeling of cylindrical rubber bushings for the simulation of wheel suspension dynamic behavior. SAE transactions, 2000, p. 78-85.

[13] HOPE, Stephem William, et al. Lower control arm rear bushing development an integrated approach. SAE Technical Paper, 2003.

[14] KANG, B. J., et al. Improving the durability of automobile suspension systems by optimizing the elastomeric bushing compliance. Proceedings of the Institution of Mechanical Engineers, Part D: Journal of Automobile Engineering, 2008, vol. 222, no 4, p. 469-484.

[15] RAHMAN, M. M., et al. Fatigue life prediction of lower suspension arm using strain-life approach. European journal of scientific research, 2009, vol. 30, no 3, p. 437-450.

[16] GOBBI, M., et al. Experimental Study and Numerical Modeling of the Dynamic Behaviour of Tyre/Suspension While Running Over an Obstacle. En ASME 2006 International Mechanical Engineering Congress and Exposition. American Society of Mechanical Engineers Digital Collection, 2006. p. 195-204.

[17] KUO, E. Y.; LI, D.; LOH, W. The Effects of Bushing Degradation on Vehicle High Mileage NVH Performance. SAE Technical Paper, 1996.

[18] PIQUET, Boris; MAAS, Clayton A.; CAPOU, Florent. Next Generation of Suspension Bushings: Review of Current Technologies and Expansion Upon New 3 rd Generation Product Data. SAE Technical Paper, 2007.

Software

[19] ADAMS/Car (ADAMS 2019) [software]. (15-03-2019): MSC.Software

[20] Microsoft Excel for Office 365 MSO 32 bits.

Consulted websites

[21] https://www.wheel-size.com/size/opel/astra/1999/

[22] es.mathworks.com

Annexes

Annex A: Mass distribution

Masses achieved by ADAMS/Car			
Component	**Mass [kg]**	**%Sprung [%]**	**Location**
Steering shaft	1.569	100	front
Rack	1.889	100	front
Steering wheel	2.150	100	front
Pinion	0.500	100	front
Rack housing	4.000	100	front
Steering column	2.000	100	front
Intermediate shaft	1.000	100	front
Powertrain	187.435	100	any
Anti-roll Bar	0.466	80	front
Left droplink	0.365	100	front
Right droplink	0.365	100	front
Lower left control arm	5.091	50	front
Lower right control arm	5.091	50	front
Left upright	20.000	0	front
Right upright	20.000	0	front
Front suspension subframe	50.000	100	front
Left upper strut	5.000	100	front
Right upper strut	5.000	100	front
Left tie-rod	0.462	50	front
Right tie-rod	0.462	50	front
Left spindle	1.103	0	front
Right spindle	1.103	0	front
Powertrain left diff output	0.696	100	front

Masses achieved by ADAMS/Car			
Component	**Mass [kg]**	**%Sprung [%]**	**Location**
Powertrain right diff output	0.696	100	front
Powertrain central diff input	0.696	100	front
Powertrain diff housing	1.000	100	front
Left tripod	1.000	100	front
Right tripod	1.000	100	front
Left half shaft	0.595	100	front
Right half shaft	0.595	100	front
Front left wheel	17.231	0	front
Front right wheel	17.231	0	front
Rear left wheel	29.600	0	rear
Rear right wheel	29.600	0	rear
Chassis	747.804	100	any
Trim mass	0.000	100	any
Rear lower left strut	3.033	50	rear
Rear lower right strut	3.033	50	rear
Rear upper left strut	4.367	100	rear
Rear upper right strut	4.367	100	rear
Left spindle	1.103	0	rear
Right spindle	1.103	0	rear
Twist beam	11.623	0	rear